Supplementary Information for

Asymmetric Catalysis in Chiral Solvents: Chirality Transfer with Amplification of Homochirality through Helical Macromolecular Scaffold

Yuuya Nagata, Ryohei Takeda, and Michinori Suginome*

Department of Synthetic Chemistry and Biological Chemistry, Graduate School of Engineering, Kyoto University, Kyoto 606-8501, Japan
615-8510, Japan

*To whom correspondence should be addressed.
E-mail: suginome@sbchem.kyoto-u.ac.jp

Contents

1 General

All reactions were carried out under an atmosphere of nitrogen with magnetic stirring. ^{1}H, ^{13}C and ^{31}P NMR spectra were recorded on a Varian 400-MR spectrometer at ambient temperature. ^{1}H NMR data are reported as follows: chemical shift in ppm downfield from tetramethylsilane (δ scale), multiplicity (s = singlet, d = doublet, t = triplet, m = multiplet, and br = broad), coupling constant (Hz), and integration. ^{13}C NMR chemical shifts are reported in ppm downfield from tetramethylsilane (δ scale). All ^{13}C NMR spectra were obtained with complete proton decoupling. ^{31}P NMR chemical shifts are reported in ppm downfield from H_3PO_4 (85%). IR spectra were obtained using a Shimadzu FTIR-8400 or IRAffinity-1S Fourier transform infrared (FT-IR) spectrometer equipped with PIKE MIRacle attenuated total reflection (MIR-ATR) attachment. The GPC analysis was carried out with TSKgel GMH_{XL} ($CHCl_3$, polystyrene standards). Preparative GPC was performed on JAI LC-908 equipped with JAIGEL-1H and - 2H columns in a series ($CHCl_3$). UV spectra were recorded on a JASCO V-750 spectrometer equipped with a JASCO ETC-505T temperature/stirring controller at 20 °C. CD spectra were recorded on a JASCO J-1500 spectrometer equipped with a JASCO PTC-510L temperature/stirring controller at 20 °C. Flash chromatography was performed using a Biotage Isolera One flash purification system with silica gel flash cartridges. The chiral HPLC analysis was carried out on TOSOH 8020 series equipped with CHIRALCEL® OZ-H or OD-H (*n*-hexane and 2-propanol).

Tetrahydrofurane (THF) and toluene were purchased from the commercial sources as anhydrous grade and were used without further purification. 3,6-dimethylcatechol, [29] acetic formic anhydride (AFA), [30] 4,7-dibromo-5,6-bis(bromomethyl)benzo[*c*][1,2,5]thiadiazole, [31] monomers **1-NC**, [31] **5-NC**, [31] $\mathbf{Q_P}$, [32] $\mathbf{Q_{PXy}}$, [33] and *o*-TolNiCl(PMe_3)$_2$, [34] were prepared according to the reported procedure. Other chemical reagents were purchased from the commercial sources and were used without further purification.

2 Experimental Procedures and Spectral Data for Synthesized Compounds

2-ethylbutyl 4-methylbenzenesulfonate: To a mixture of 4-methylbenzenesulfonyl chloride (8.54g, 44.8 mmol) and anhydrous pyridine (14.7 mL) was added 2-ethylbutan-1-ol (4.16 g, 40.7 mmol, 5.0 mL) at 0 °C. After stirring for 4 h at 0 °C, the reaction mixture was quenched with water (50 mL) and extracted with Et_2O (50 mL × 3). The combined organic layer was washed with saturated $CuSO_4$ aq (50 mL), saturated $NaHCO_3$ aq (50 mL × 2), and brine (50 mL). The organic layer was dried over Na_2SO_4, filtered, and dried under reduced pressure. The crude product was subjected to silica gel column chromatography (hexane/AcOEt = 90/10), giving 2-ethylbutyl 4-methylbenzenesulfonate (10.2 g, 97% yield) as colorless oil. ^{1}H NMR ($CDCl_3$) δ 7.81-7.80 (2H, m), 7.36-7.35 (2H, m), 3.93 (2H, d, *J* = 5.6 Hz), 2.45 (3H, s), 1.52-1.51 (1H, m), 1.36-1.34 (4H, m), 0.80 (3H, t, *J* = 7.4 Hz); ^{13}C NMR ($CDCl_3$) δ 144.30, 132.71, 129.43, 127.39, 71.65, 40.12, 22.36, 21.05, 10.29; IR (ATR, neat) 2962.5 1355.9 1174.6 931.6 812.0 665.4HRMS (APCI$^+$) m/z calcd for $C_{13}H_{20}O_3S_1$+Na^+ (M+Na^+): 279.1025, found: 279.1023.

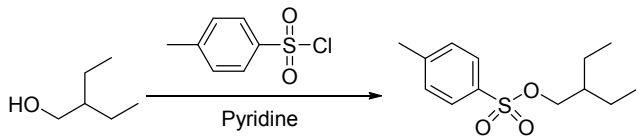

Scheme S1. Synthesis of 2-ethylbutyl 4-methylbenzenesulfonate.

Synthesis of 2-H: To a mixture of 3,6-dimethylcatechol (1.44 g, 10.4 mmol), a potassium hydroxide (1.75 g, 31.2 mmol), and 2-ethylbutyl 4-methylbenzenesulfonate (8.00 g, 31.2 mmol) was added dimethyl sulfoxide (10.4 mL). After stirring for 19 h at room temperature, the reaction mixture was quenched with water (50 mL) and extracted with Et_2O (50 mL). The combined organic layer was washed with water (50 mL × 3) and brine (50 mL). The organic layer was dried over Na_2SO_4, filtered, and dried under reduced pressure. The crude product was subjected to silica gel column chromatography (hexane/AcOEt = 90/10), and purified with preparative GPC, giving **2-H** (2.47 g, 78% yield) as colorless oil. ^{1}H NMR ($CDCl_3$) δ 6.78 (2H, s), 3.80 (4H, d, *J* = 6.40 Hz), 1.71-1.40 (10H, m), 0.94 (12H, t, *J* = 7.60 Hz); ^{13}C NMR ($CDCl_3$) δ 151.0, 129.7, 125.2, 75.4, 42.2, 23.2, 16.0, 11.2; IR (ATR, neat) 2961, 1460, 1277, 1074, 799 cm^{-1}; HRMS (EI$^+$) m/z calcd for $C_{20}H_{34}O_2$+H^+ (M+H^+): 306.2553, found: 306.2559.

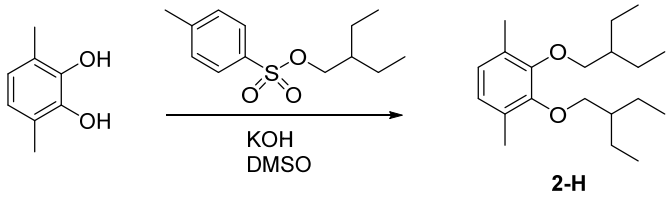

Scheme S2. Synthesis of **2-H**.

Synthesis of 2-NO_2: To mixed solution of fuming nitric acid (6.89 mL) and concentrated sulfuric acid was added dropwise an $CHCl_3$ (16 mL) solution of **2-H** (2.47 g, 8.06 mmol) at 0 °C. After stirring for 1 h, the reaction mixture was quenched with iced water and extracted with $CHCl_3$ (50 mL). The organic layer was washed with water (50 mL × 2), and brine (50 mL). The organic layer was dried over Na_2SO_4, filtered, and concentrated under reduced pressure. The crude product was subjected to silica gel column chromatography (hexane/AcOEt = 95/5), and purified with preparative GPC, giving **2-NO_2** (1.86 g, 58% yield) as yellow oil. ^{1}H NMR ($CDCl_3$) δ 3.86 (4H, d, J = 6.40 Hz), 2.29 (6H, s), 1.74-1.65 (2H, m), 1.58-1.41(8H, m), 0.95(12H, t, J = 7.60 Hz); ^{13}C NMR ($CDCl_3$) δ 153.2, 140.3, 125.7, 76.6, 41.9, 23.0, 11.7, 11.0; IR (ATR, neat) 2963, 1537, 1352, 1092, 756 cm^{-1}; HRMS (ESI$^+$) m/z calcd for $C_{20}H_{32}N_2O_6$+NH_4^+ (M+NH_4^+): 414.2559, found: 414.2592.

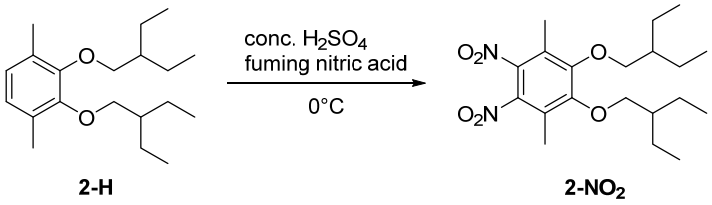

Scheme S3. Synthesis of **2-NO_2**.

Synthesis of 2-NC: A mixture of **2-NO_2** (1.86 g, 4.69 mmol), HCO_2NH_4 (1.92 g, 30.5 mmol), and 10 wt% Pd/C (0.250 g, 0.235 mmol) in EtOH (23 mL) was stirred for 7 h. The mixture was filtered through a pad of Celite and evaporated under vacuum. The residue was dissolved in AcOEt (20 mL), and washed with water (20 mL) and brine (20 mL). The organic layer was dried over Na_2SO_4, filtered, and concentrated under reduced pressure to give a diamine compound as yellow oil. Then, To a CH_2Cl_2 (19 mL) solution of the diamine compound (1.26 g, 3.74 mmol) was added AFA (2.63 g, 29.9 mmol) at 0 °C. The mixture was stirred for 10 h with gradual warming up to room temperature. The

mixture containing a diformamide compound was subjected to evaporation of volatile materials in vacuo and used for the next step without further purification. $POCl_3$ (0.91 mL, 1.50 g, 9.76 mmol) was added to a suspension of the diformate (1.28 g, 3.25 mmol) in Et_3N (4.52 mL) and CH_2Cl_2 (50 mL) at 0 °C. After stirring at 0 °C for 30 min, the reaction mixture was washed with saturated $NaHCO_3$ aq (50 mL). The organic layer was dried over Na_2SO_4, filtered, and concentrated under reduced pressure. The residue was purified with silica gel column chromatography (hexane to hexane/CH_2Cl_2 = 50/50) to give **2m** as white solid (0.714 g, 62%). ^{1}H NMR ($CDCl_3$) δ 3.79 (4H, d, J = 6.00 Hz), 2.33 (6H, s), 1.69-1.63 (2H, m), 1.57-1.41 (8H, m), 0.94 (12H, t, J = 7.40 Hz); ^{13}C NMR ($CDCl_3$) δ 171.6 , 151.9, 128.6, 119.9, 76.3, 42.0, 23.1, 12.7, 11.1; IR (ATR, neat) 2961, 2116 1454, 1335, 1269, 951 cm^{-1}; HRMS (ESI$^+$) m/z calcd for $C_{22}H_{32}N_2O_2$+NH_4^+ (M+NH_4^+): 374.2802, found: 374.2788.

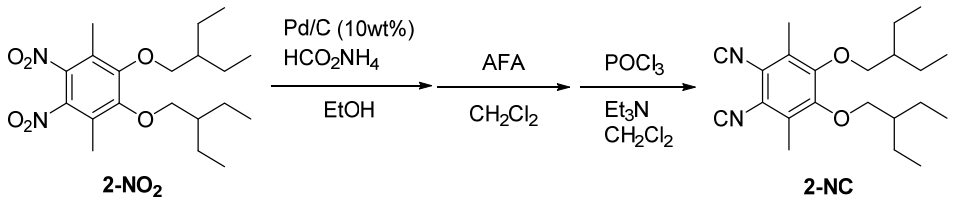

Scheme S4. Synthesis of **2-NC**.

Synthesis of 3-Br: To a solution of 5-nonanol (3.76 g, 26.1 mmol) in THF (10 mL) was added EtMgBr (1.09 M in THF, 21 mL, 24.0 mmol) at 0 °C. After stirring at room temperature for 30 min, hexamethylphosphoramide (HMPA, 10.9 mL, 62.5 mmol) and 4,7-dibromo-5,6- bis(bromomethyl)benzo[c][1,2,5]thiadiazole (5.0 g, 10.4 mmol) were added. The mixture was refluxed for 12 h. After concentration under reduced pressure, the mixture was diluted with water and extracted with Et_2O. The organic phase was washed with water and brine, and dried over Na_2SO_4. After evaporation of the solvent, the residue was purified by silica gel column chromatography (hexane: CH_2Cl_2 =1:1) to give **3-Br** (4.00 g, 63% yield). ^{1}H NMR ($CDCl_3$) δ 5.00 (4H, s), 3.49 (2H, quin, J = 5.70 Hz), 1.63-1.50 (8H, m), 1.42-1.29 (16H, m), 0.90 (12H, t, J = 7.00 Hz); ^{13}C NMR ($CDCl_3$) δ 152.7, 140.1, 117.6, 80.4, 67.5, 33.4, 27.6, 22.9, 14.1; IR (ATR, neat) 2955, 2930, 2859, 1466, 1377, 1344, 1271, 1125, 1057, 985, 881, 840, 732 cm^{-1}; HRMS (APCI$^+$) m/z calcd for $C_{26}H_{42}Br_2N_2O_2S$+H^+ (M+H^+):605.1407, found: 605.1386.

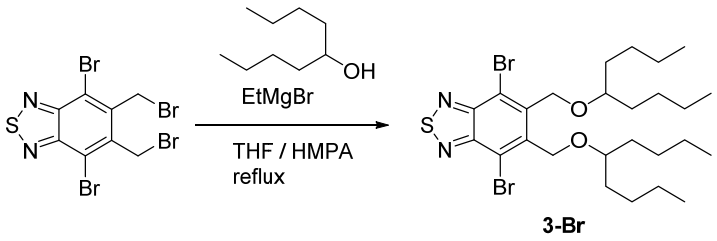

Scheme S5. Synthesis of **3-Br**.

Synthesis of 3-Me: To a mixture of **3-Br** (3.50 g, 5.77 mmol), KF (2.21 g, 38.1 mmol), and $(MeBO)_3$ (0.72 g, 5.77 mmol) was added a solution of $Pd(dba)_2$ (66.4 mg, 0.115 mmol), tri-*tert*-butylphosphine(46.7 mg, 0.231 mmol), and H_2O (0.208 mL, 11.5 mmol) in THF (12 mL). The mixture was heated under reflux for 14 h. The reaction mixture was cooled to room temperature and filtrated through a pad of Celite. To the mixture was added water and extracted with Et_2O. The organic phase was washed with water and brine and dried over $MgSO_4$. After evaporation of the solvent, the residue was purified by silica gel column chromatography (hexane:Et_2O = 10:1) to give **3-Me** (2.74 g, quant.). ^{1}H NMR ($CDCl_3$) δ 4.73 (4H, s), 3.46 (2H, quin, J = 5.70 Hz), 2.79 (6H, s), 1.66-1.53 (8H, m), 1.46-1.28 (16H, m), 0.92 (12H, t, J = 6.80 Hz); ^{13}C NMR ($CDCl_3$) δ 155.4, 136.3, 128.7, 80.3, 64.7, 33.4, 27.7, 23.0, 14.4, 14.1; IR (ATR, neat) 2955, 2930, 2859, 1456, 1379, 1344, 1126, 1051, 988, 880, 729 cm^{-1}; HRMS (APCI$^+$) m/z calcd for $C_{28}H_{48}N_2O_2S+H^+$ ($M+H^+$): 477.3509, found: 477.3493.

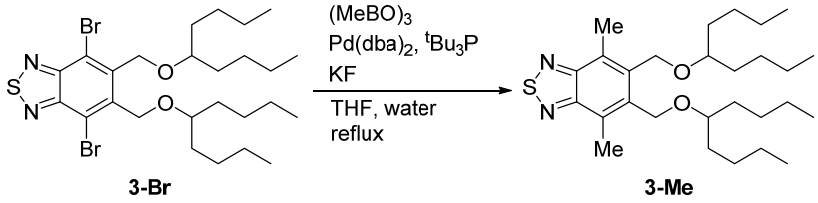

Scheme S6. Synthesis of **3-Me**.

Synthesis of 3-NH_2: To a solution of **3-Me** (2.50 g, 5.24 mmol) in EtOH (50 mL) were added $NaBH_4$ (1.98 g, 52.4 mmol) and $CoCl_2 \cdot 6H_2O$ (62.4 mg, 0.262 mmol). The mixture was heated gradually to 50 °C and stirred for 2 h, and passed through a pad of Celite. The resultant solution was evaporated in vacuo. Extraction with AcOEt followed by column chromatography on silica gel (hexane:AcOEt = 2:3) afforded diamine **3-NH_2** (1.42 g, 60% yield). ^{1}H NMR ($CDCl_3$) δ 4.50 (4H, s), 3.38-3.34 (6H, m), 2.21 (6H, s), 1.62-1.49(8H, m), 1.44-1.29(16H, m), 0.92 (6H, t, J = 7.0 Hz); ^{13}C NMR ($CDCl_3$) δ 132.9, 127.4, 121.0, 79.5, 65.3, 33.5, 27.8, 23.0, 14.1, 13.1; IR (ATR, neat) 3356, 2953, 2927,

2857, 1674, 1464, 1348, 1117, 1078, 1040, 785, 731 cm^{-1}; HRMS ($APCI^+$) m/z calcd for $C_{28}H_{52}N_2O_2+H^+$ ($M+H^+$): 449.4102, found: 449.4084.

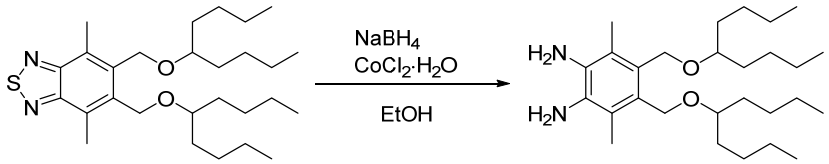

Scheme S7. Synthesis of **3-NH₂**.

Synthesis of 3-NC: To a CH_2Cl_2 (16 mL) solution of the diamine compound **3-NH₂** (1.42 g, 3.18 mmol) was added AFA (2.80 g, 31.8 mmol) at 0 °C. The mixture was stirred for 12 h with gradual warming up to room temperature. The mixture containing a diformamide compound was subjected to evaporation of volatile materials in vacuo and used for the next step without further purification. To a CH_2Cl_2 (5 mL) suspension of the diformamide compound (300 mg, 0.594 mmol) and Et_3N (0.824 mL, 5.94 mmol) cooled to 0 °C, $POCl_3$ (0.166 mL, 0.273 g, 1.78 mmol) was added. After stirring for 1 h at 0 °C, the reaction mixture was added saturated $NaHCO_3$ aq and extracted with CH_2Cl_2. The organic phase was washed with water and brine and dried over Na_2SO_4. After evaporation of the solvent, the residue was purified by column chromatography on silica gel (hexane:Et_2O = 4:1) gave **3-NC** (72.3 mg, 36% yield). ^1H NMR (C_6D_6) δ 4.28 (4H, s) 3.24 (2H, quin), 2.15 (4H, s), 1.57-1.27 (24H, m), 0.94 (6H, t, J = 7.0 Hz); ^{13}C NMR (C_6D_6) δ 175.5, 138.5, 133.9, 124.2, 80.5, 64.6, 33.7, 28.0, 23.4, 15.4, 14.4; IR (ATR, neat) 3233, 2955, 2859, 2116, 1667, 1466, 1379, 1344, 1082, 1049, 731 cm^{-1}; HRMS ($APCI^+$) m/z calcd for $C_{30}H_{48}N_2O_2+H^+$ ($M+H^+$): 469.3789, found: 469.3778.

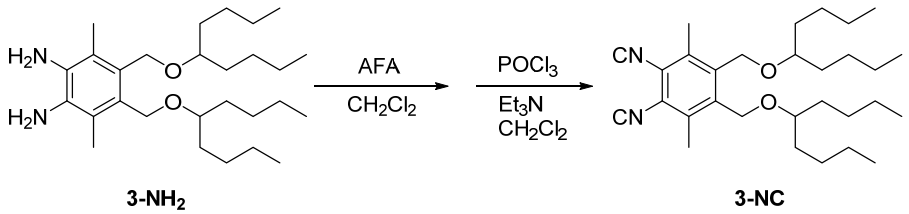

Scheme S8. Synthesis of **3m**.

Synthesis of 4-Br: To a solution of 1-heptanol (5.28 g, 45.4 mmol) in THF (10 mL) was added EtMgBr (1.10 M in THF, 38 mL, 41.8 mmol) at 0 °C. After stirring at room temperature for 30 min, hexamethylphosphoramide (HMPA, 19.0 mL, 109 mmol) and 4,7-dibromo-5,6- bis(bromomethyl)benzo[*c*][1,2,5]thiadiazole (8.72 g, 18.2 mmol) were added. The mixture was refluxed for 12 h. After concentration under reduced pressure,

the mixture was diluted with water and extracted with Et_2O. The organic phase was washed with water and brine, and dried over Na_2SO_4. After evaporation of the solvent, the residue was purified by silica gel column chromatography (hexane: AcOEt = 9:1) to give **4-Br** as white solid (9.32 g, 93% yield). ^{1}H NMR ($CDCl_3$) δ 5.01 (4H, s), 3.60 (4H, t, J = 6.60 Hz), 1.62 (4H, quin, J = 7.00 Hz), 1.39-1.23 (16H, m), 0.87 (6H, t, J = 6.80 Hz); ^{13}C NMR ($CDCl_3$) δ152.6, 139.6, 117.6, 71.2, 69.2, 31.8, 29.7, 29.0, 26.1, 22.6, 14.0; IR (ATR, neat) 2918, 1466, 1369, 1252, 1096, 847 cm^{-1}; HRMS (ESI$^+$) m/z calcd for $C_{22}H_{34}Br_2N_2O_2S+H^+$ (M+H$^+$): 549.0781, found: 549.0776.

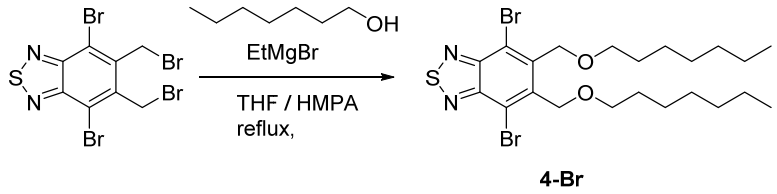

Scheme S9. Synthesis of **4-Br**.

Synthesis of 4-Me: To a mixture of **4-Br** (9.32 g, 16.9 mmol), KF (6.49 g, 112 mmol), and $(MeBO)_3$ (2.13 g, 16.9 mmol) was added a solution of bis(dibenzylideneacetone)palladium(0) ($Pd(dba)_2$, 195 mg, 0.339 mmol), tri-*tert*-butylphosphine (137 mg, 0.677 mmol), and H_2O (0.610 mL, 33.9 mmol) in THF (30 mL). The mixture was refluxed for 13 h. The reaction mixture was cooled to room temperature. The mixture was added water and extracted with Et_2O. The organic phase was washed with water and brine and dried over Na_2SO_4. After evaporation of the solvent, the residue was purified by silica gel column chromatography (hexane:Et_2O = 5:1) to give **4-Me** as white solid (5.70 g, 80% yield). ^{1}H NMR ($CDCl_3$) δ 4.72 (4H, s), 3.58 (4H, t, J = 6.60 Hz), 2.79 (6H, s), 1.634 (4H, quin, J = 7.00 Hz), 1.42-1.23 (16H, m), 0.88 (6H, t, J = 6.80 Hz); ^{13}C NMR ($CDCl_3$) δ 155.3, 136.0, 128.6, 71.2, 66.7, 31.8, 29.8, 29.1, 26.2, 22.6, 14.4, 14.1; IR (ATR, neat) 2926, 1466, 1354, 1094, 876 cm^{-1}; HRMS (ESI$^+$) m/z calcd for $C_{24}H_{40}N_2O_2S+H^+$ (M+H$^+$): 421.2883, found: 421.2873.

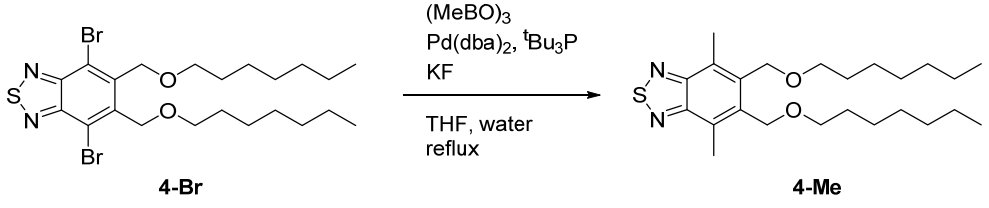

Scheme S10. Synthesis of **4-Me**.

Synthesis of 4-NC: To a solution of **4-Me** (5.60 g, 13.3 mmol) in EtOH (130 mL) were added $NaBH_4$ (5.04 g, 133 mmol) and $CoCl_2 \cdot 6H_2O$ (158 mg, 0.666 mmol). The mixture was heated gradually to reflux and stirred for 1 h, and passed through a pad of Celite. The resultant solution was evaporated in vacuo. Extraction with AcOEt followed by column chromatography on silica gel (hexane:AcOEt = 2:3) afforded diamine (5.12 g, 98% yield). Then, acetic formic anhydride (11.5 g, 130 mmol) was added to the diamine (5.12 g, 13.0 mmol) dissolved in CH_2Cl_2 (65 mL). After stirring for 12 h, removal of volatiles under reduced pressure gave a diformate compound as white powder (5.63 g, 96% yield). $POCl_3$ (0.22 mL, 0.356 g, 2.32 mmol) was added to a suspension of the diformate (0.347 g, 0.773 mmol) in Et_3N (1.08 mL) and CH_2Cl_2 (12 mL) at 0 °C. After stirring at 0 °C for 1 h, the reaction mixture was washed with saturated $NaHCO_3$ aq (20 mL). The organic layer was dried over Na_2SO_4, filtered, and concentrated under reduced pressure. The residue was purified with silica gel column chromatography (hexane to hexane/CH_2Cl_2 = 1/1) to give **4-NC** as colorless oily compound (0.151 g, 47%). ^{1}H NMR ($CDCl_3$) δ 4.19 (4H, s), 3.27 (4H, t, J = 6.40 Hz), 2.11 (6H, s), 1.53 (4H, quin, J = 6.90), 1.36-1.23 (16H, m), 0.89 (6H, t, J = 7.0Hz); ^{13}C NMR (C_6D_6) δ 172.9, 138.1, 134.1, 123.9, 71.5, 66.3, 31.8, 29.7, 29.0, 26.1, 22.6, 15.6, 14.0; IR (ATR, neat) 2926, 2114, 1466, 1356, 1099 cm^{-1}; HRMS (ESI$^+$) m/z calcd for $C_{26}H_{40}N_2O_2$+NH_4^+ (M+NH_4^+): 430.3428, found: 413.3429.

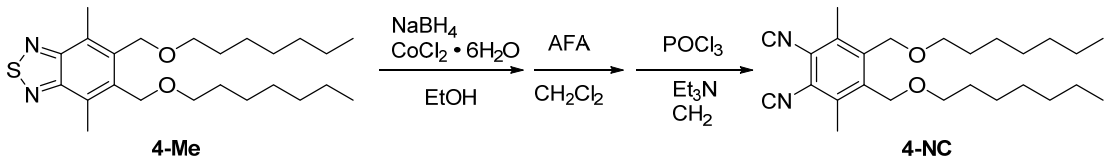

Scheme S11. Synthesis of **4-NC**.

Synthesis of 1(40): A THF solution of *o*-TolNiCl(PMe_3)$_2$ (50.0 mM, 33.3 μL, 1.67 μmol) was diluted with THF (1 mL). A THF solution of **1-NC** (20.0 mg, 66.6 μmol) was diluted with THF (1 mL). The monomer solution was added to the solution of *o*-TolNiCl(PMe_3)$_2$. After stirring for 18 h, $NaBH_4$ (2.52 mg, 66.6 μmol) was added to the reaction mixture at room temperature. After stirring for 1 h at room temperature, saturated NH_4Cl aq (10 mL) was added and extracted with CH_2Cl_2 (10 mL). The organic extract was washed with water (10 mL) and brine (10 mL) and dried over Na_2SO_4 followed by preparative GPC gave **1(40)** as a beige solid (19.5 mg, 97%). ^{1}H NMR ($CDCl_3$) δ 9.95 (1H, s), 3.98 (2H×40, br s), 3.83 (2H×40, br s), 2.84–2.04 (6H×40, br m), 1.74–1.72 (6H×40, br m), 1.57–1.26

(4H×40, br m), 1.03–0.87 (6H×40, br m); GPC ($CHCl_3$, g/mol): $M_n = 7.87 \times 10^3$, $M_w/M_n = 1.12$.

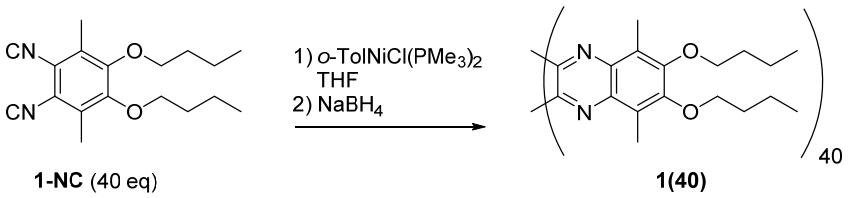

Scheme S12. Synthesis of **1(40)**.

Synthesis of 2(40): A THF solution of *o*-TolNiCl(PMe_3)$_2$ (50.0 mM, 28.1 μL, 1.40 μmol) was diluted with THF (1 mL). A THF solution of **2-NC** (20.0 mg, 56.1 μmol) was diluted with THF (1 mL). The monomer solution was added to the solution of *o*-TolNiCl(PMe_3)$_2$. After stirring for 18 h, $NaBH_4$ (2.12 mg, 56.1 μmol) was added to the reaction mixture at room temperature. After stirring for 1 h at room temperature, saturated NH_4Cl aq (10 mL) was added and extracted with CH_2Cl_2 (10 mL). The organic extract was washed with water (10 mL) and brine (10 mL) and dried over Na_2SO_4 followed by preparative GPC gave **2(40)** as a beige solid (19.3 mg, 96%). ^{1}H NMR ($CDCl_3$) δ 3.93–3.60 (4H×40, br m), 2.26–1.88 (6H×40, br m), 1.68–1.26 (8H×40, br m), 0.99–0.72 (12H×40, br m); GPC ($CHCl_3$, g/mol): $M_n = 4.02 \times 10^3$, $M_w/M_n = 1.18$.

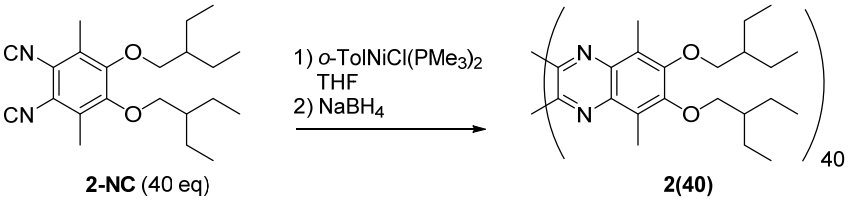

Scheme S13. Synthesis of **2(40)**.

Synthesis of 3(40): A THF solution of *o*-TolNiCl(PMe_3)$_2$ (50.0 mM, 24.1 μL, 1.21 μmol) was diluted with THF (1 mL). A THF solution of **3-NC** (22.6 mg, 48.2 μmol) was diluted with THF (1 mL). The monomer solution was added to the solution of *o*-TolNiCl(PMe_3)$_2$. After stirring for 18 h, $NaBH_4$ (1.82 mg, 48.2 μmol) was added to the reaction mixture at room temperature. After stirring for 1 h at room temperature, saturated NH_4Cl aq (10 mL) was added and extracted with CH_2Cl_2 (10 mL). The organic extract was washed with water (10 mL) and brine (10 mL) and dried over Na_2SO_4 followed by preparative GPC gave **3(40)** as a beige solid (18.7 mg, 83%). ^{1}H NMR ($CDCl_3$) δ 4.82–4.57 (4H×40, br

m), 3.46–3.22 (2H×40, br m), 2.66–2.09 (6H×40, br m), 1.56–1.24 (24H×40, br m), 0.96–0.67 (12H×40, br m); GPC ($CHCl_3$, g/mol): $M_n = 5.75 \times 10^3$, $M_w/M_n = 1.15$.

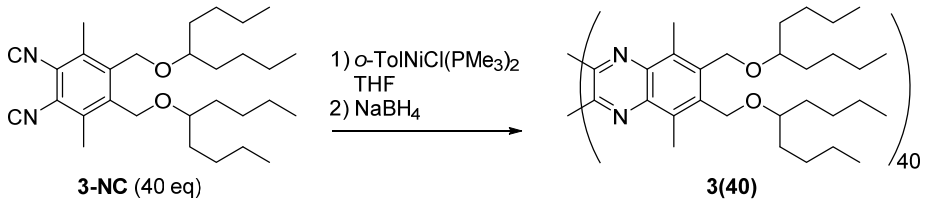

Scheme S14. Synthesis of **3(40)**.

Synthesis of 4(40): A THF solution of *o*-TolNiCl(PMe_3)$_2$ (50.0 mM, 27.4 μL, 1.37 μmol) was diluted with THF (1 mL). A THF solution of **4-NC** (22.6 mg, 54.8 μmol) was diluted with THF (1 mL). The monomer solution was added to the solution of *o*-TolNiCl(PMe_3)$_2$. After stirring for 18 h, $NaBH_4$ (2.07 mg, 54.8 μmol) was added to the reaction mixture at room temperature. After stirring for 1 h at room temperature, saturated NH_4Cl aq (10 mL) was added and extracted with CH_2Cl_2 (10 mL). The organic extract was washed with water (10 mL) and brine (10 mL) and dried over Na_2SO_4 followed by preparative GPC gave **4(40)** as a beige solid (20.7 mg, 92%). ^{1}H NMR ($CDCl_3$) δ 4.82–4.53 (2H×40, br m), 3.65–3.41 (4H×40, br m), 2.49–2.05 (6H×40, br m), 1.66–1.48 (4H×40, br m), 1.24 (16H×40, br s), 0.93–0.83 (6H×40, br s); GPC ($CHCl_3$, g/mol): $M_n = 4.16 \times 10^3$, $M_w/M_n = 1.23$.

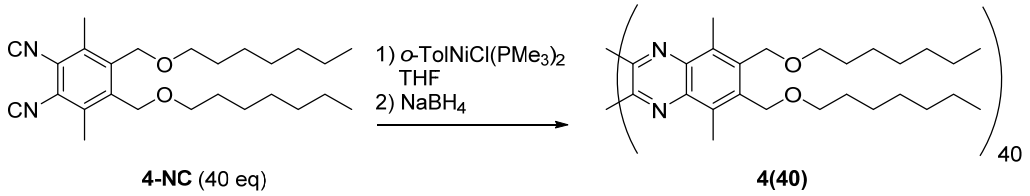

Scheme S15. Synthesis of **4(40)**.

Synthesis of 5(30): A THF solution of *o*-TolNiCl(PMe$_3$)$_2$ (50.0 mM, 30.7 μL, 1.53 μmol) was diluted with THF (1 mL). A THF solution of **5-NC** (13.8 mg, 45.9 μmol) was diluted with THF (1 mL). The monomer solution was added to the solution of *o*-TolNiCl(PMe$_3$)$_2$. After stirring for 12 h, $NaBH_4$ (1.74 mg, 45.9 μmol) was added to the reaction mixture at room temperature. After stirring for 1 h at room temperature, saturated NH_4Cl aq (10 mL) was added and extracted with CH_2Cl_2 (10 mL). The organic extract was washed with water (10 mL) and brine (10 mL) and dried over Na_2SO_4 followed by preparative GPC gave **5(30)** as a beige solid (13.6 mg, 94%). ^{1}H NMR ($CDCl_3$) δ 10.06 (1H, s), 4.84–4.41 (4H×30, m), 3.56–3.35 (4H×30, m), 2.45–2.03 (6H×30, m), 1.71–1.47 (4H×30, m), 0.99–0.79 (6H×30, m); GPC ($CHCl_3$, g/mol): $M_n = 4.13 \times 10^3$, $M_w/M_n = 1.18$.

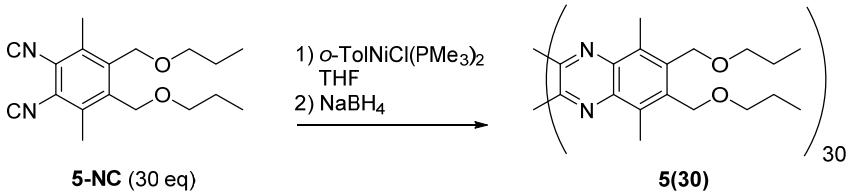

Scheme S16. Synthesis of **5(30)**.

Synthesis of 5(40): A THF solution of *o*-TolNiCl(PMe$_3$)$_2$ (50.0 mM, 13.4 μL, 0.67 μmol) was diluted with THF (3 mL). A THF solution of **5-NC** (20.1 mg, 66.9 μmol) was diluted with THF (1 mL). The monomer solution was added to the solution of *o*-TolNiCl(PMe$_3$)$_2$. After stirring for 18 h, $NaBH_4$ (2.53 mg, 66.9 μmol) was added to the reaction mixture at room temperature. After stirring for 1 h at room temperature, saturated NH_4Cl aq (10 mL) was added and extracted with CH_2Cl_2 (10 mL). The organic extract was washed with water (10 mL) and brine (10 mL) and dried over Na_2SO_4 followed by preparative GPC gave **5(40)** as a beige solid (17.6 mg, 88%). ^{1}H NMR ($CDCl_3$) δ10.06 (1H, s), 4.81-4.44 (4H×40, br m), 3.57–3.35 (4H×40, m), 3.05–2.02 (6H×40, m), 1.70–149 (4H×40, br m), 0.99–0.79 (6H×40, br m); GPC ($CHCl_3$, g/mol): $M_n = 7.87 \times 10^3$, $M_w/M_n = 1.12$.

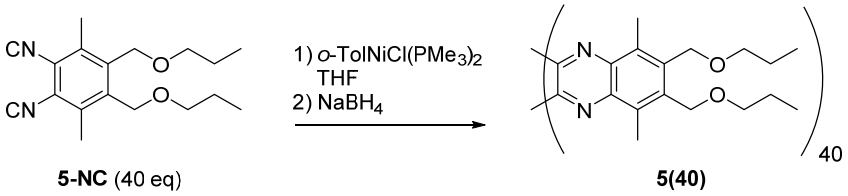

Scheme S17. Synthesis of **5(40)**.

Synthesis of 5(60): A THF solution of *o*-TolNiCl(PMe$_3$)$_2$ (50.0 mM, 15.3 μL, 0.766 μmol) was diluted with THF (3 mL). A THF solution of **5-NC** (14.2 mg, 47.3 μmol) was diluted with THF (3mL). The monomer solution was added to the solution of *o*-TolNiCl(PMe$_3$)$_2$. After stirring for 12 h, NaBH$_4$ (1.79 mg, 47.3 μmol) was added to the reaction mixture at room temperature. After stirring for 1 h at room temperature, saturated NH$_4$Cl aq (10 mL) was added and extracted with CH_2Cl_2 (10 mL). The organic extract was washed with water (10 mL) and brine (10 mL) and dried over Na_2SO_4 followed by preparative GPC gave **5(60)** as a beige solid (13.7 mg, 99%). ^{1}H NMR ($CDCl_3$) δ10.06 (1H, s), 4.80-4.37 (4H×60, br m), 3.65–3.35 (4H×60, br s), 2.67–2.03 (6H×60, m), 1.67–1.51 (4H×60, br m), 0.99–0.79 (6H×60, br m); GPC ($CHCl_3$, g/mol): M_n = 11.2 × 10^3, M_w/M_n = 1.13.

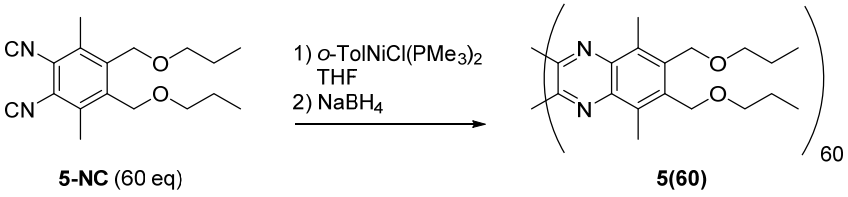

Scheme S18. Synthesis of **5(60)**.

Synthesis of 5(100): A THF solution of *o*-TolNiCl(PMe$_3$)$_2$ (50.0 mM, 13.4 μL, 0.669 μmol) was diluted with THF (1 mL). A THF solution of **5-NC** (20.1 mg, 66.9 μmol) was diluted with THF (1 mL). The monomer solution was added to the solution of o-TolNiCl(PMe$_3$)$_2$. After stirring for 18 h, NaBH$_4$ (2.53 mg, 66.9 μmol) was added to the reaction mixture at room temperature. After stirring for 1 h at room temperature, saturated NH$_4$Cl aq (10 mL) was added and extracted with CH_2Cl_2 (10 mL). The organic extract was washed with water (10 mL) and brine (10 mL) and dried over Na_2SO_4 followed by preparative GPC gave **5(100)** as a beige solid (18.7 mg, 93%). ^{1}H NMR ($CDCl_3$) δ 10.06 (1H, s) 4.6 6-4.57 (4H×100, br m), 3.47 (4H×100, br s), 2.66–2.03 (6H×100, br m), 1.69–

1.49 (4H×100, br m), 0.98–0.81 (6H×100, br m); GPC ($CHCl_3$, g/mol): $M_n = 15.1 \times 10^3$, $M_w/M_n = 1.13$.

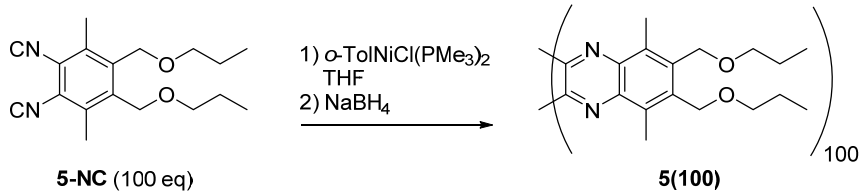

Scheme S19. Synthesis of **5(100)**.

Synthesis of 5(150): A THF solution of *o*-TolNiCl(PMe_3)$_2$ (50.0 mM, 6.13 μL, 0.306 μmol) was diluted with THF (3 mL). A THF solution of **5-NC** (14.1 mg, 46.9 μmol) was diluted with THF (3mL). The monomer solution was added to the solution of *o*-TolNiCl(PMe_3)$_2$. After stirring for 12 h, $NaBH_4$ (1.77 mg, 46.8 μmol) was added to the reaction mixture at room temperature. After stirring for 1 h at room temperature, saturated NH_4Cl aq (10 mL) was added and extracted with CH_2Cl_2 (10 mL). The organic extract was washed with water (10 mL) and brine (10 mL) and dried over Na_2SO_4 followed by preparative GPC gave **5(150)** as a beige solid (13.2 mg, 95%). ^{1}H NMR ($CDCl_3$) δ 4.67–4.57 (4H×150, br m), 3.46 (4H×150, br s), 2.34–2.30 (6H×150, br m), 1.61–1.55 (4H×150, m), 0.99–0.83 (6H×150, br m); GPC ($CHCl_3$, g/mol): $M_n = 33.9 \times 10^3$, $M_w/M_n = 1.08$.

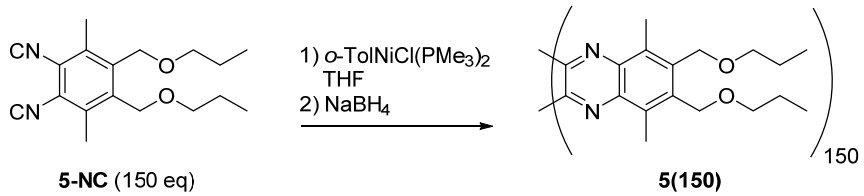

Scheme S20. Synthesis of **5(150)**.

Synthesis of 5(200): A THF solution of *o*-TolNiCl(PMe_3)$_2$ (50.0 mM, 4.60 μL, 0.241 μmol) was diluted with THF (1 mL). A THF solution of **5-NC** (14.5 mg, 48.1 μmol) was diluted with THF (1 mL). The monomer solution was added to the solution of *o*-TolNiCl(PMe_3)$_2$. After stirring for 16 h, $NaBH_4$ (1.82 mg, 48.1 μmol) was added to the reaction mixture at room temperature. After stirring for 1 h at room temperature, saturated NH_4Cl aq (10 mL) was added and extracted with CH_2Cl_2 (10 mL). The organic extract was washed with water (10 mL) and brine (10 mL) and dried over Na_2SO_4 followed by preparative GPC gave **5(200)** as a beige solid (11.9 mg, 89%). ^{1}H NMR ($CDCl_3$) δ 4.68–

4.56 (4H×200, br m), 3.46 (4H×200, br s), 2.35 (6H×200, br s), 1.61–1.59 (4H×200, m), 0.90 (6H×200, br t, J = 6.80 Hz); GPC ($CHCl_3$, g/mol): M_n = 52.1 × 10^3, M_w/M_n = 1.08.

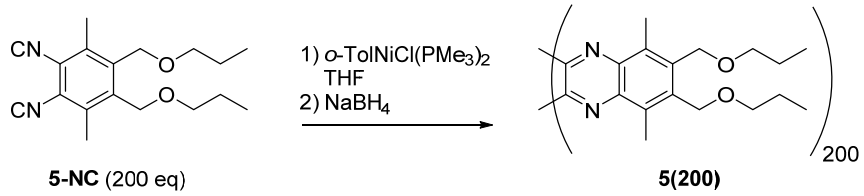

Scheme S21. Synthesis of **5(200)**.

Synthesis of 5(250): A THF solution of *o*-TolNiCl(PMe_3)$_2$ (50.0 mM, 3.68 μL, 0.184 μmol) was diluted with THF (3 mL). A THF solution of **5-NC** (14.1 mg, 46.9 μmol) was diluted with THF (3mL). The monomer solution was added to the solution of *o*-TolNiCl(PMe_3)$_2$. After stirring for 16 h, $NaBH_4$ (1.78 mg, 46.9 μmol) was added to the reaction mixture at room temperature. After stirring for 1 h at room temperature, saturated NH_4Cl aq (10 mL) was added and extracted with CH_2Cl_2 (10 mL). The organic extract was washed with water (10 mL) and brine (10 mL) and dried over Na_2SO_4 followed by preparative GPC gave **5(250)** as a beige solid (13.2 mg, 96%). ^{1}H NMR ($CDCl_3$) δ 4.67–4.58 (4H×250, br m), 3.47 (4H×250, br s), 2.35 (6H×250, br s), 1.61– 1.59 (4H×250, br m), 0.90 (6H×250, br t, J = 6.80 Hz); GPC ($CHCl_3$, g/mol): M_n = 55.2 × 10^3, M_w/M_n = 1.12.

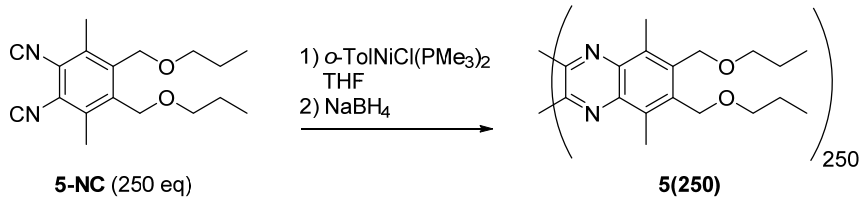

Scheme S22. Synthesis of **5(250)**.

Synthesis of 5(300): A THF solution of *o*-TolNiCl(PMe_3)$_2$ (50.0 mM, 3.07 μL, 0.153 μmol) was diluted with THF (3 mL). A THF solution of **5-NC** (14.1 mg, 47.1 μmol) was diluted with THF (3mL). The monomer solution was added to the solution of *o*-TolNiCl(PMe_3)$_2$. After stirring for 16 h, $NaBH_4$ (1.78 mg, 47.1 μmol) was added to the reaction mixture at room temperature. After stirring for 1 h at room temperature, saturated NH_4Cl aq (10 mL) was added and extracted with CH_2Cl_2 (10 mL). The organic extract was washed with water (10 mL) and brine (10 mL) and dried over Na_2SO_4 followed by

preparative GPC gave **5(300)** as a beige solid (13.6 mg, 98%). ^{1}H NMR ($CDCl_3$) δ 4.68–4.57 (4H×300, br m), 3.46 (4H×300, br s), 2.35 (6H×300, br s), 1.61– 1.59 (4H×300, br m), 0.90 (6H×300, br t, J = 7.00 Hz); GPC ($CHCl_3$, g/mol): M_n = 66.0 × 10^3, M_w/M_n = 1.08.

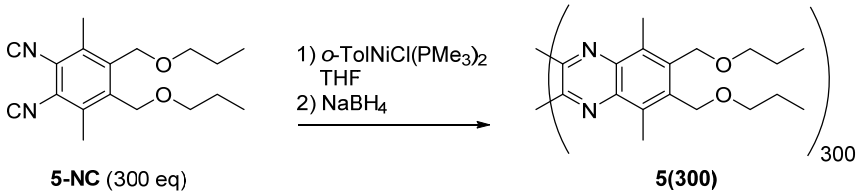

Scheme S23. Synthesis of **5(300)**.

Synthesis of 5(1000): A THF solution of *o*-TolNiCl(PMe_3)$_2$ (50.0 mM, 1.33 μL, 0.0666 μmol) was diluted with THF (1 mL). A THF solution of **5-NC** (20.0 mg, 66.7 μmol) was diluted with THF (1 mL). The monomer solution was added to the solution of *o*-TolNiCl(PMe_3)$_2$. After stirring for 18 h, $NaBH_4$ (2.52 mg, 66.7 μmol) was added to the reaction mixture at room temperature. After stirring for 1 h at room temperature, saturated NH_4Cl aq (10 mL) was added and extracted with CH_2Cl_2 (10 mL). The organic extract was washed with water (10 mL) and brine (10 mL) and dried over Na_2SO_4 followed by preparative GPC gave **5(1000)** as a beige solid (19.2 mg, 96%). ^{1}H NMR ($CDCl_3$) δ 4.57 (4H×1000, br s), 3.46 (4H×1000, br s), 2.35 (6H ×1000, br s), 1.59 (4H×1000, br s), 0.90 (6H×1000, br s); GPC ($CHCl_3$, g/mol): M_n = 35.0 × 10^4, M_w/M_n = 1.56.

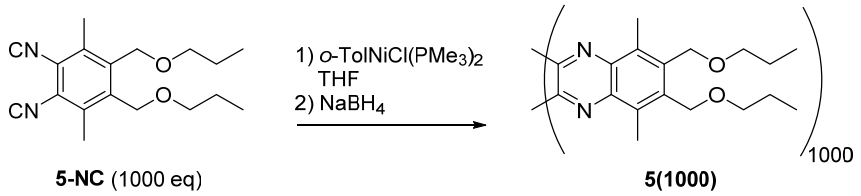

Scheme S24. Synthesis of **5(1000)**.

Synthesis of L1: A THF solution of o-TolNiCl(PMe_3)$_2$ (50.7 mM, 14.0 μL, 0.711 μmol) was added to the solution of monomer **5-NC** (211.5 mg, 704 μmol) and $\mathbf{Q_P}$ (3.09 mg, 7.11 μmol) in THF (30 mL). The mixture was stirred for 24 h at room temperature. To the reaction mixture was added $NaBH_4$ (10.8 mg, 285 μmol), and the mixture was stirred for 1 h. The mixture was poured into vigorously stirred methanol (300 mL), and precipitated polymer was collected by filtration. After drying in vacuo, **L1-S** was obtained as fibriform solid.

Reduction of phosphine sulfide: A mixture of **L1-S** (7.11 μmol P) and $P(NMe_2)_3$ (52 μL, 287 μmol) in toluene (4 mL) was stirred at 110 °C for 19 h. The mixture was poured into vigorously stirred MeOH (300 mL). Precipitated material was collected by filtration to give **L1** as fibriform solid (187 mg, 82%). ^{1}H NMR ($CDCl_3$) δ 4.65 (4×990H, br s), 3.45 (4H×990, br s), 2.35 (6H×990, br s), 1.61 (4H×990, br s), 0.91 (6H×990, br s); ^{31}P NMR ($CDCl_3$) δ -15.3 (br s); GPC ($CHCl_3$, g/mol): $M_n = 34.9 \times 10^4$, $M_w/M_n = 1.43$.

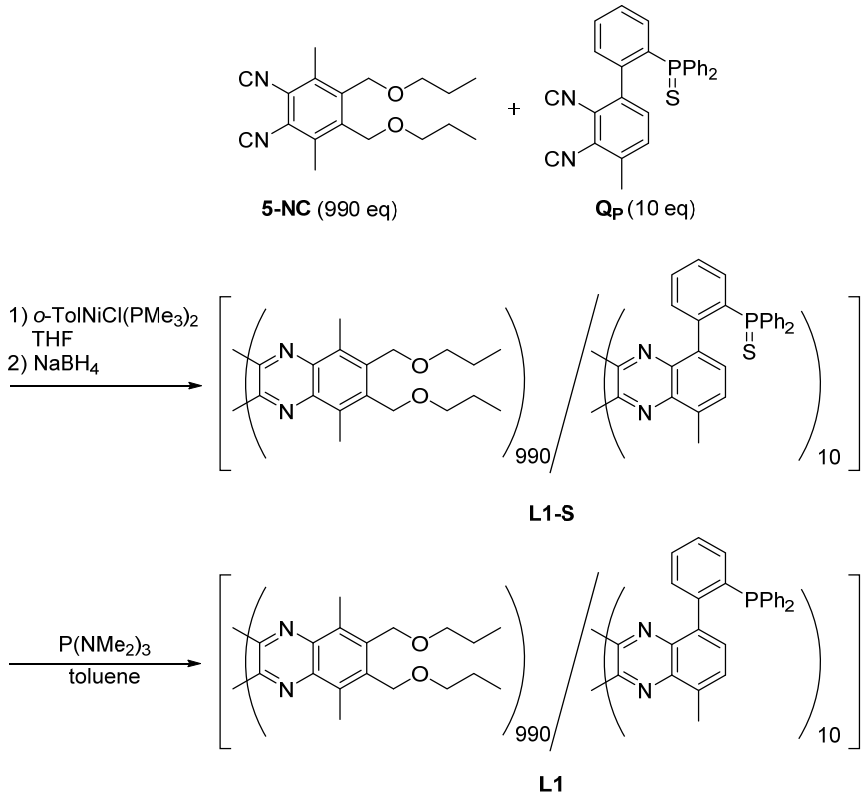

Scheme S25. Synthesis of **L1**.

Synthesis of L2: A THF solution of *o*-$TolNiCl(PMe_3)_2$ (50.7 mM, 14.0 μL, 0.711 μmol) was added to the solution of monomer **5-NC** (203.0 mg, 704 μmol) and $\mathbf{Q_p}$ (15.5 mg, 35.6 μmol) in THF (30 mL). The mixture was stirred for 24 h at room temperature. To the reaction mixture was added $NaBH_4$ (10.8 mg, 285 μmol), and the mixture was stirred for 1 h. The mixture was poured into vigorously stirred methanol (300 mL), and precipitated polymer was collected by filtration. After drying in vacuo, **L2-S** was obtained as fibriform solid.

Reduction of phosphine sulfide: A mixture of **L2-S** (35.6 μmol P) and $P(NMe_2)_3$ (272 μL, 1.49 mmol) in toluene (4 mL) was stirred at 110 °C for 24 h. The mixture was poured

into vigorously stirred MeOH (300 mL). Precipitated material was collected by filtration to give **L2** as fibriform solid (202 mg, 93%). ^{1}H NMR ($CDCl_3$) δ 4.55 (4×950H, br s), 3.44 (4H×950, br s), 2.35 (6H×950, br s), 1.59 (4H×950, br s), 0.88 (6H×950, br s); ^{31}P NMR ($CDCl_3$) δ -15.4 (br s); GPC ($CHCl_3$, g/mol): M_n = 23.5 × 10^4, M_w/M_n = 1.37.

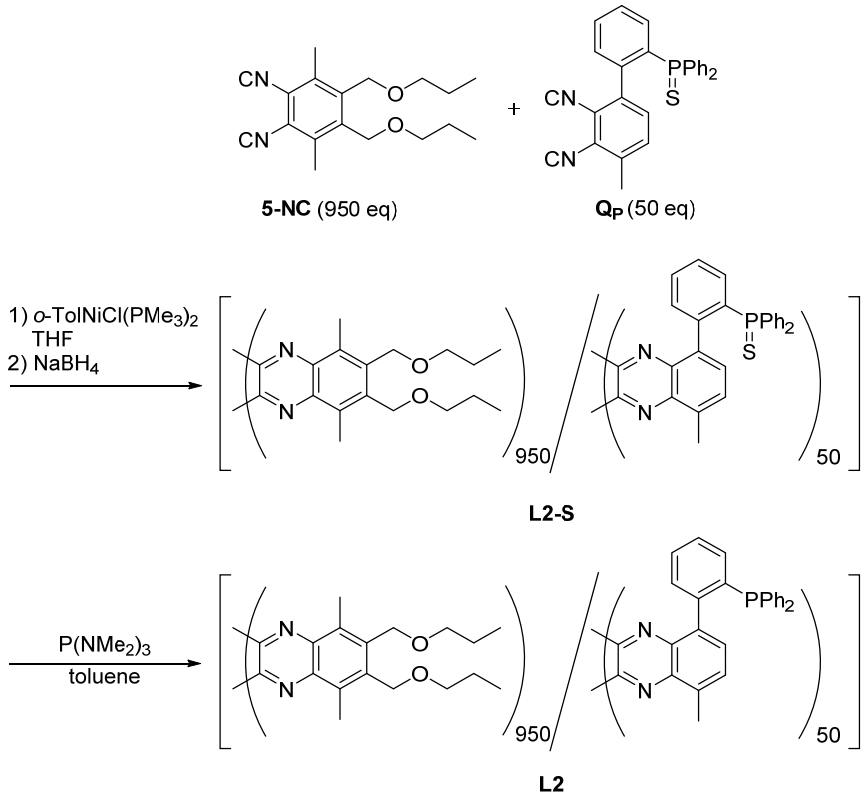

Scheme S26. Synthesis of **L2**.

Synthesis of L6: A THF solution of *o*-TolNiCl(PMe_3)$_2$ (50.7 mM, 20.0 μL, 1.02 μmol) was added to the solution of monomer **5-NC** (301.9 mg, 1.00 mmol) and $\mathbf{Q_{PXy}}$ (4.97 mg, 10.2 μmol) in THF (50 mL). The mixture was stirred for 24 h at room temperature. To the reaction mixture was added $NaBH_4$ (15.4 mg, 406 μmol), and the mixture was stirred for 1 h. The mixture was poured into vigorously stirred methanol (300 mL), and precipitated polymer was collected by filtration. After drying in vacuo, **L6-S** was obtained as fibriform solid.

Reduction of phosphine sulfide: A mixture of **L6-S** (10.2 μmol P) and $P(NMe_2)_3$ (73.4 μL, 404 μmol) in toluene (5 mL) was stirred at 110 °C for 24 h. The mixture was poured into vigorously stirred MeOH (300 mL). Precipitated material was collected by filtration to give **L6** as fibriform solid (295 mg, 98%). ^{1}H NMR ($CDCl_3$) δ 4.62 (4×990H, br s),

3.47 (4H×990, br s), 2.35 (6H×990, br s), 1.60 (4H×990, br s), 0.90 (6H×990, br s); ^{31}P NMR ($CDCl_3$) δ -15.7 (br s) GPC ($CHCl_3$, g/mol): $M_n = 28.7 \times 10^4$, $M_w/M_n = 1.71$.

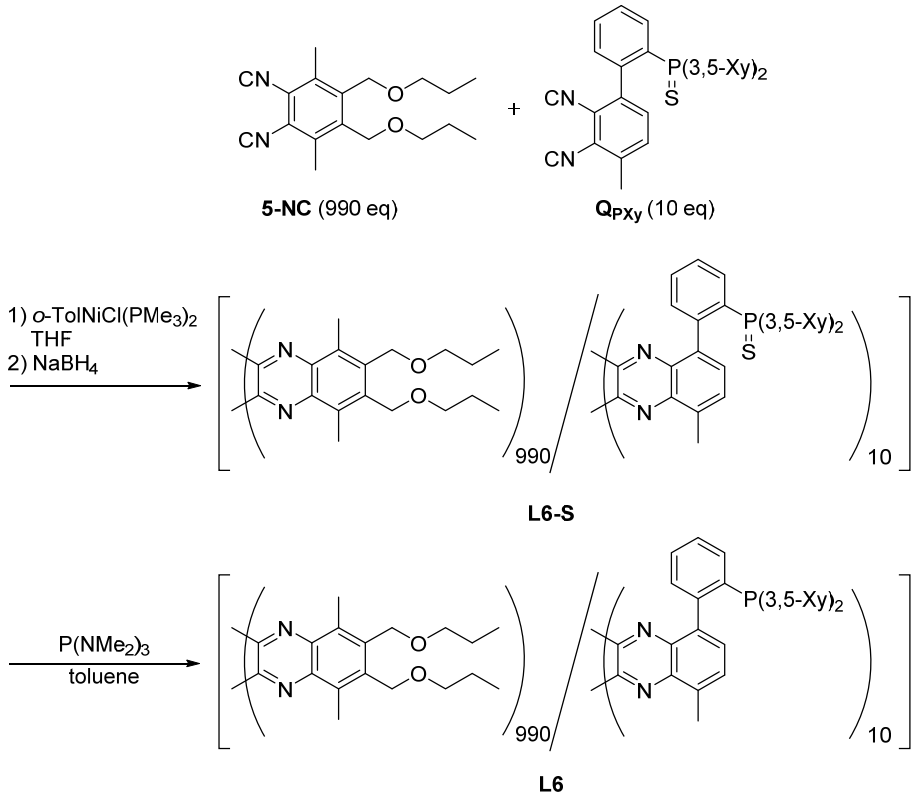

Scheme S27. Synthesis of **L6**.

Asymmetric Suzuki-Miyaura cross coupling

A PQX (61 mg of **L1** (2.00 μmol of phosphorus atom), 12 mg of **L2** (2.00 μmol of phosphorus atom) or 12 mg of **1(1000)**) was dissolved in chiral solvent at room temperature for 12 hours. Within 15 minutes after an addition of $[PdCl(\eta^3\text{-}C_3H_5)]_2$ (8.50 mM in THF, 58.8 μL, 0.50 μmol) to the solution, dimethyl(1-bromonaphtahlen-2-yl)phophonate (0.05 mmol), (4-methy-1-naphthalene)boronic acid (0.10 mmol), K_3PO_4 (31.8 mg, 0.15 mmol) and H_2O (50 μL) were added in this order. The reaction was stirred at room temperature for 24 h. After the reaction, subsequent addition of MeCN (10mL) resulted in precipitation of the PQXphos. The suspension was filtrated using MeCN as an eluent. The crude product was subjected to PTLC (hexane/AcOEt = 3/7). Further purification was performed by GPC. The enantiomeric excess of the product was determined by HPLC with CHIRALCEL® OZ-H (Eluent: *n*-hexane/2-PrOH = 80/20, Flow rate: 0.6 mL/min, Retention time: t_R of (−)-isomer = 12.7 min, t_R of (+)-isomer = 15.5 min).

Asymmetric Hydrosilylation Reaction

L1 (7.68 mg, 0.240 μmol of phosphorus atom) was dissolved in (*R*)-limonene at room temperature for 12 hours. $[PdCl(\eta^3\text{-}C_3H_5)]_2$ (9.50 mM in THF, 10.5 μL, 0.10 μmol) was added to the solution. After an addition of styrene (23.0 μL, 20.8 mg, 200 μmol), trichlorosilane (40.4 μL, 400 μmol) was added to the reaction solution. It was stirred for 24 h under room temperature. After the reaction mixture was subjected to bulb-to-bulb distillation to afford the hydrosilylation product (93% ^{1}H NMR yield). To determine enantiomeric excess of the hydrosilylation product, KF (64.8 mg, 1.12 mol), and $KHCO_3$ (167 mg, 1.67 mmol) in THF (1 mL) and MeOH (1 mL) was added hydrogen peroxide (30 wt. %, 253 μL, 75.9 mmol) at room temperature. The mixture was stirred at room temperature for 12 h. To the mixture was added sat. $Na_2S_2O_3$ aq. Organic materials were extracted with ether (20 mL), washed with water (20 mL) and brine (20 mL), and dried over Na_2SO_4. After evaporation of the solvent, the residue was subjected to preparative GPC, giving enantioenriched 1-phenylpropanol (15.8 mg, 0.13 mmol, 65% isolated yield in two steps). The enantiomeric excess of the product was determined to be 92% by HPLC with CHIRALCEL® OD-H (Eluent: *n*-hexane/2-PrOH = 97/3, Flow rate: 0.6 mL/min, Retention time: t_R of (*R*)-isomer = 14.0 min, t_R of (*S*)-isomer = 16.0 min).

Silaboration reaction of methylene cyclopropane

To a solution of **L6** (1.20 μmol of phosphorous atom) in (*S*)-limonene (950 μL) was added Pd_2dba_3 (0.01 M in toluene, 50 μL, 0.50 μmol). The mixture was stirred at room temperature for 12 hours. To the mixture was added methylenecyclopropane (75 μmol) and $MePh_2Si$-B(pin) (16.2 mg, 0.05 mmol), and the resulting mixture was heated at 50 °C with stirring for 24 h and then 60 °C for 24 h. Subsequent addition of MeCN (10 mL) resulted in precipitation of the **L6**. The suspension was passed through a pad of Celite® using MeCN as an eluent. To determine the enantiomeric excess, the silylated alkenylborane obtained was converted to *β*-silyl ketone. To a methanol solution (2 mL) of the 2-boryl-4-silyl-1-butene derivative was added NaOH aq (3 mol/L, 2.5 mL) and the mixture was cooled to 0 °C. H_2O_2 aq (30 wt. %, 1.5 mL) was slowly added to the mixture. The resulting solution was stirred at room temperature for 12 h. The resulting mixture was extracted with Et_2O and the extracts were washed with water. After drying with anhydrous $MgSO_4$, the concentrated mixture was purified by a preparative thin layer chromatography to give a corresponding *β*-silylketone. The enantiomeric excess of the product was determined to be 89% (*R*) by HPLC with CHIRALCEL® OD-H (Eluent: *n*-hexane/2-PrOH = 99.7/0.3, Flow rate: 0.6 mL/min, Retention time: t_R of (*R*)-isomer = 8.0 min, t_R of (*S*)-isomer = 7.4 min).

3 CD spectra of 5(100) in the mixed solvent of (*R*)-limonene and cyclohexane

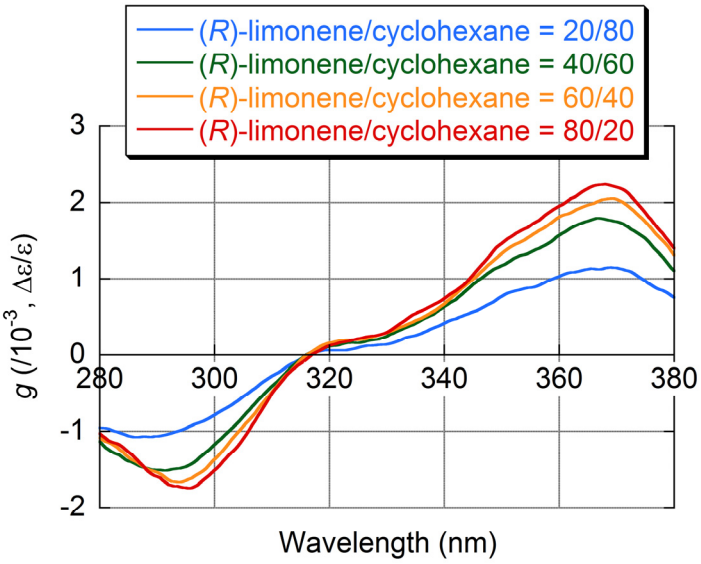

Figure S1. CD spectra of **5(100)** in mixed solvents of (*R*)-limonene and cyclohexane (v/v = 20/80, 40/60, 60/40, and 80/20; 9.35×10^{-2} g/L, path length = 2.0 mm).

4 References

(29) Fields, D. L.; Reynolds, D. D.; Miller, J. B. Preparation of Acetoxybenzyl Bromides. *J. Org. Chem.* **1964**, *29*, 2640-2647.

(30) Krimen, L. I. Acetic Formic Anhydride. *Org. Synth.* **1970**, *50*, 1-3.

(31) Ito, Y.; Ihara, E.; Uesaka, T.; Murakami, M. Synthesis of Novel Thermotropic Liquid-Crystalline Poly(2,3-Quinoxaline)s. *Macromolecules* **1992**, *25*, 6711-6713.

(32) Yamamoto, T.; Yamada, T.; Nagata, Y.; Suginome, M. High-Molecular-Weight Polyquinoxaline-Based Helically Chiral Phosphine (PQXphos) as Chirality-Switchable, Reusable, and Highly Enantioselective Monodentate Ligand in Catalytic Asymmetric Hydrosilylation of Styrenes. *J. Am. Chem. Soc.* **2010**, *132*, 7899-7901.

(33) Akai, Y.; Yamamoto, T.; Nagata, Y.; Ohmura, T.; Suginome, M. Enhanced Catalyst Activity and Enantioselectivity with Chirality-Switchable Polymer Ligand PQXphos in Pd-Catalyzed Asymmetric Silaborative Cleavage of meso-Methylenecyclopropanes. *J. Am. Chem. Soc.* **2012**, *134*, 11092-11095.

(34) Carmona, E.; Paneque, M.; Poveda, M. L. Synthesis and Characterization of Some New Organometallic Complexes of Nickel(II) Containing Trimethylphosphine. *Polyhedron* **1989**, *8*, 285-291.

5 UV-vis and CD Spectra of New Compounds

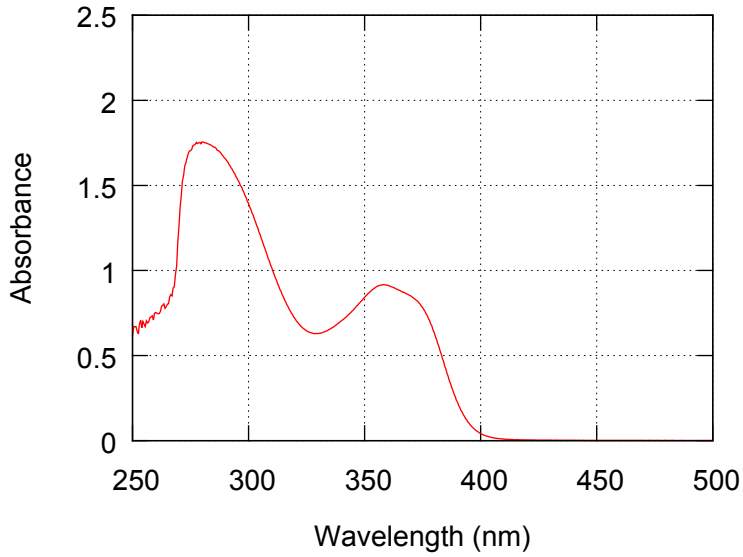

Figure S2. UV-vis absorption spectrum of **1(40)** in α-PIN (1.54×10^{-1} g/L, path length = 2.0 mm).

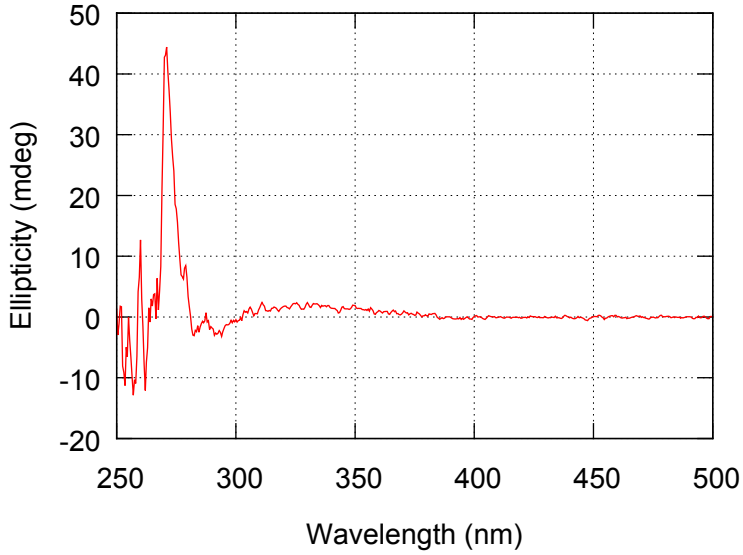

Figure S3. CD spectrum of **1(40)** in α-PIN (1.54×10^{-1} g/L, path length = 2.0 mm).

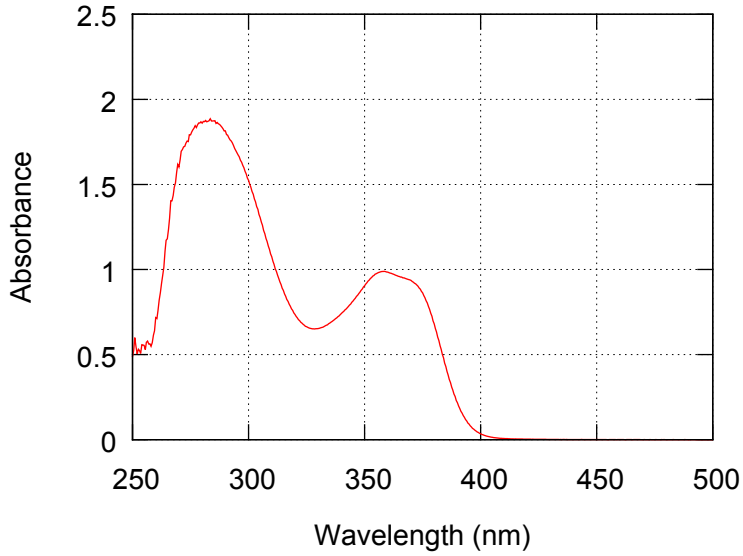

Figure S4. UV-vis absorption spectrum of **1(40)** in (*R*)-limonene (1.54×10^{-1} g/L, path length = 2.0 mm).

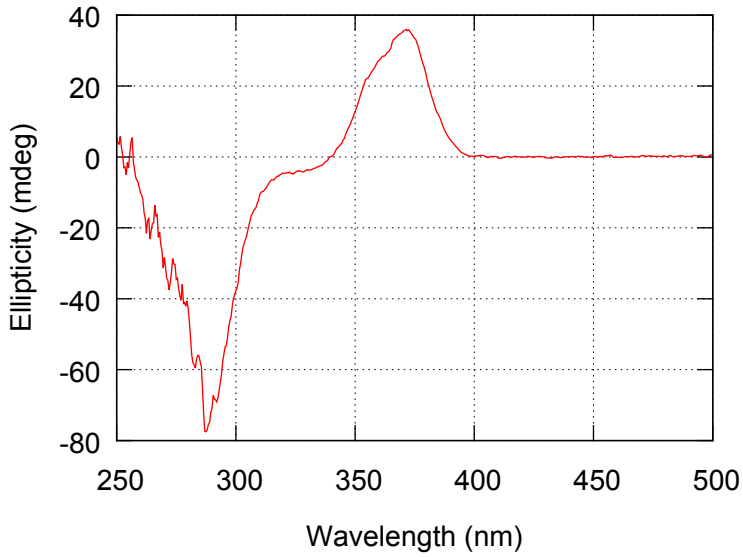

Figure S5. CD spectrum of **1(40)** in (*R*)-limonene (1.54×10^{-1} g/L, path length = 2.0 mm).

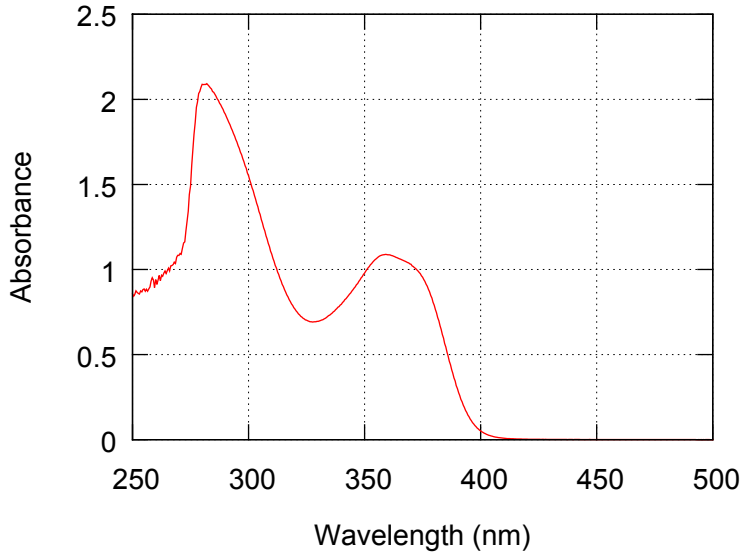

Figure S6. UV-vis absorption spectrum of **2(40)** in (*S*)-CMB (1.90×10^{-1} g/L, path length = 2.0 mm).

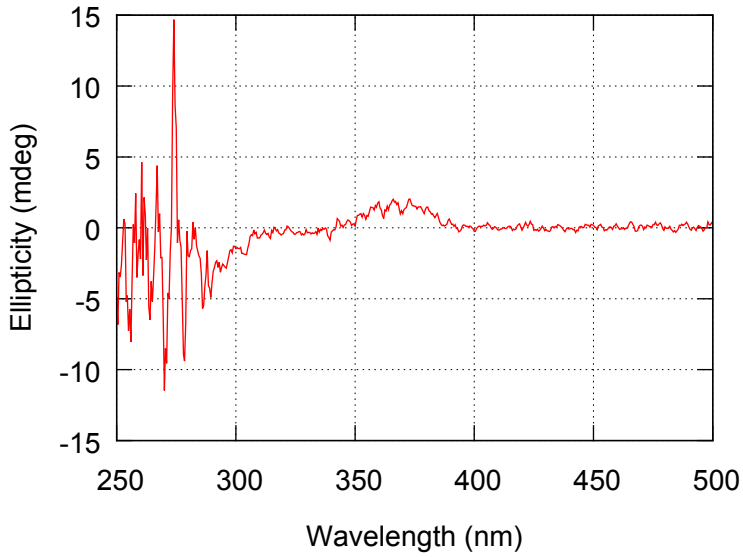

Figure S7. CD spectrum of **2(40)** in (*S*)-CMB (1.90×10^{-1} g/L, path length = 2.0 mm).

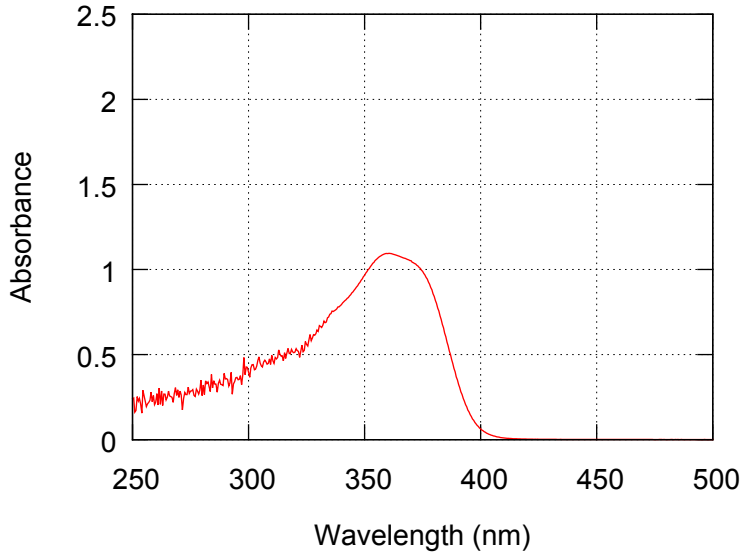

Figure S8. UV-vis absorption spectrum of **2(40)** in (*S*)-CIT (1.91×10^{-1} g/L, path length = 2.0 mm).

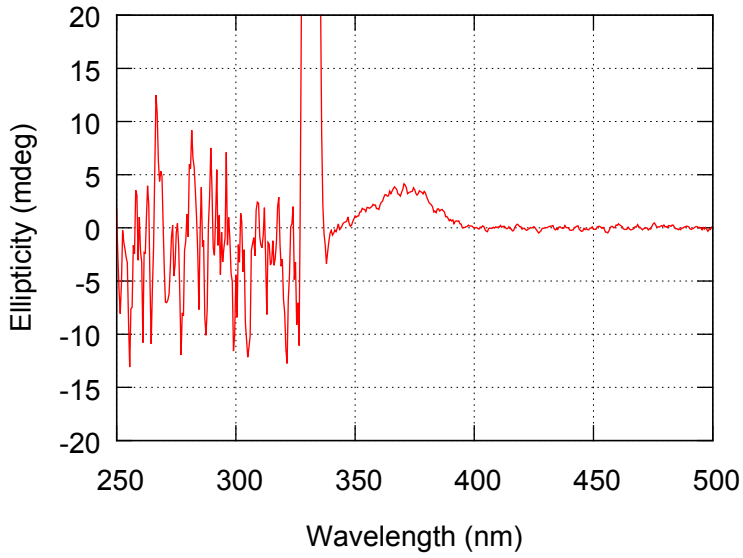

Figure S9. CD spectrum of **2(40)** in (*S*)-CIT (1.91×10^{-1} g/L, path length = 2.0 mm).

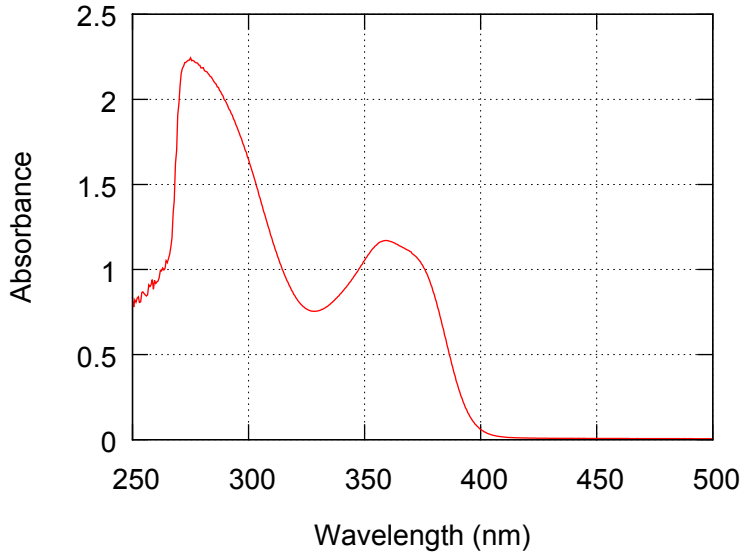

Figure S10. UV-vis absorption spectrum of **2(40)** in α-PIN (1.91×10^{-1} g/L, path length = 2.0 mm).

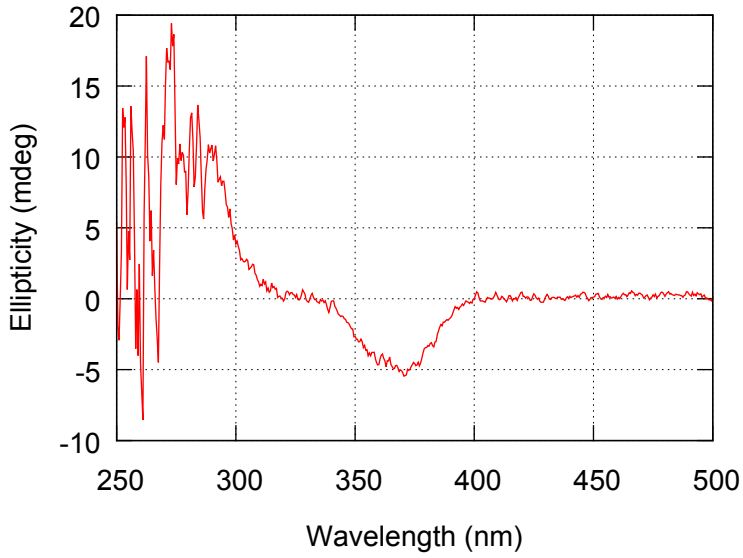

Figure S11. CD spectrum of **2(40)** in α-PIN (1.91×10^{-1} g/L, path length = 2.0 mm).

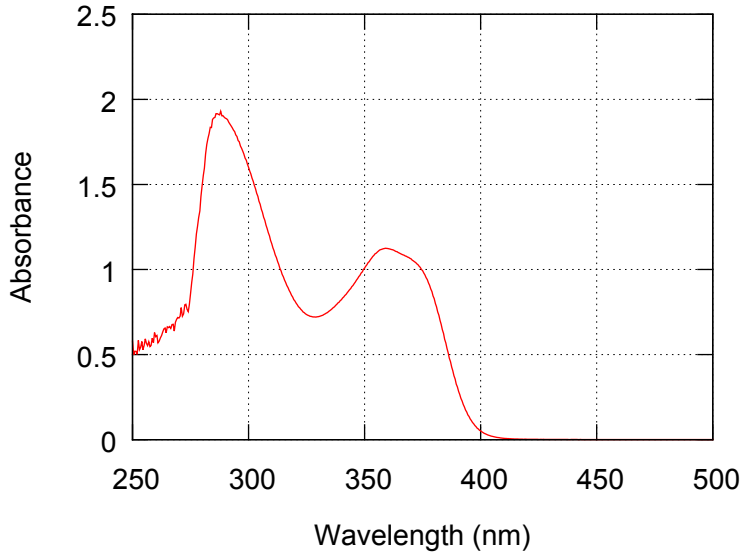

Figure S12. UV-vis absorption spectrum of **2(40)** in β-PIN (1.96×10^{-1} g/L, path length = 2.0 mm).

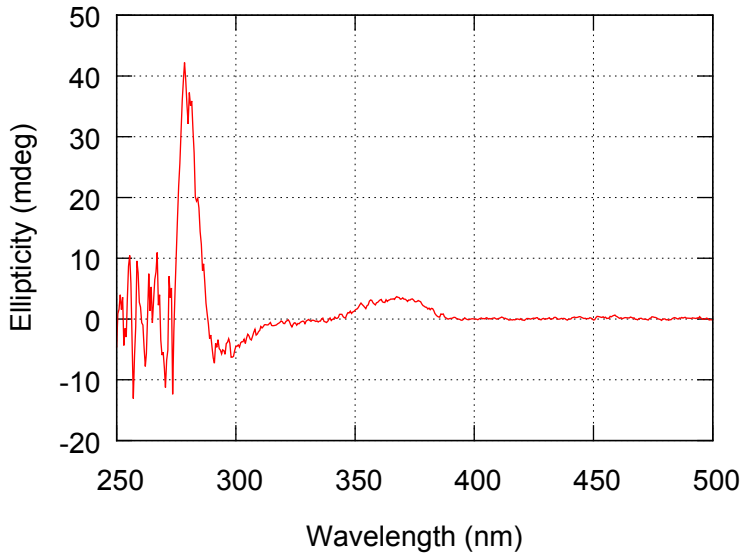

Figure S13. CD spectrum of **2(40)** in β-PIN (1.96×10^{-1} g/L, path length = 2.0 mm).

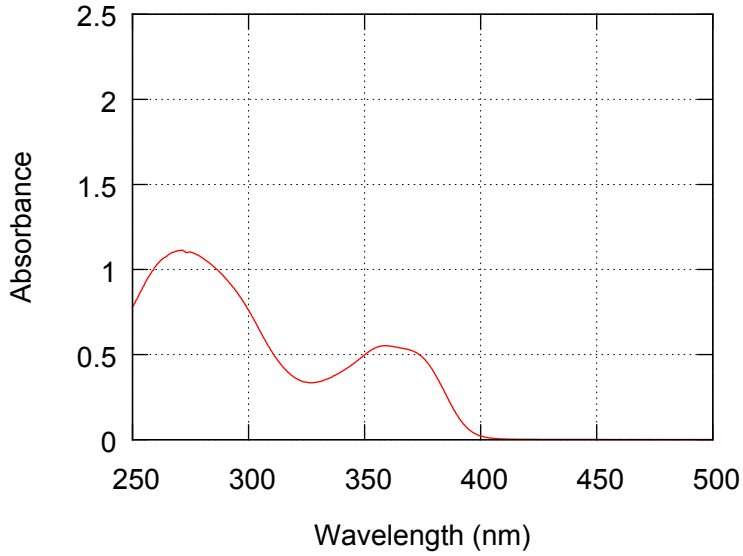

Figure S14. UV-vis absorption spectrum of **2(40)** in (*R*)-MEN (9.55×10^{-2} g/L, path length = 2.0 mm).

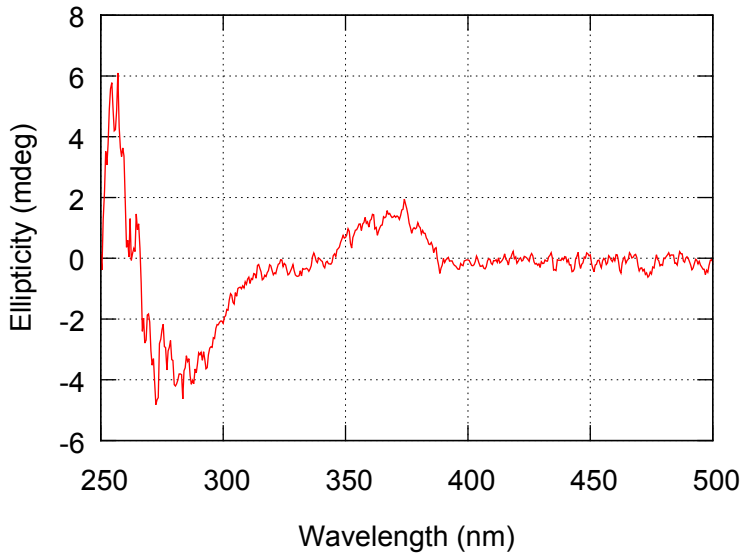

Figure S15. CD spectrum of **2(40)** in (*R*)-MEN (9.55×10^{-2} g/L, path length = 2.0 mm).

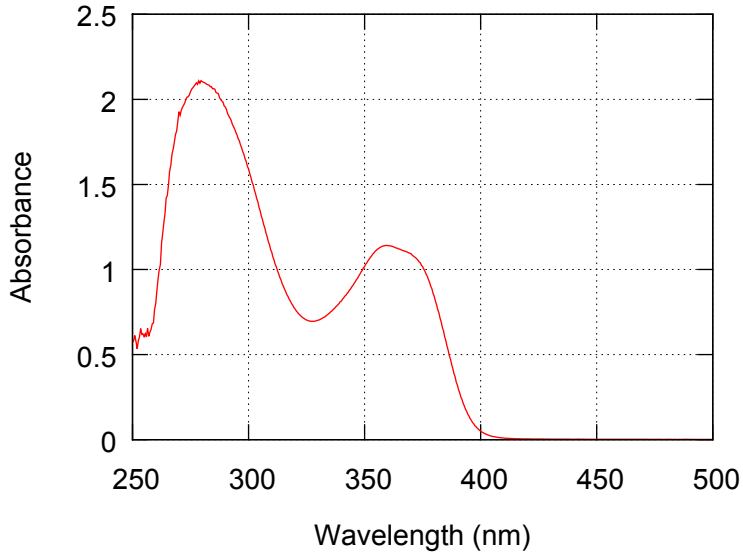

Figure S16. UV-vis absorption spectrum of **2(40)** in (*R*)-limonene (1.91×10^{-1} g/L, path length = 2.0 mm).

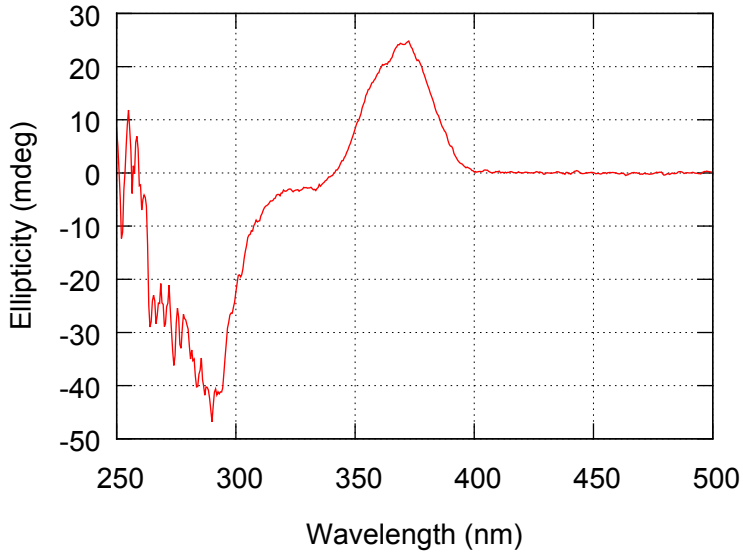

Figure S17. CD spectrum of **2(40)** in (*R*)-limonene (1.91×10^{-1} g/L, path length = 2.0 mm).

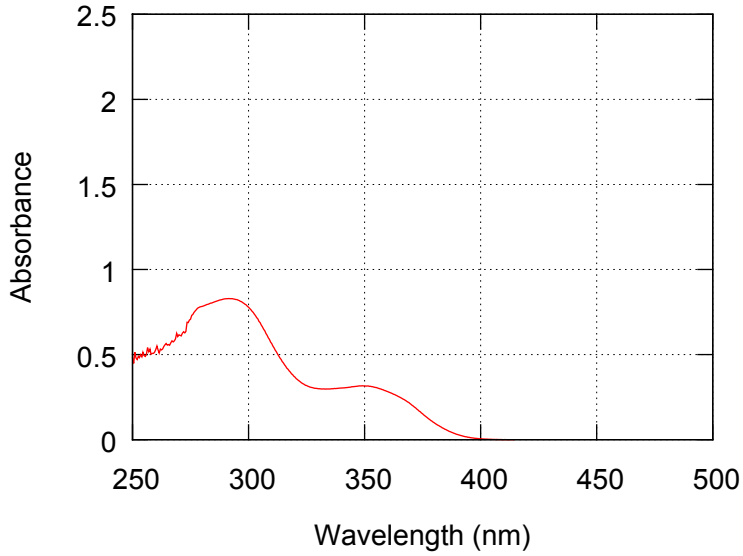

Figure S18. UV-vis absorption spectrum of **3(40)** in (*S*)-CMB (1.45×10^{-1} g/L, path length = 2.0 mm).

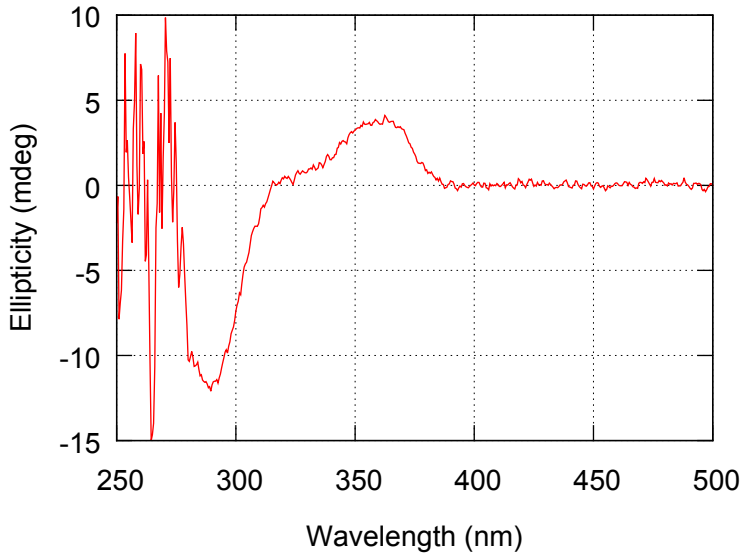

Figure S19. CD spectrum of **3(40)** in (*S*)-CMB (1.45×10^{-1} g/L, path length = 2.0 mm).

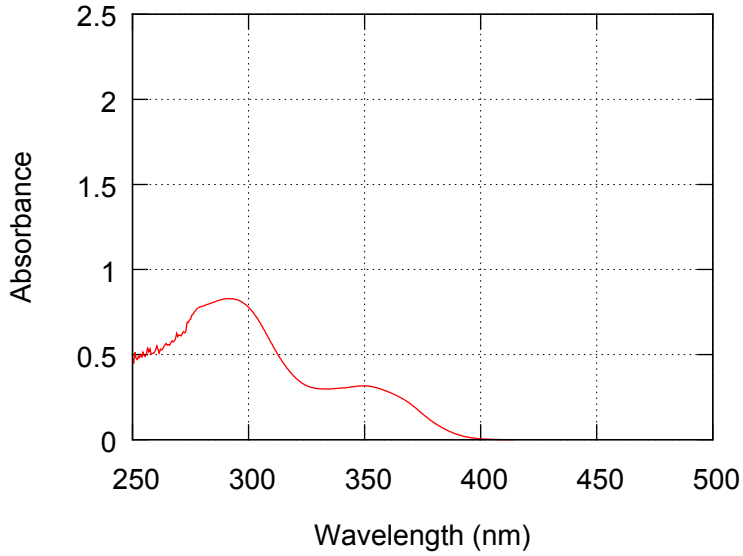

Figure S20. UV-vis absorption spectrum of **3(40)** in (*S*)-HMB (1.45×10^{-1} g/L, path length = 2.0 mm).

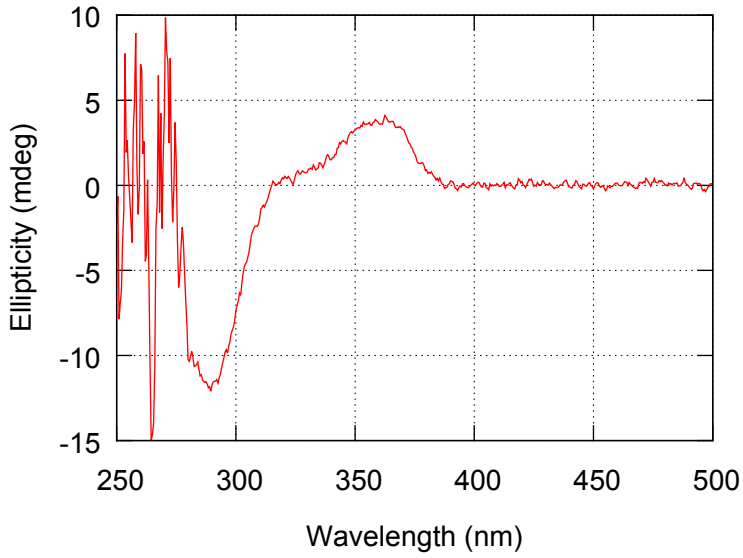

Figure S21. CD spectrum of **3(40)** in (*S*)-HMB (1.45×10^{-1} g/L, path length = 2.0 mm).

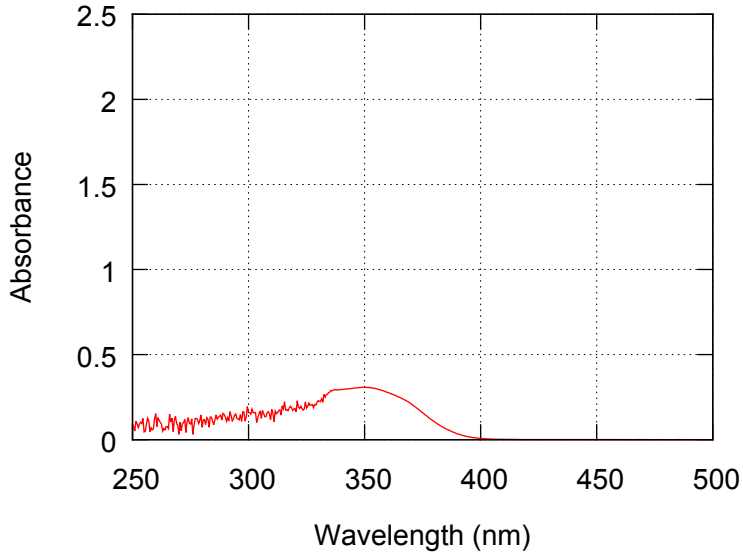

Figure S22. UV-vis absorption spectrum of **3(40)** in (*S*)-CIT (1.45×10^{-1} g/L, path length = 2.0 mm).

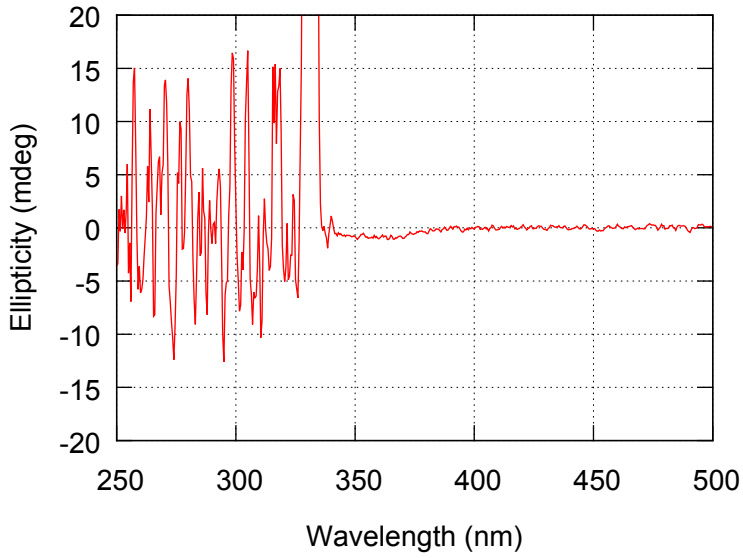

Figure S23. CD spectrum of **3(40)** in (*S*)-CIT (1.45×10^{-1} g/L, path length = 2.0 mm).

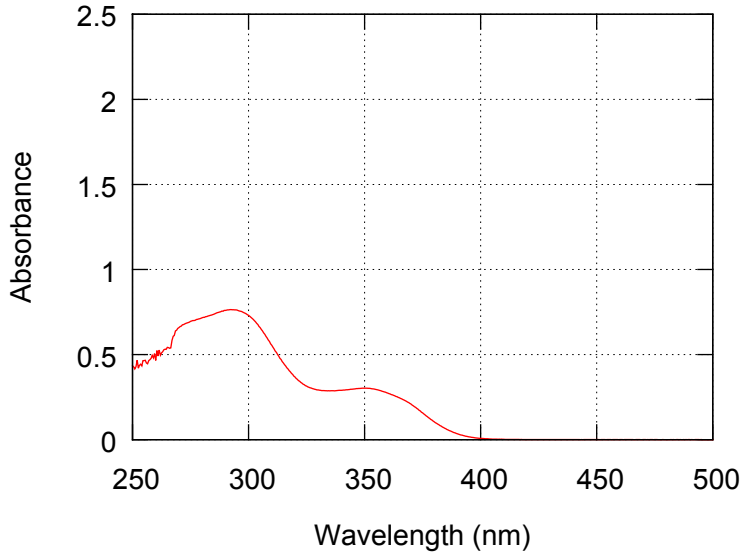

Figure S24. UV-vis absorption spectrum of **3(40)** in α-PIN (1.45×10^{-1} g/L, path length = 2.0 mm).

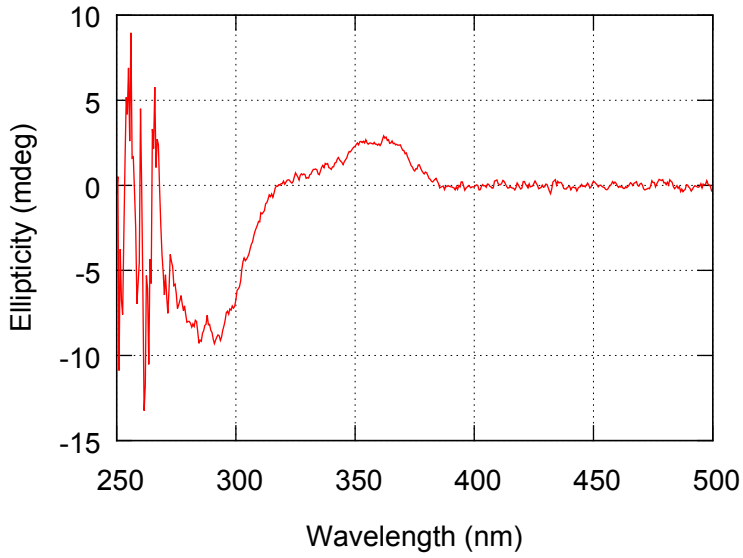

Figure S25. CD spectrum of **3(40)** in α-PIN (1.45×10^{-1} g/L, path length = 2.0 mm).

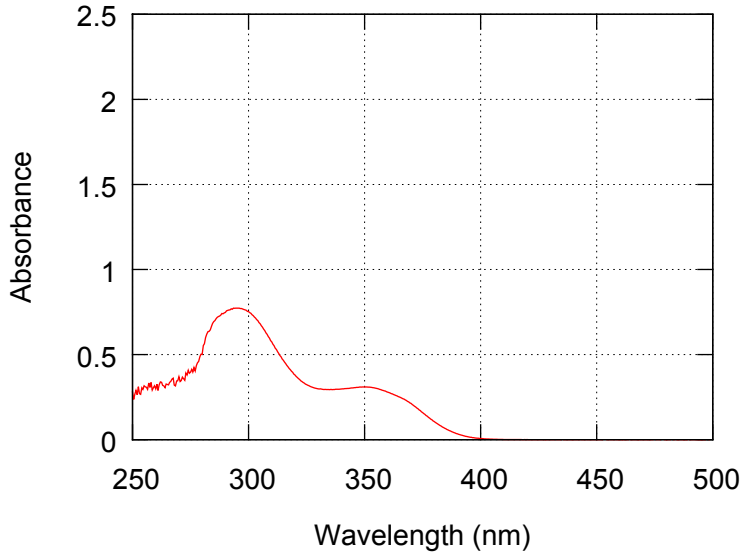

Figure S26. UV-vis absorption spectrum of **3(40)** in β-PIN (1.45×10^{-1} g/L, path length = 2.0 mm).

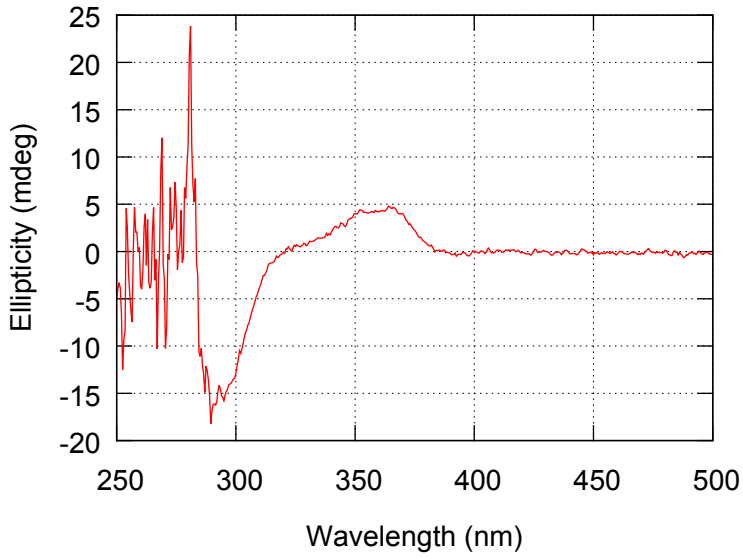

Figure S27. CD spectrum of **3(40)** in β-PIN (1.45×10^{-1} g/L, path length = 2.0 mm).

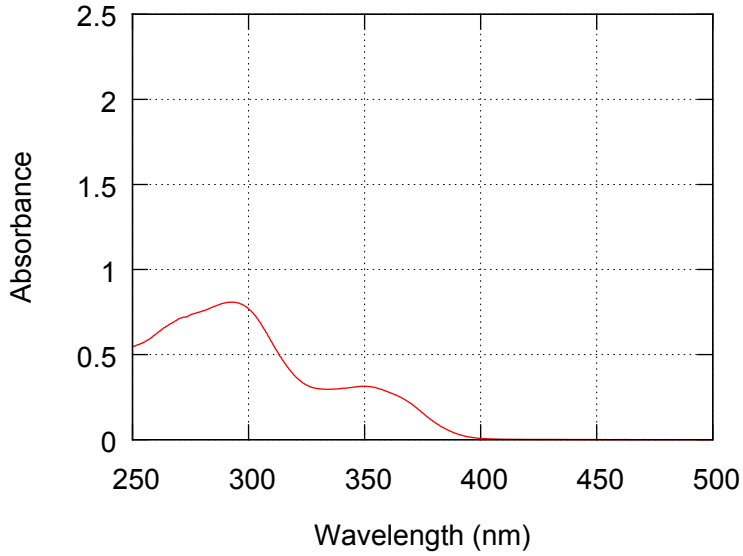

Figure S28. UV-vis absorption spectrum of **3(40)** in (*R*)-MEN (1.45×10^{-1} g/L, path length = 2.0 mm).

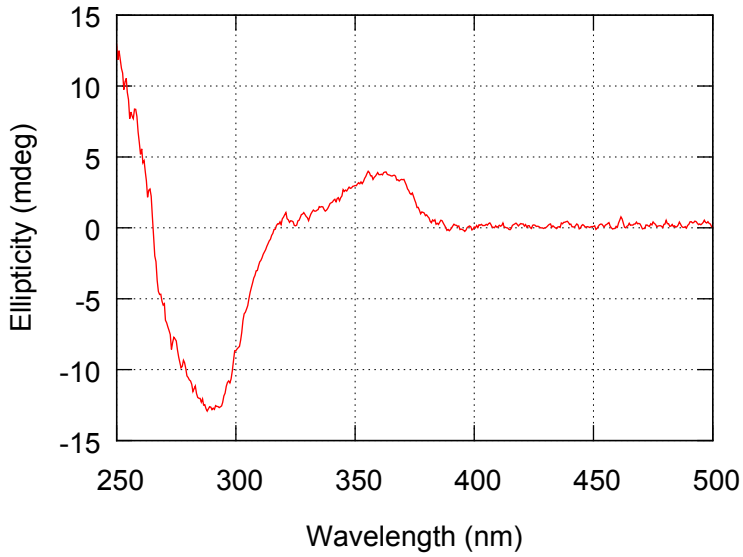

Figure S29. CD spectrum of **3(40)** in (*R*)-MEN (1.45×10^{-1} g/L, path length = 2.0 mm).

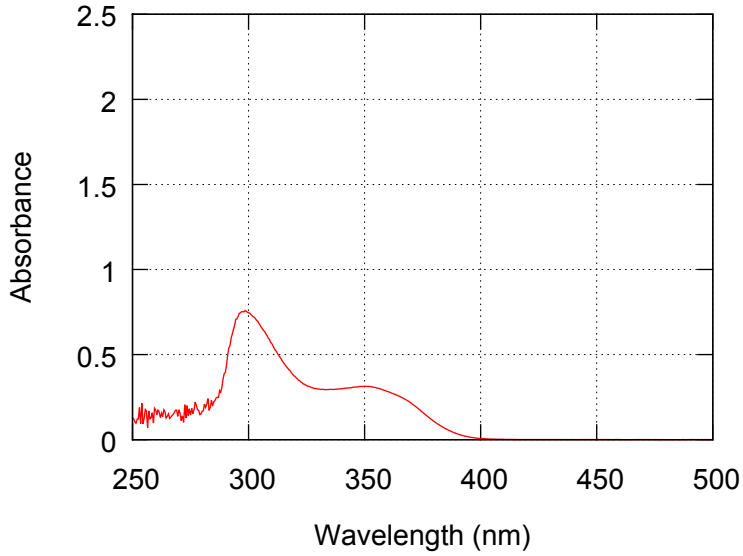

Figure S30. UV-vis absorption spectrum of **3(40)** in (*R*)-limonene (2.90×10^{-2} g/L, path length = 10.0 mm).

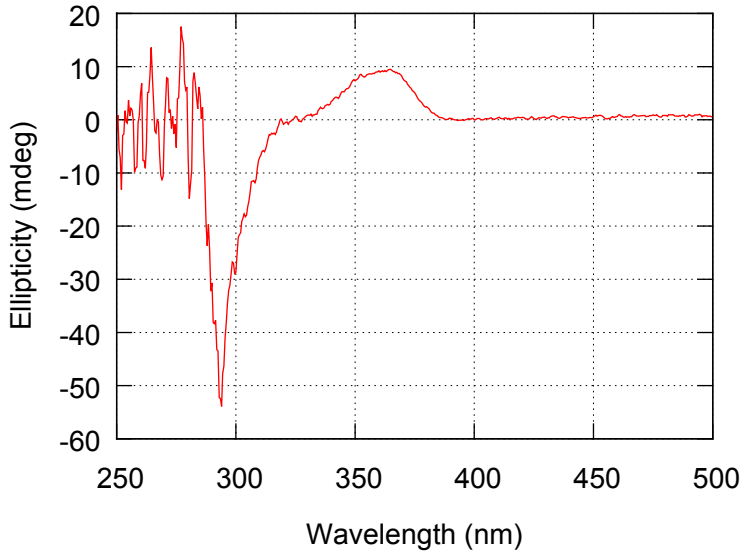

Figure S31. CD spectrum of **3(40)** in (*R*)-limonene (2.90×10^{-2} g/L, path length = 10.0 mm).

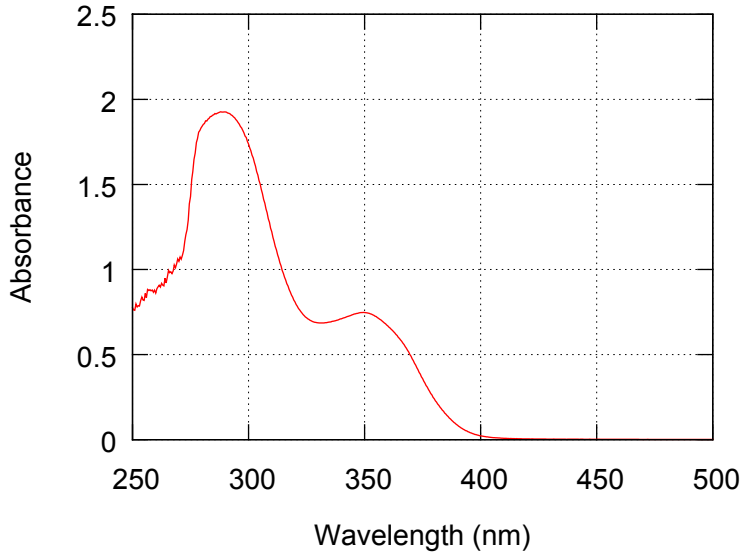

Figure S32. UV-vis absorption spectrum of **4(40)** in (*S*)-CMB (1.22×10^{-1} g/L, path length = 2.0 mm).

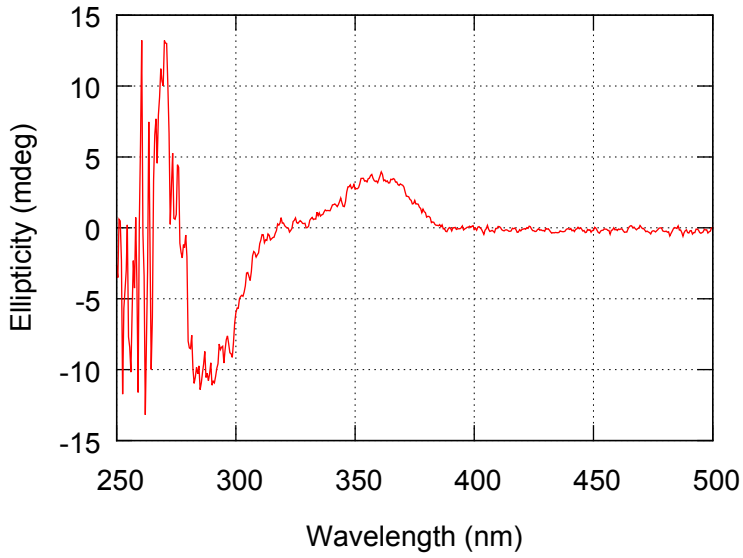

Figure S33. CD spectrum of **4(40)** in (*S*)-CMB (1.22×10^{-1} g/L, path length = 2.0 mm).

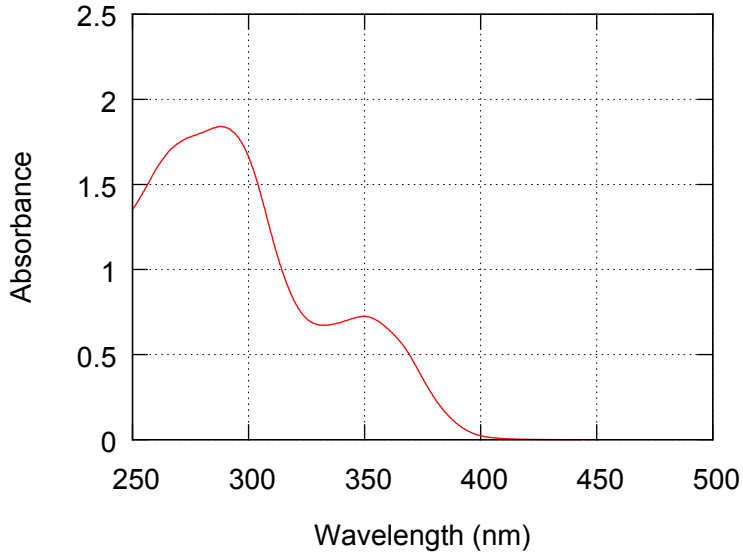

Figure S34. UV-vis absorption spectrum of **4(40)** in (*S*)-HMB (1.22×10^{-1} g/L, path length = 2.0 mm).

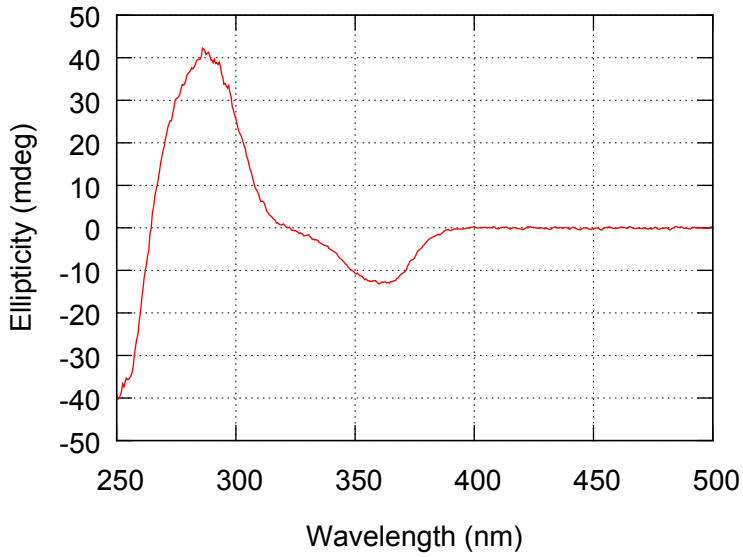

Figure S35. CD spectrum of **4(40)** in (*S*)-HMB (1.22×10^{-1} g/L, path length = 2.0 mm).

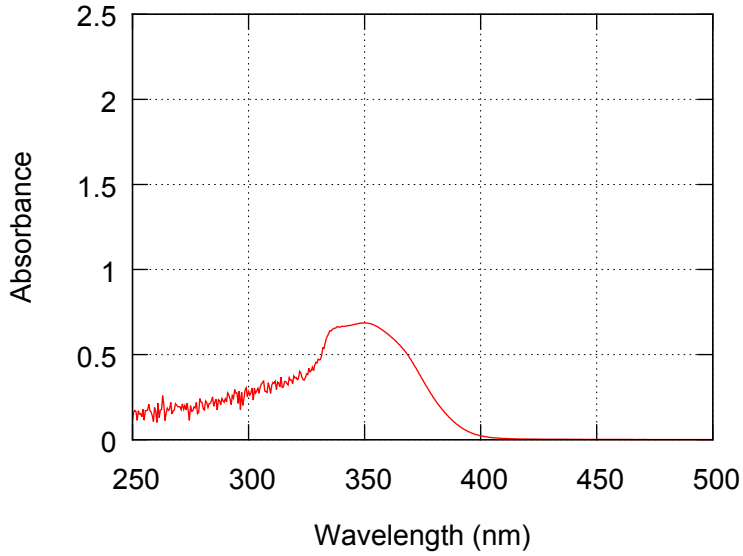

Figure S36. UV-vis absorption spectrum of **4(40)** in (*S*)-CIT (1.22×10^{-1} g/L, path length = 2.0 mm).

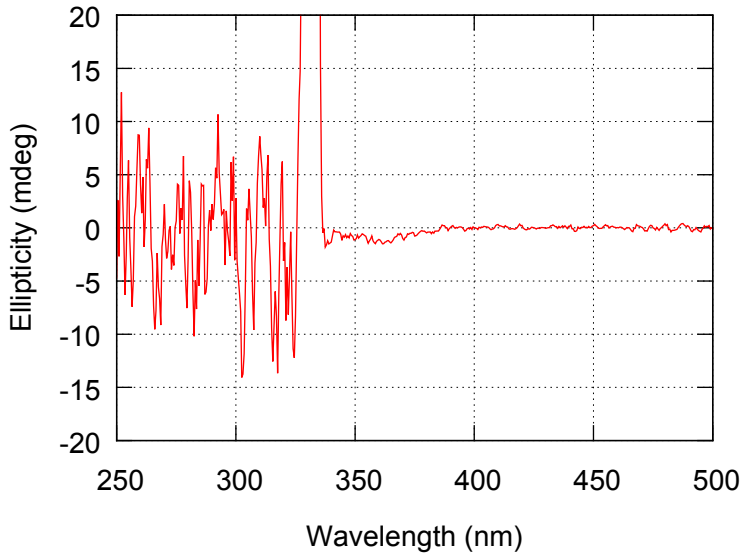

Figure S37. CD spectrum of **4(40)** in (*S*)-CIT (1.22×10^{-1} g/L, path length = 2.0 mm).

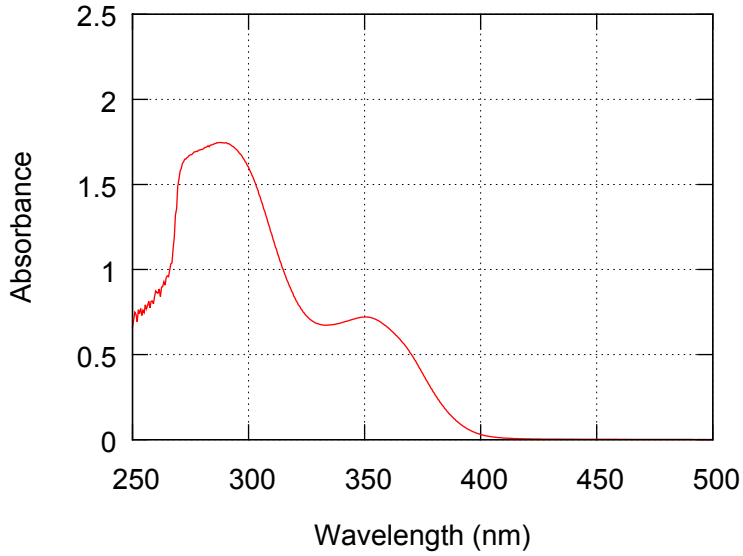

Figure S38. UV-vis absorption spectrum of **4(40)** in α-PIN (1.22×10^{-1} g/L, path length = 2.0 mm).

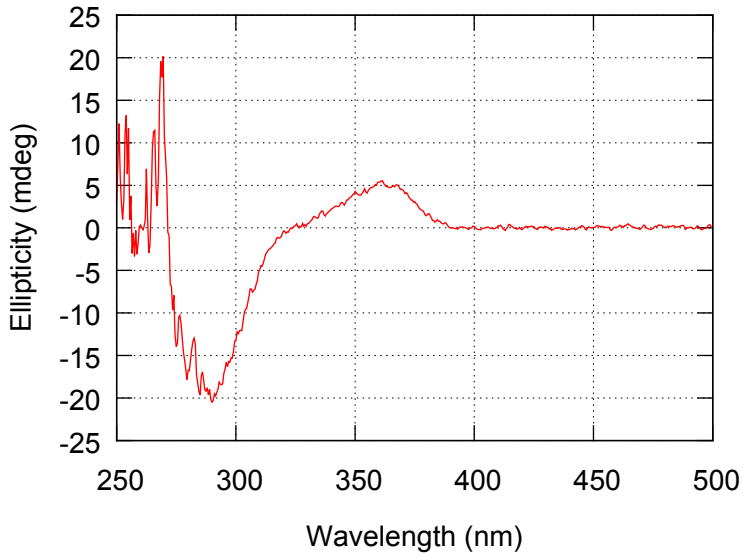

Figure S39. CD spectrum of **4(40)** in α-PIN (1.22×10^{-1} g/L, path length = 2.0 mm).

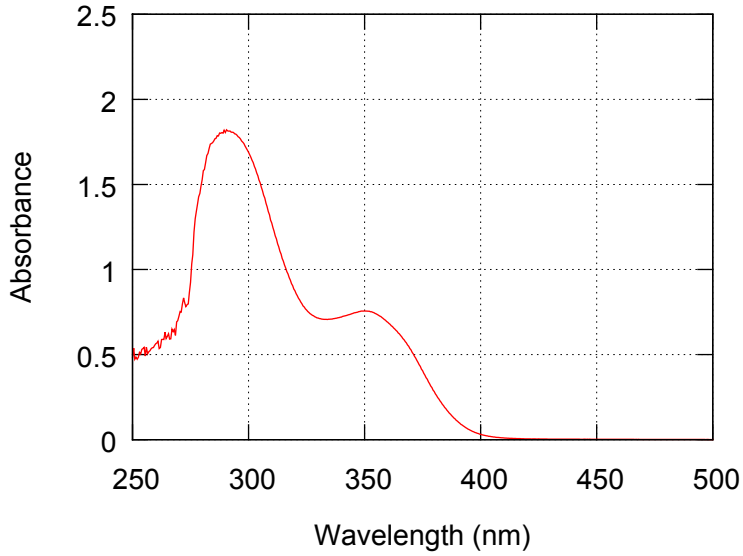

Figure S40. UV-vis absorption spectrum of **4(40)** in β-PIN (1.22×10^{-1} g/L, path length = 2.0 mm).

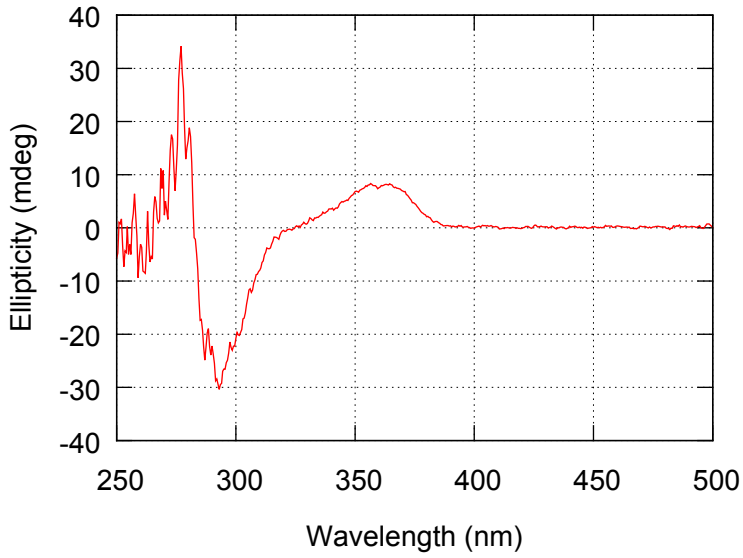

Figure S41. CD spectrum of **4(40)** in β-PIN (1.22×10^{-1} g/L, path length = 2.0 mm).

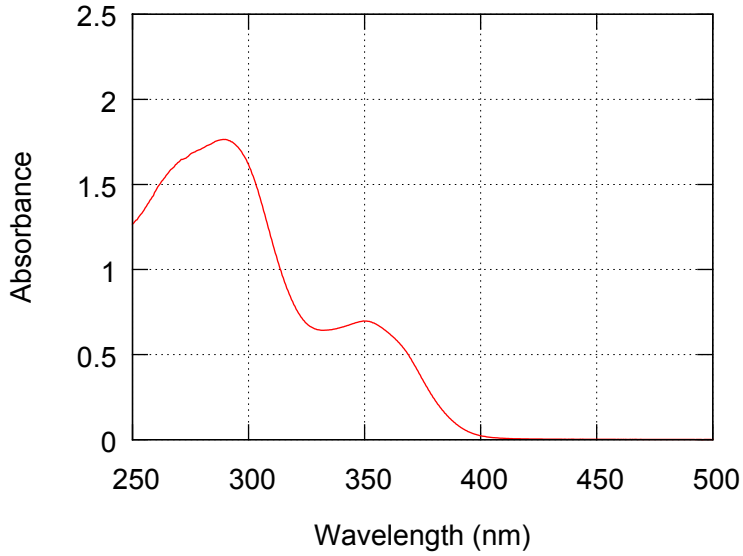

Figure S42. UV-vis absorption spectrum of **4(40)** in (*R*)-MEN (1.22×10^{-1} g/L, path length = 2.0 mm).

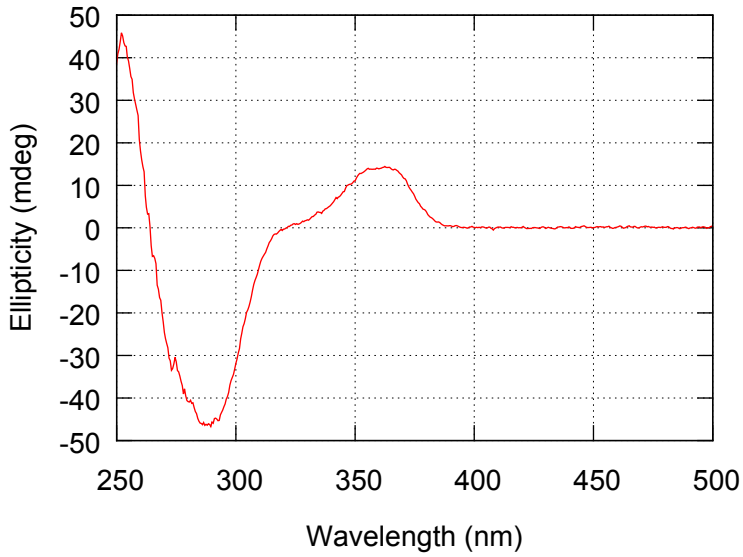

Figure S43. CD spectrum of **4(40)** in (*R*)-MEN (1.22×10^{-1} g/L, path length = 2.0 mm).

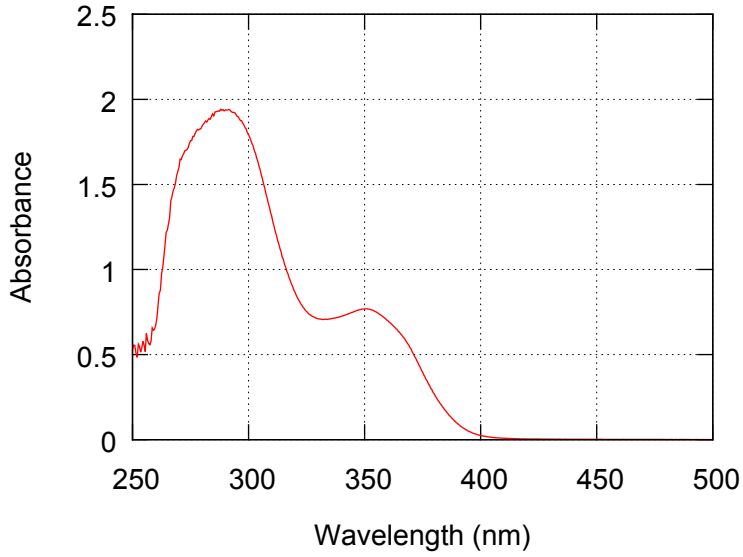

Figure S44. UV-vis absorption spectrum of **4(40)** in (*R*)-limonene (1.22×10^{-1} g/L, path length = 2.0 mm).

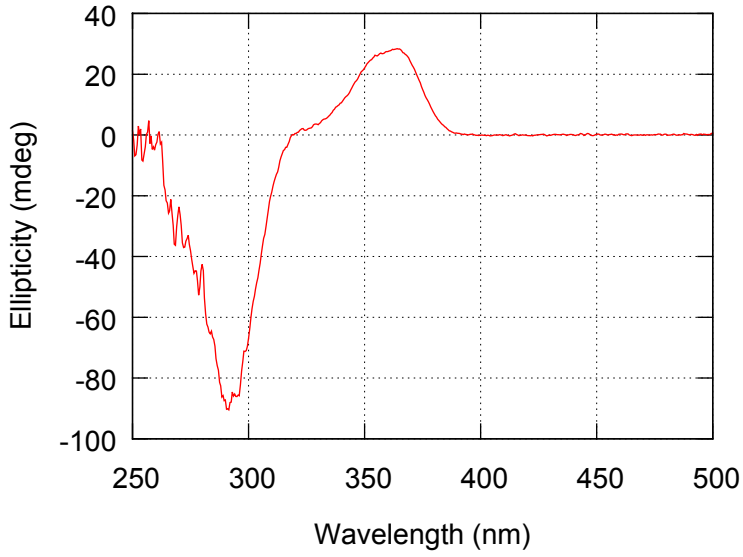

Figure S45. CD spectrum of **4(40)** in (*R*)-limonene (1.22×10^{-1} g/L, path length = 2.0 mm).

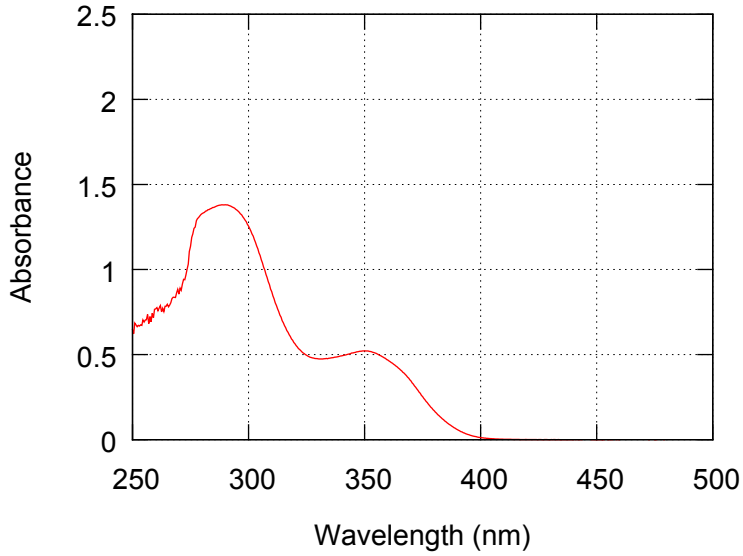

Figure S46. UV-vis absorption spectrum of **5(40)** in (*S*)-CMB (1.28×10^{-1} g/L, path length = 2.0 mm).

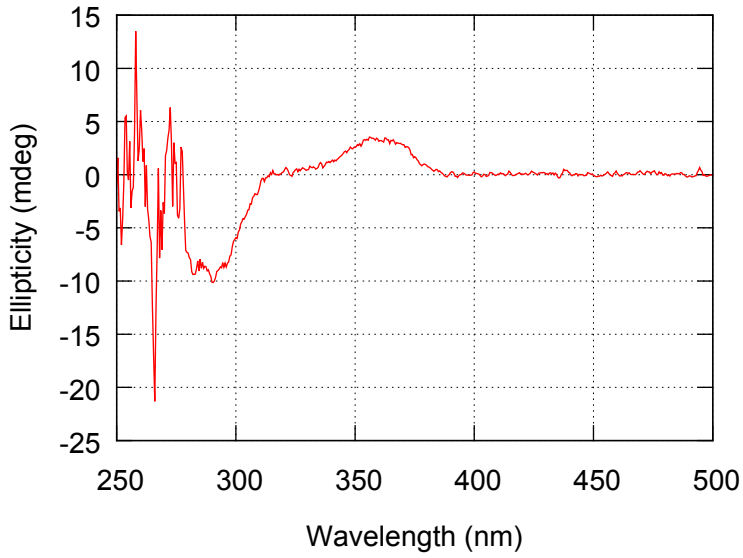

Figure S47. CD spectrum of **5(40)** in (*S*)-CMB (1.28×10^{-1} g/L, path length = 2.0 mm).

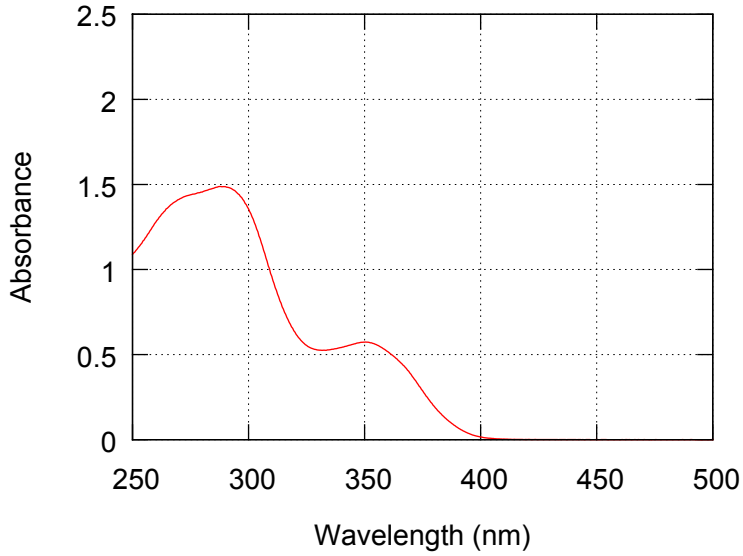

Figure S48. UV-vis absorption spectrum of **5(40)** in (*S*)-HMB (1.28×10^{-1} g/L, path length = 2.0 mm).

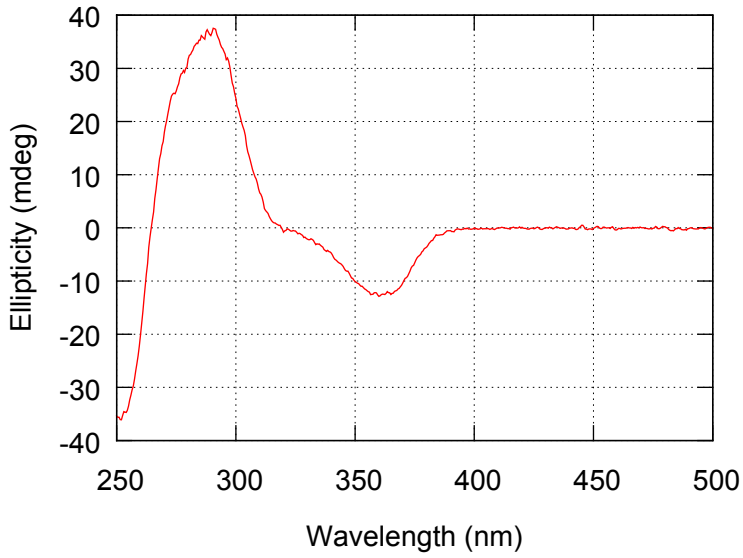

Figure S49. CD spectrum of **5(40)** in (*S*)-HMB (1.28×10^{-1} g/L, path length = 2.0 mm).

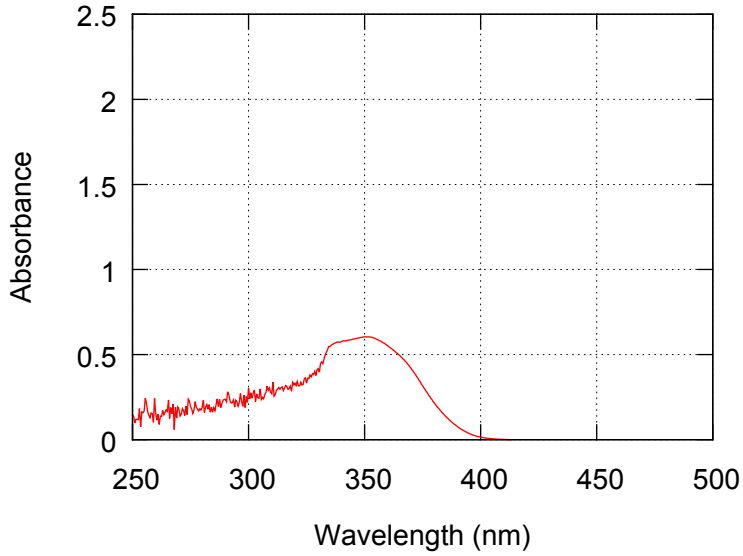

Figure S50. UV-vis absorption spectrum of **5(40)** in (*S*)-CIT (1.28×10^{-1} g/L, path length = 2.0 mm).

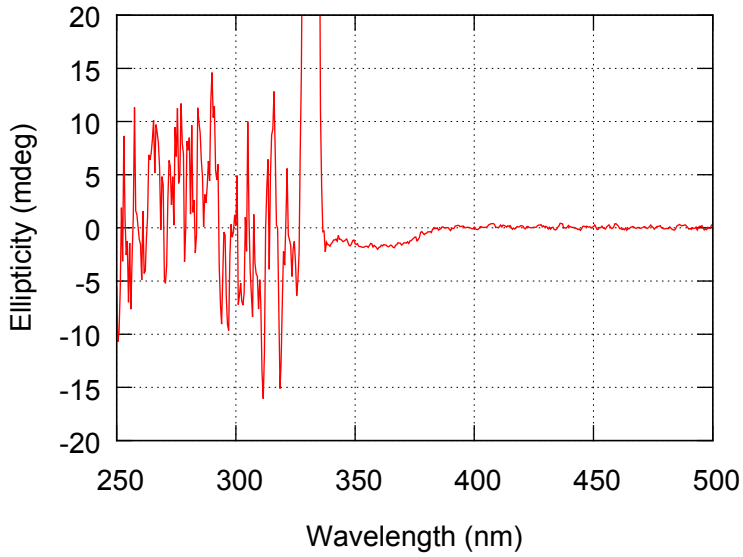

Figure S51. CD spectrum of **5(40)** in (*S*)-CIT (1.28×10^{-1} g/L, path length = 2.0 mm).

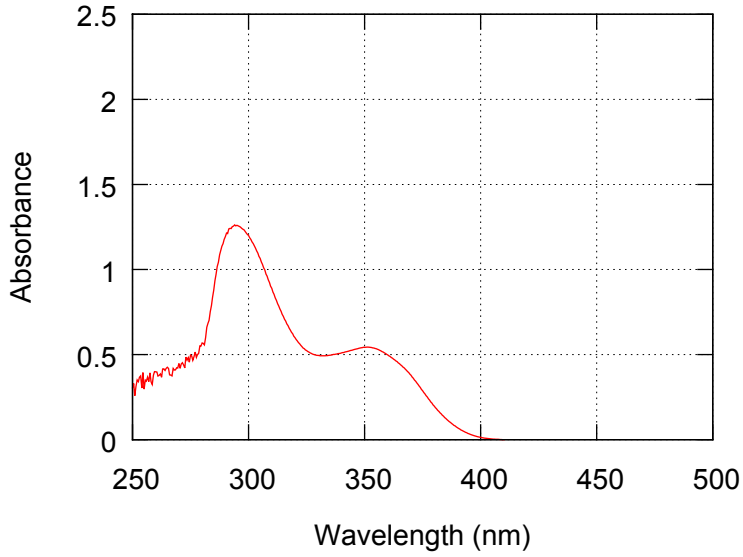

Figure S52. UV-vis absorption spectrum of **5(40)** in α-PIN (1.28×10^{-2} g/L, path length = 10.0 mm).

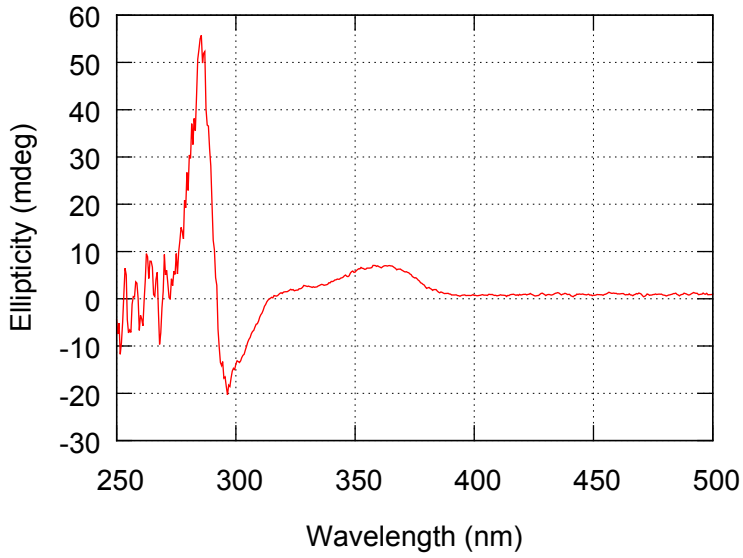

Figure S53. CD spectrum of **5(40)** in α-PIN (1.28×10^{-2} g/L, path length = 10.0 mm).

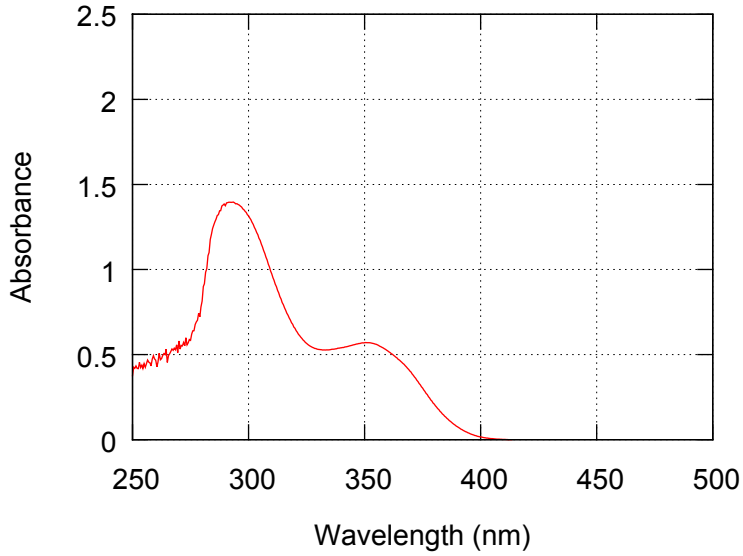

Figure S54. UV-vis absorption spectrum of **5(40)** in β-PIN (1.28×10^{-1} g/L, path length = 2.0 mm).

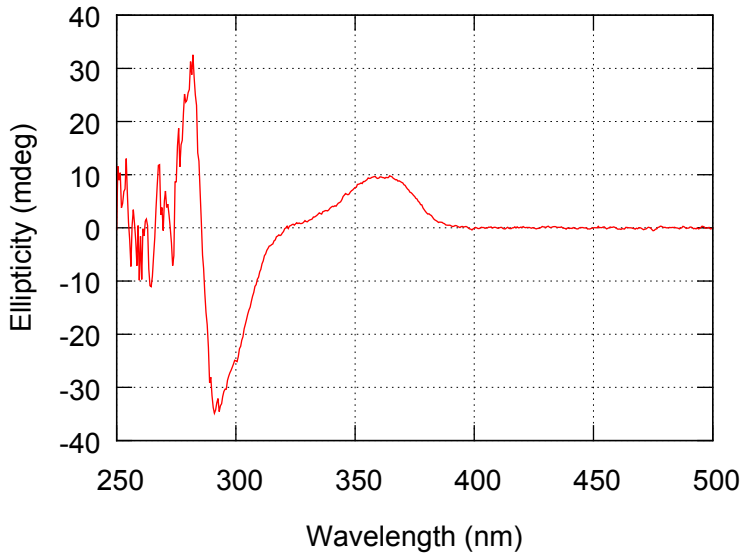

Figure S55. CD spectrum of **5(40)** in β-PIN (1.28×10^{-1} g/L, path length = 2.0 mm).

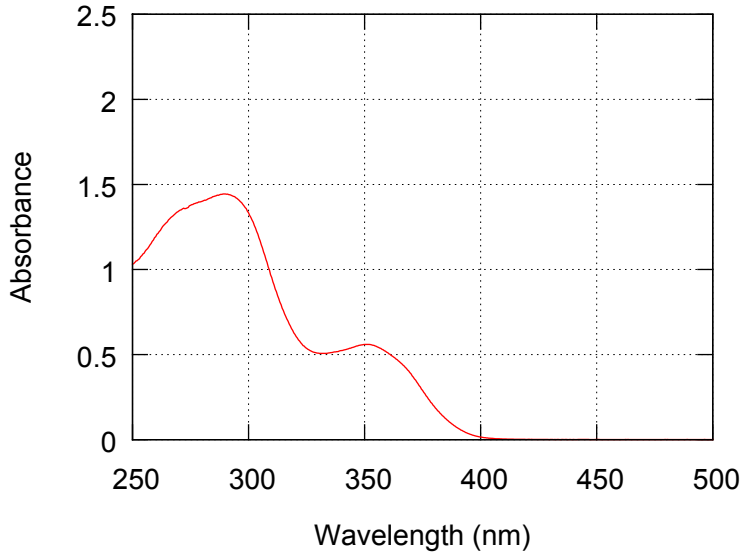

Figure S56. UV-vis absorption spectrum of **5(40)** in (*R*)-MEN (1.28×10^{-1} g/L, path length = 2.0 mm).

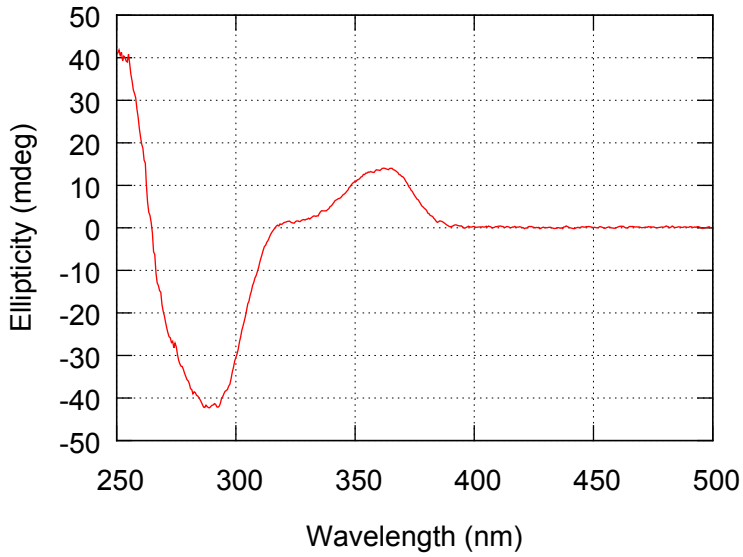

Figure S57. CD spectrum of **5(40)** in (*R*)-MEN (1.28×10^{-1} g/L, path length = 2.0 mm).

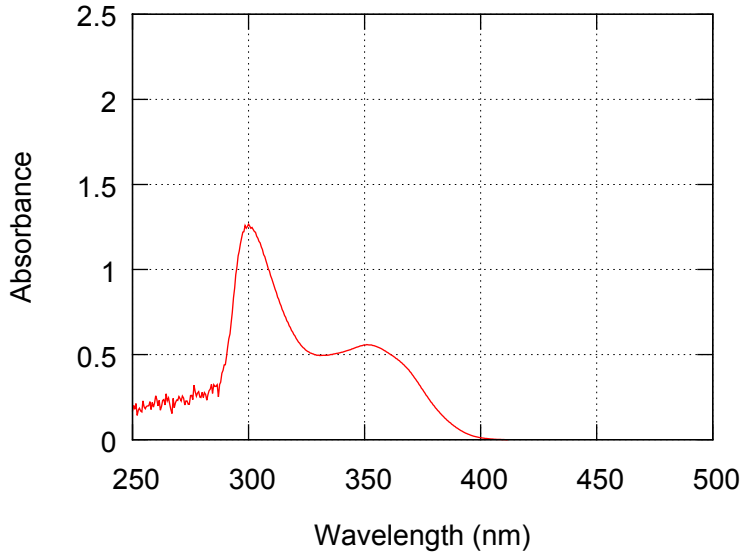

Figure S58. UV-vis absorption spectrum of **5(40)** in (*R*)-limonene (3.00×10^{-2} g/L, path length = 10.0 mm).

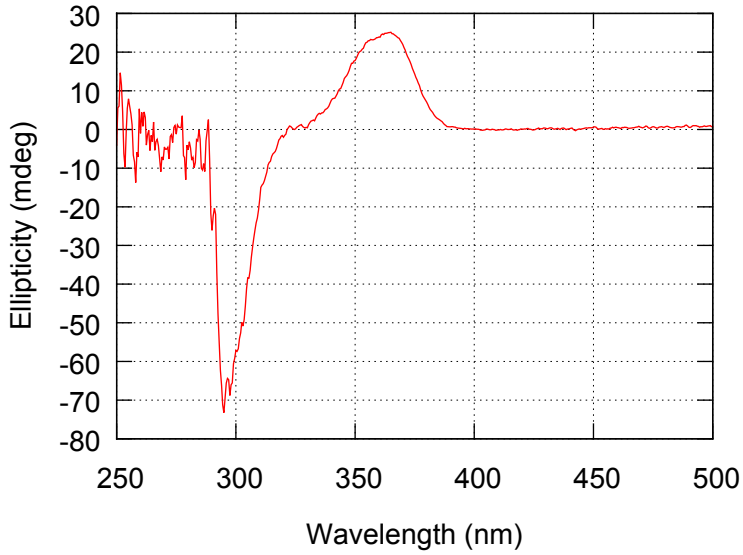

Figure S59. CD spectrum of **5(40)** in (*R*)-limonene (3.00×10^{-2} g/L, path length = 10.0 mm).

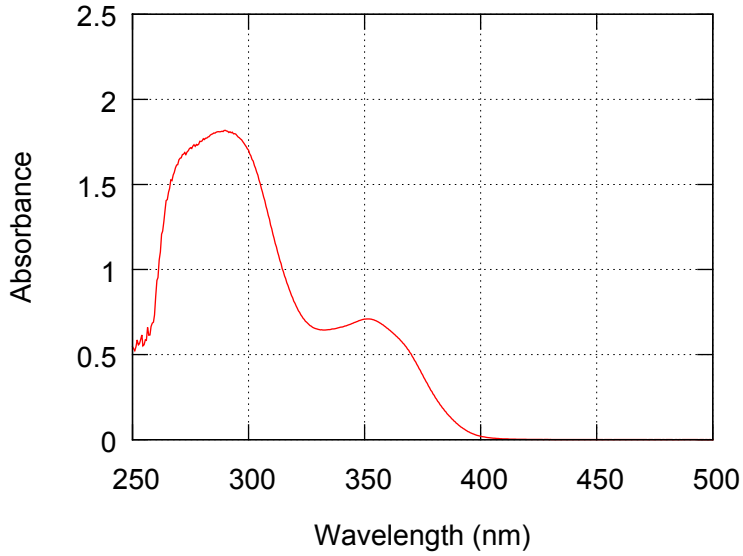

Figure S60. UV-vis absorption spectrum of **5(30)** in (*R*)-limonene (1.88×10^{-1} g/L, path length = 2.0 mm).

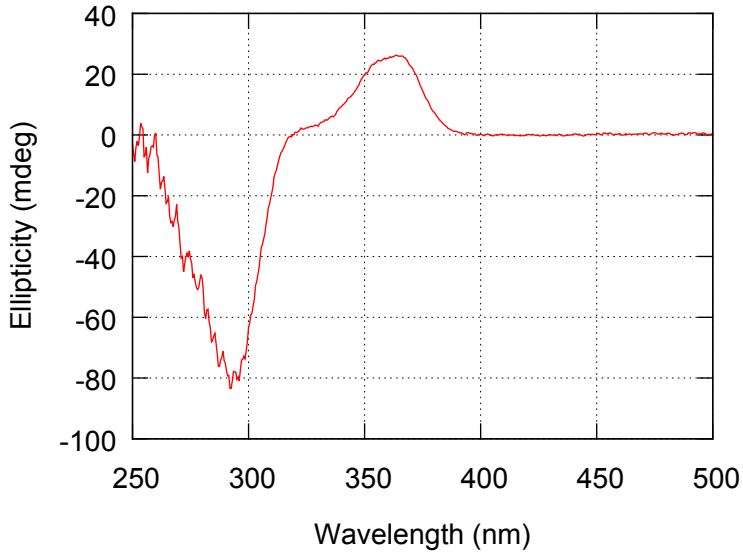

Figure S61. CD spectrum of **5(30)** in (*R*)-limonene (1.88×10^{-1} g/L, path length = 2.0 mm).

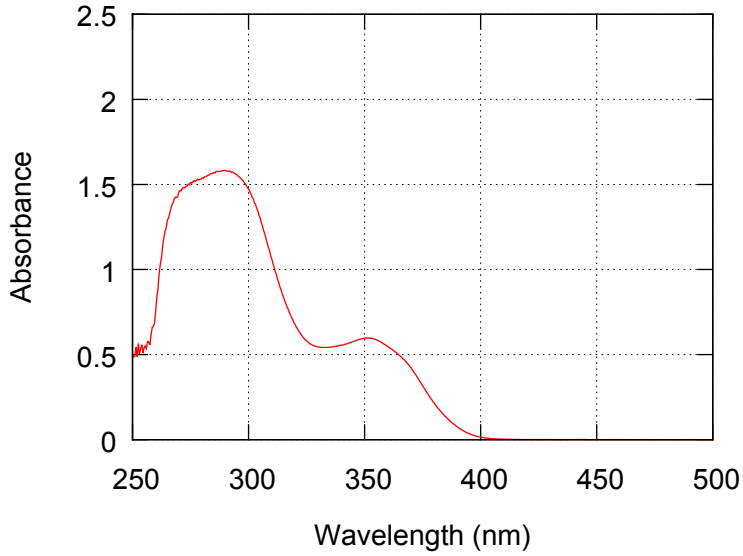

Figure S62. UV-vis absorption spectrum of **5(60)** in (*R*)-limonene (1.48×10^{-1} g/L, path length = 2.0 mm).

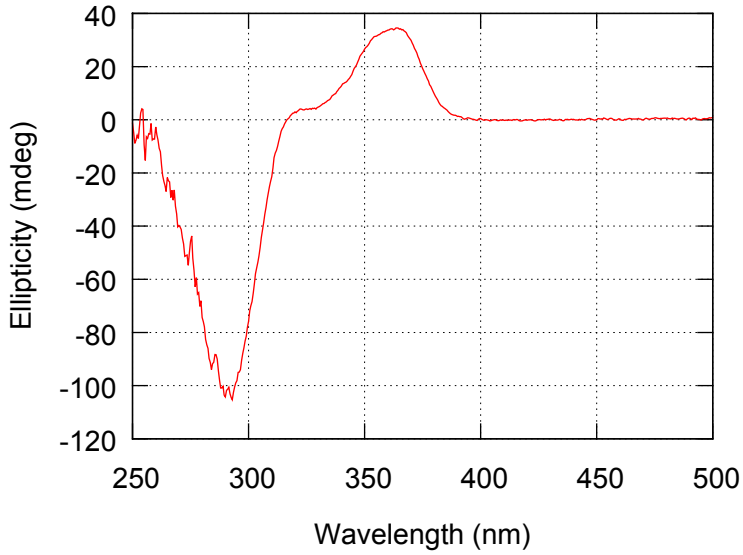

Figure S63. CD spectrum of **5(60)** in (*R*)-limonene (1.48×10^{-1} g/L, path length = 2.0 mm).

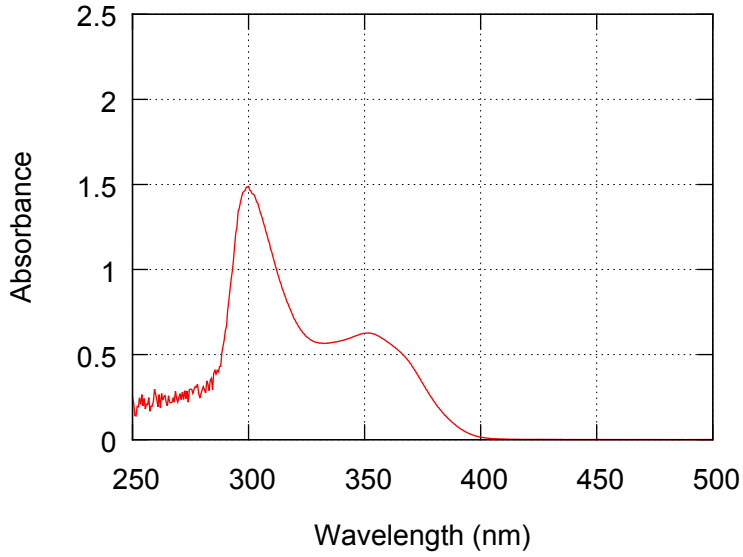

Figure S64. UV-vis absorption spectrum of **5(100)** in (*R*)-limonene (2.54×10^{-2} g/L, path length = 10 mm).

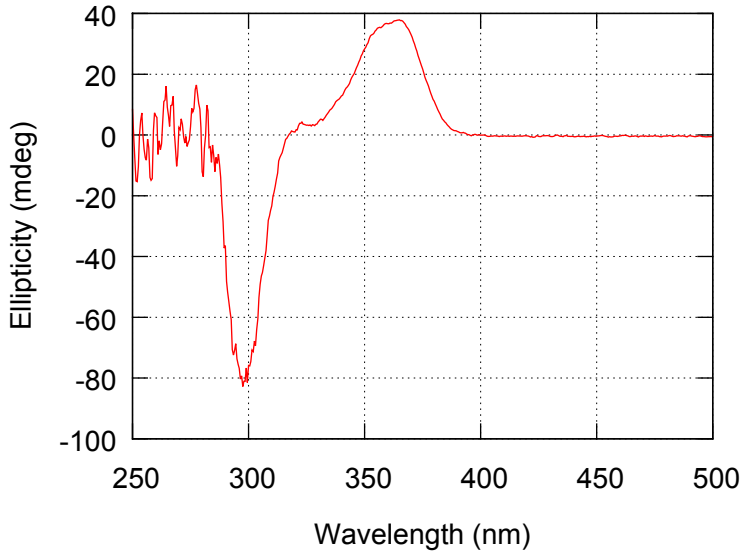

Figure S65. CD spectrum of **5(100)** in (*R*)-limonene (2.54×10^{-2} g/L, path length = 10 mm).

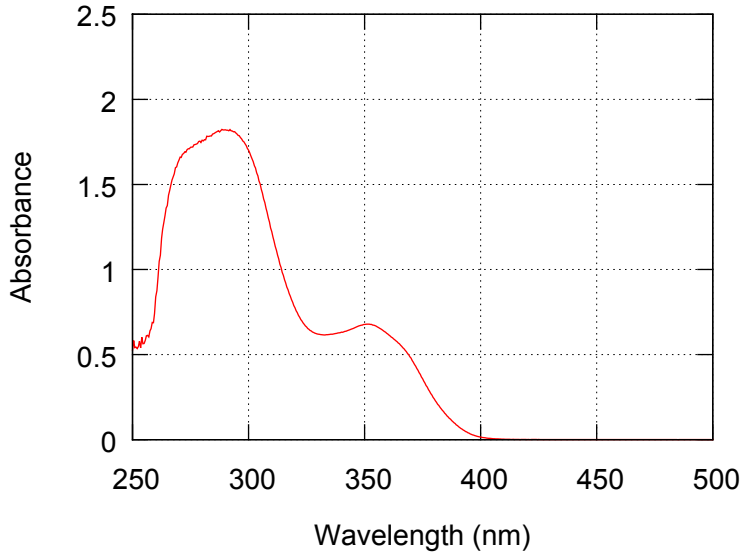

Figure S66. UV-vis absorption spectrum of **5(150)** in (*R*)-limonene (1.88×10^{-1} g/L, path length = 2.0 mm).

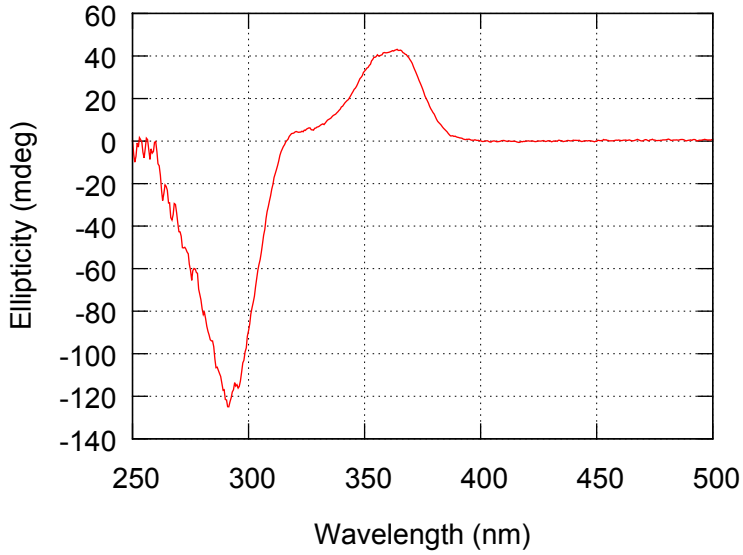

Figure S67. CD spectrum of **5(150)** in (*R*)-limonene (1.88×10^{-1} g/L, path length = 2.0 mm).

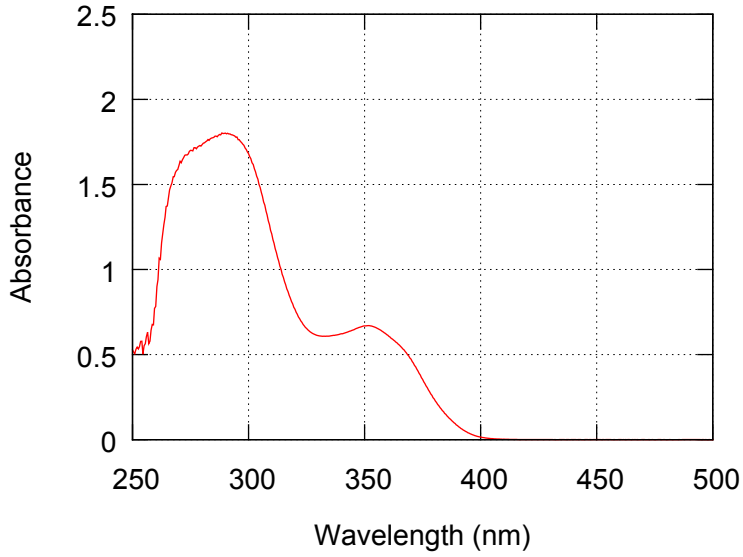

Figure S68. UV-vis absorption spectrum of **5(200)** in (*R*)-limonene (1.42×10^{-1} g/L, path length = 2.0 mm).

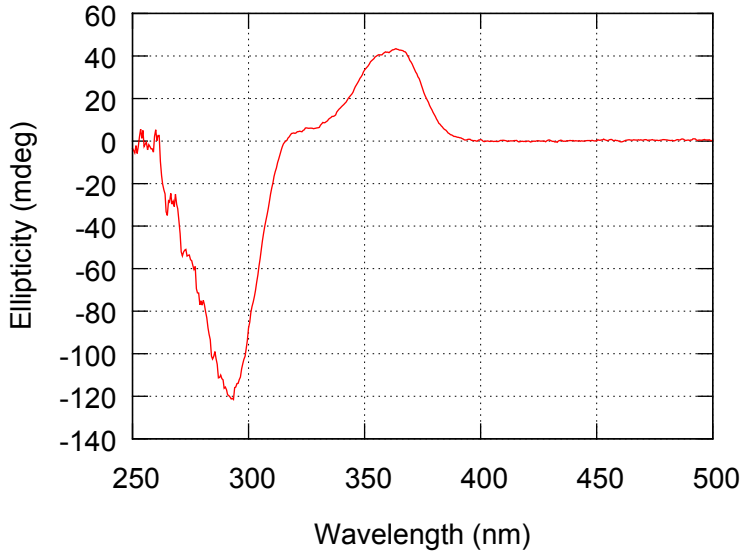

Figure S69. CD spectrum of **5(200)** in (*R*)-limonene (1.42×10^{-1} g/L, path length = 2.0 mm).

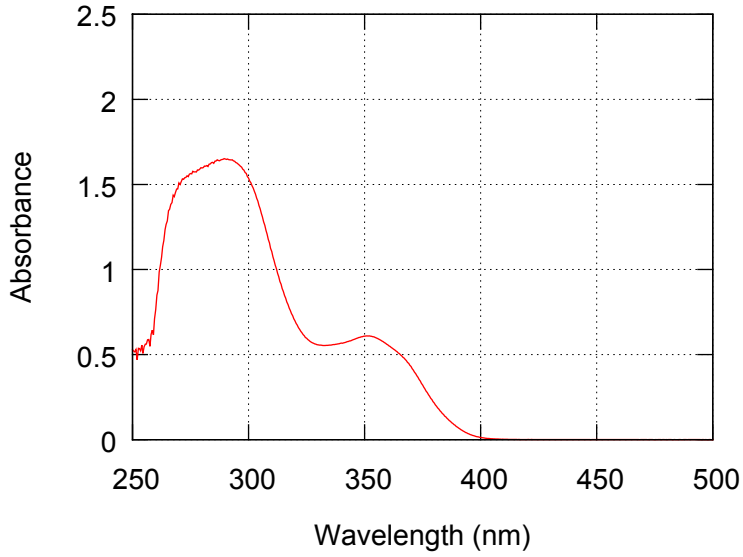

Figure S70. UV-vis absorption spectrum of **5(250)** in (*R*)-limonene (1.70×10^{-1} g/L, path length = 2.0 mm).

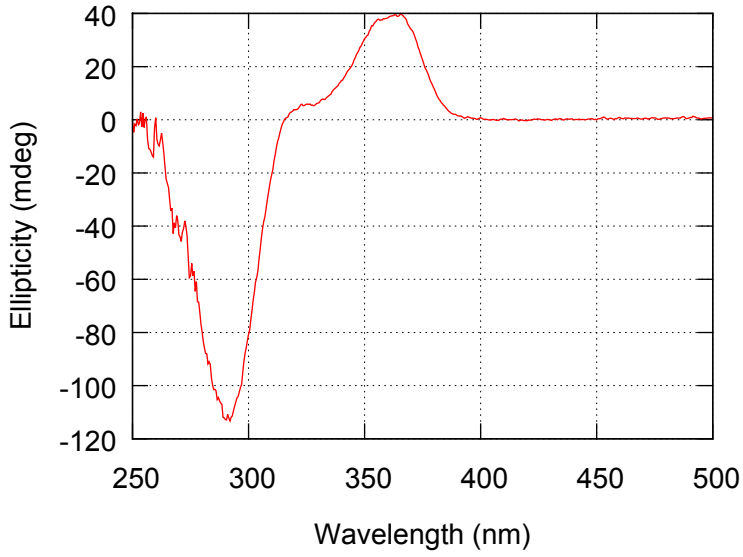

Figure S71. CD spectrum of **5(250)** in (*R*)-limonene (1.70×10^{-1} g/L, path length = 2.0 mm).

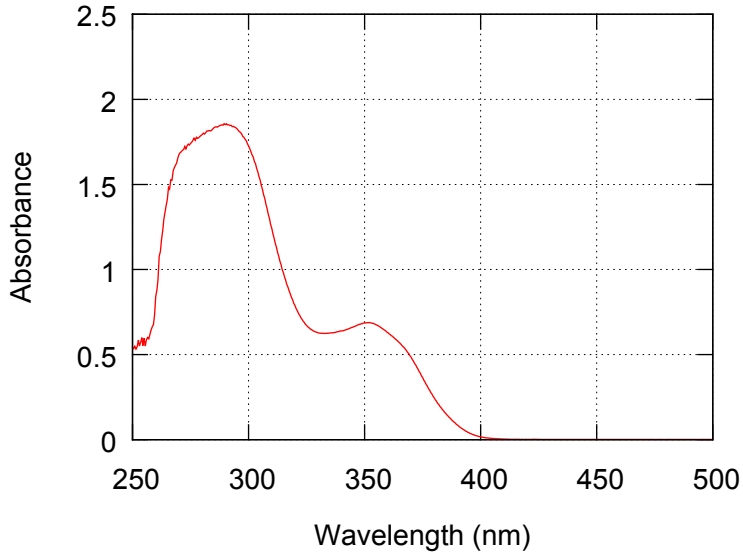

Figure S72. UV-vis absorption spectrum of **5(300)** in (*R*)-limonene (1.52×10^{-1} g/L, path length = 2.0 mm).

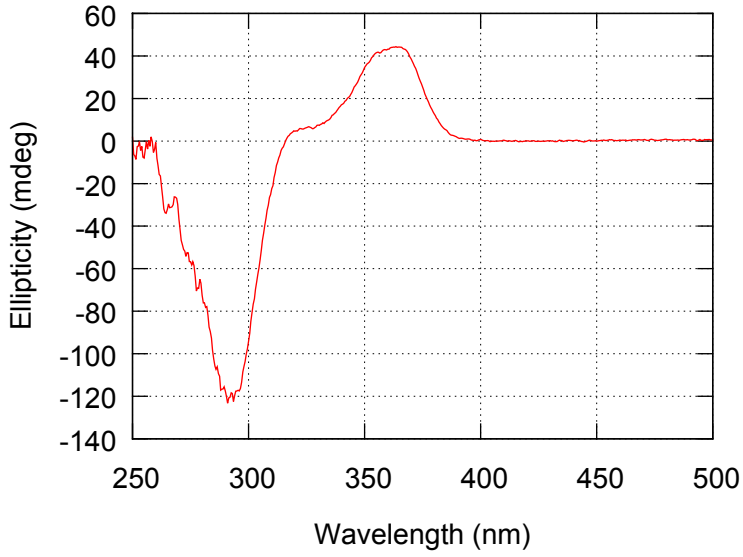

Figure S73. CD spectrum of **5(300)** in (*R*)-limonene (1.52×10^{-1} g/L, path length = 2.0 mm).

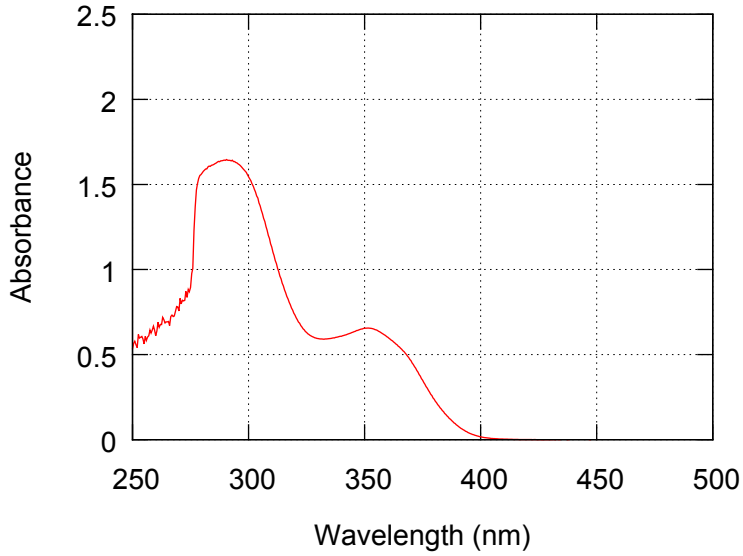

Figure S74. UV-vis absorption spectrum of **5(40)** in (*R*)-limonene (1.40×10^{-1} g/L, path length = 2.0 mm).

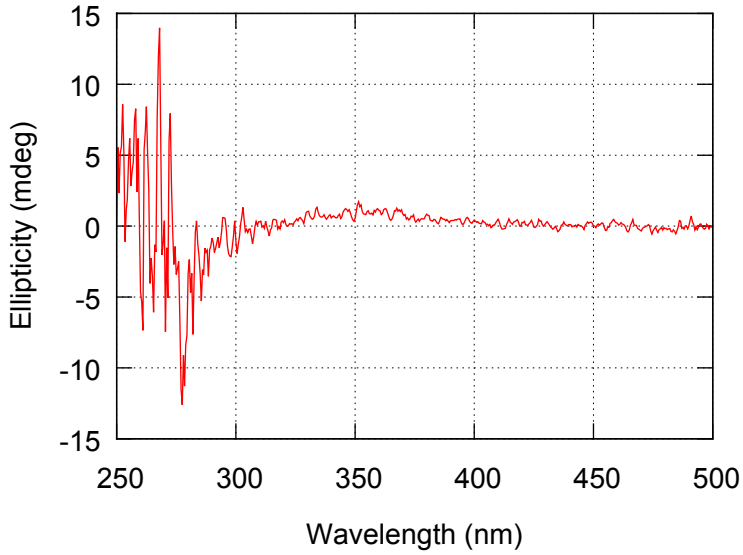

Figure S75. CD spectrum of **5(40)** in (*R*)-limonene (1.40×10^{-1} g/L, path length = 2.0 mm).

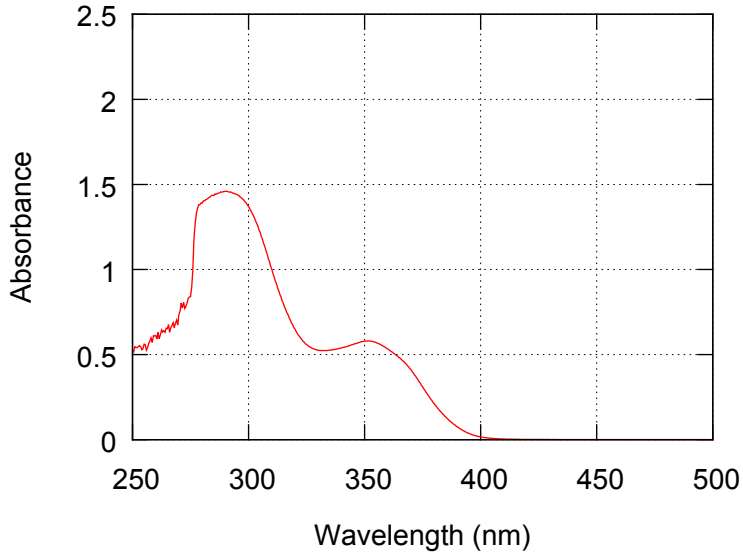

Figure S76. UV-vis absorption spectrum of **5(40)** in (*R*)-limonene (1.13×10^{-1} g/L, path length = 2.0 mm).

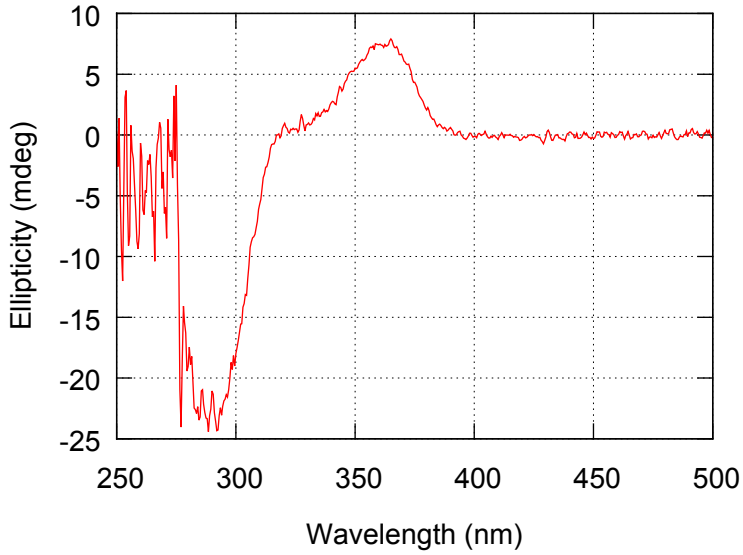

Figure S77. CD spectrum of **5(40)** in (*R*)-limonene (1.13×10^{-1} g/L, path length = 2.0 mm).

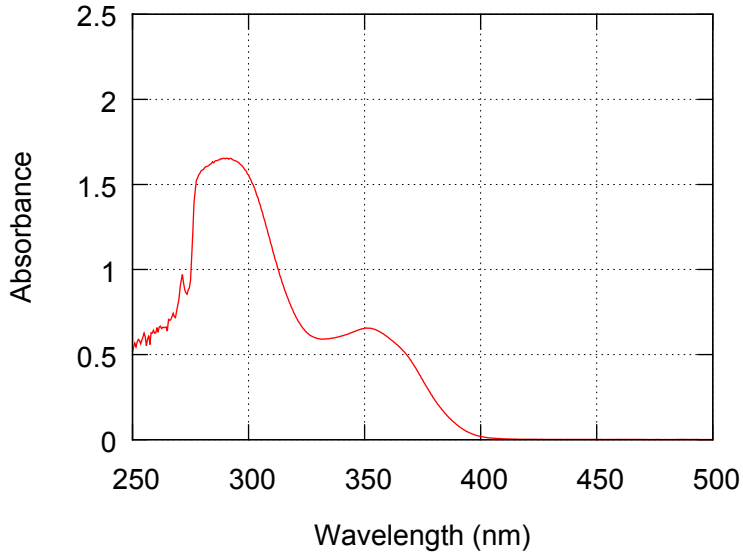

Figure S78. UV-vis absorption spectrum of **5(40)** in (*R*)-limonene (1.29×10^{-1} g/L, path length = 2.0 mm).

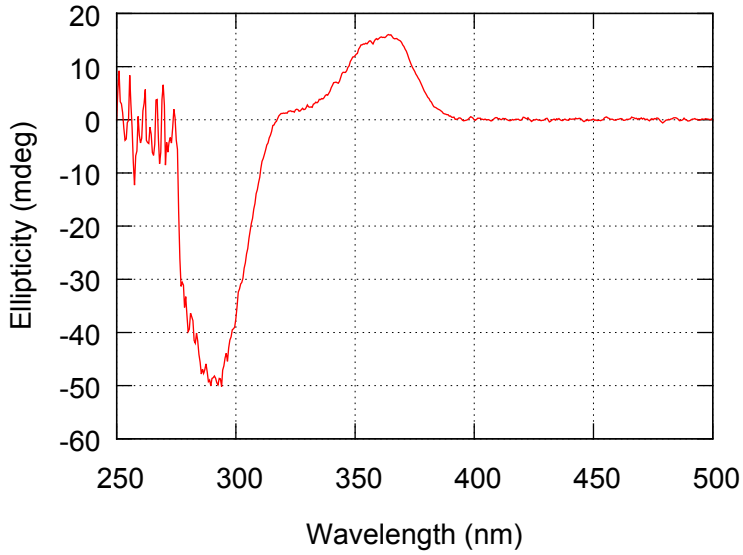

Figure S79. CD spectrum of **5(40)** in (*R*)-limonene (1.29×10^{-1} g/L, path length = 2.0 mm).

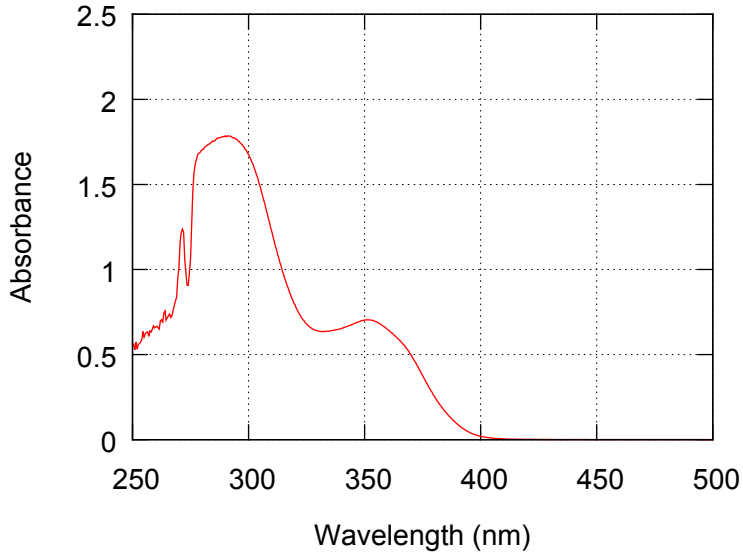

Figure S80. UV-vis absorption spectrum of **5(40)** in (*R*)-limonene (1.24×10^{-1} g/L, path length = 2.0 mm).

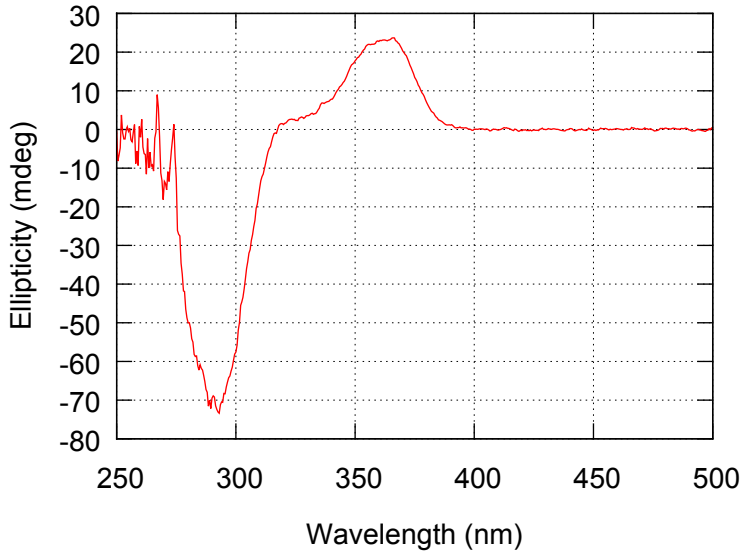

Figure S81. CD spectrum of **5(40)** in (*R*)-limonene (1.24×10^{-1} g/L, path length = 2.0 mm).

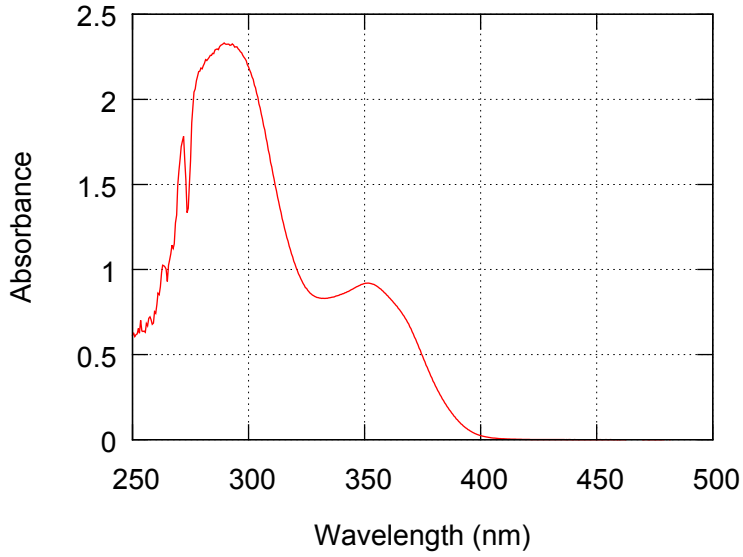

Figure S82. UV-vis absorption spectrum of **5(40)** in (*R*)-limonene (1.30×10^{-1} g/L, path length = 2.0 mm).

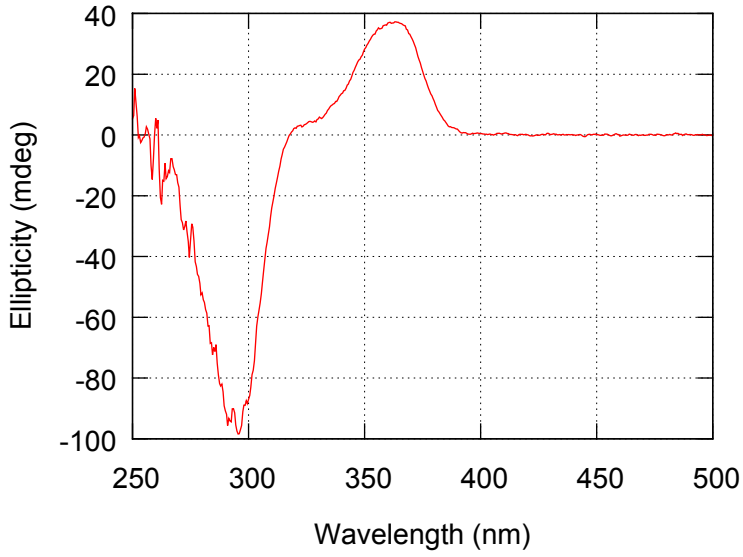

Figure S83. CD spectrum of **5(40)** in (*R*)-limonene (1.30×10^{-1} g/L, path length = 2.0 mm).

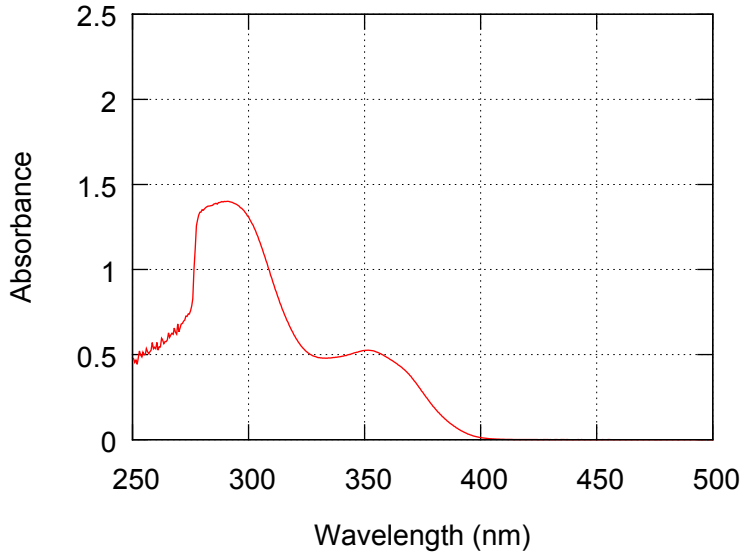

Figure S84. UV-vis absorption spectrum of **5(200)** in (*R*)-limonene (1.21×10^{-1} g/L, path length = 2.0 mm).

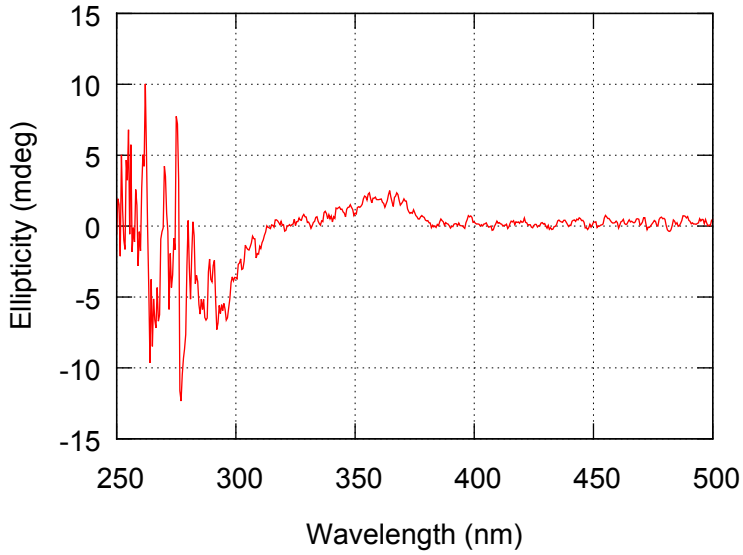

Figure S85. CD spectrum of **5(200)** in (*R*)-limonene (1.21×10^{-1} g/L, path length = 2.0 mm).

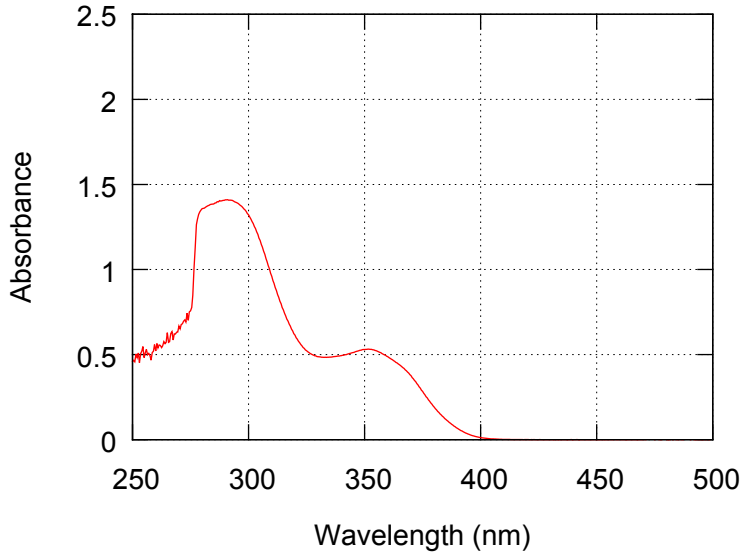

Figure S86. UV-vis absorption spectrum of **5(200)** in (*R*)-limonene (1.21×10^{-1} g/L, path length = 2.0 mm).

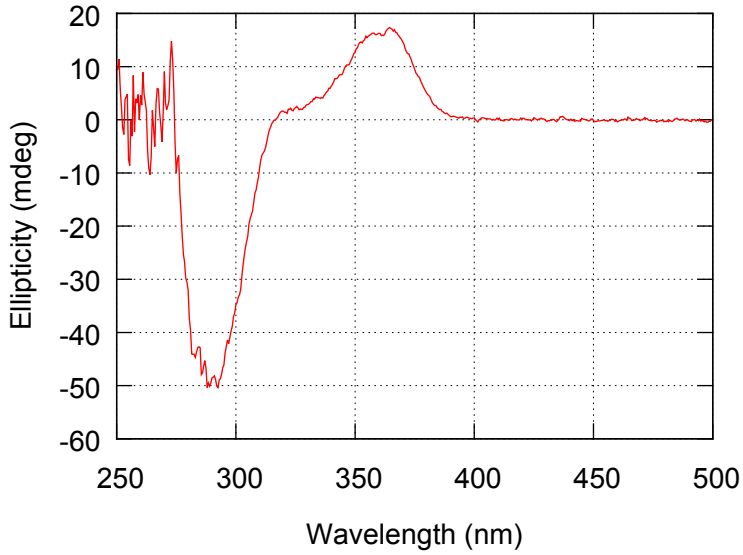

Figure S87. CD spectrum of **5(200)** in (*R*)-limonene (1.21×10^{-1} g/L, path length = 2.0 mm).

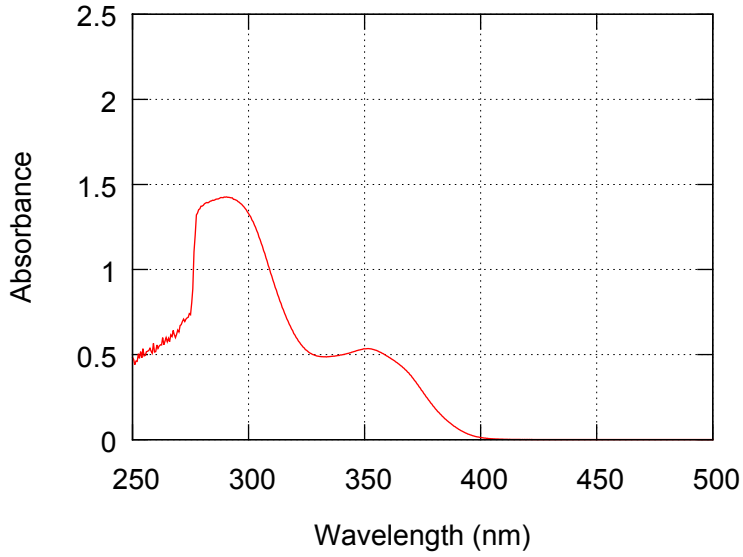

Figure S88. UV-vis absorption spectrum of **5(200)** in (*R*)-limonene (1.21×10^{-1} g/L, path length = 2.0 mm).

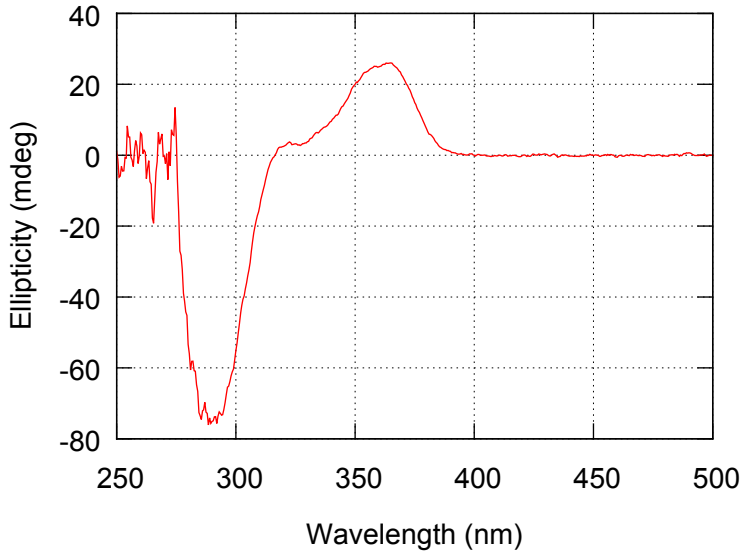

Figure S89. CD spectrum of **5(200)** in (*R*)-limonene (1.21×10^{-1} g/L, path length = 2.0 mm).

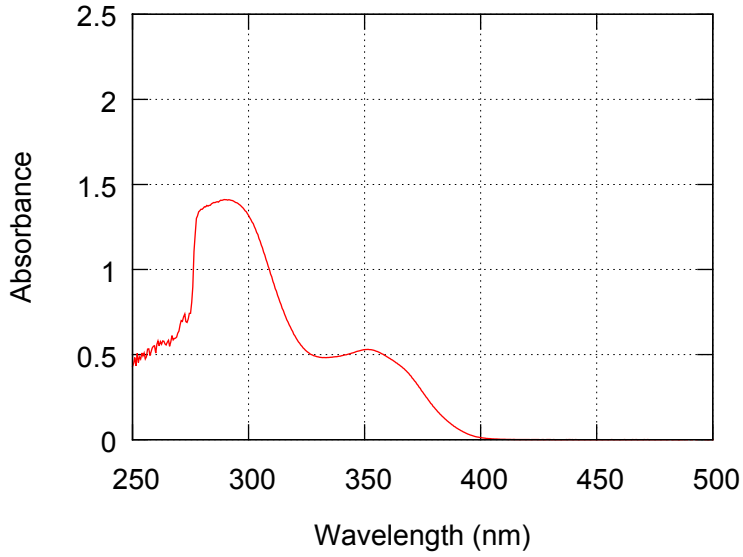

Figure S90. UV-vis absorption spectrum of **5(200)** in (*R*)-limonene (1.21×10^{-1} g/L, path length = 2.0 mm).

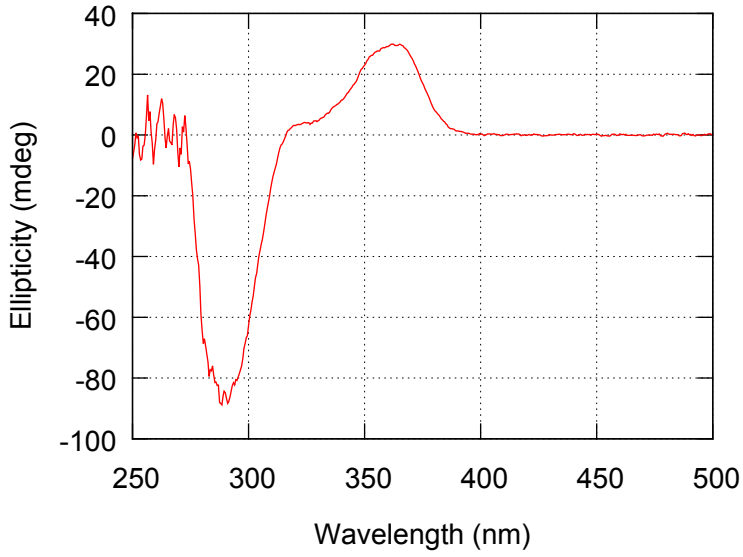

Figure S91. CD spectrum of **5(200)** in (*R*)-limonene (1.21×10^{-1} g/L, path length = 2.0 mm).

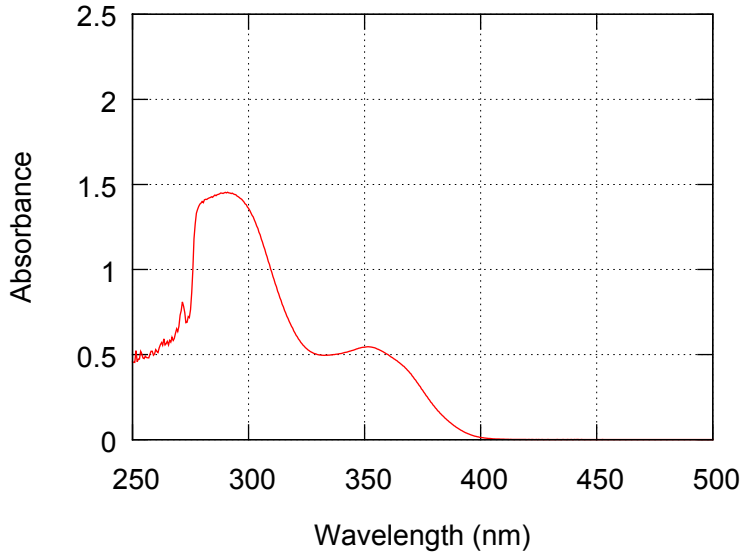

Figure S92. UV-vis absorption spectrum of **5(200)** in (*R*)-limonene (1.21×10^{-1} g/L, path length = 2.0 mm).

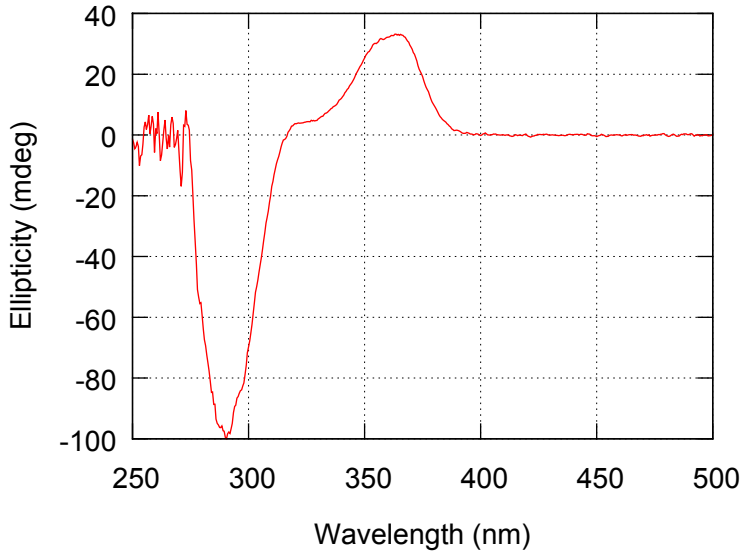

Figure S93. CD spectrum of **5(200)** in (*R*)-limonene (1.21×10^{-1} g/L, path length = 2.0 mm).

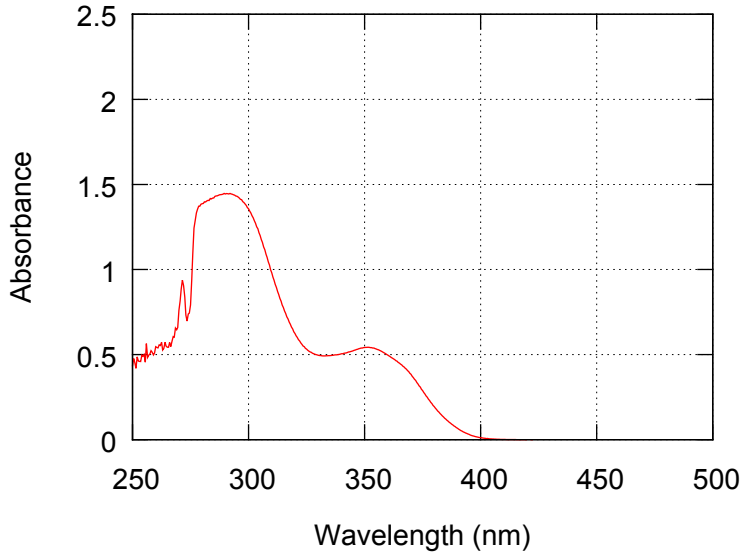

Figure S94. UV-vis absorption spectrum of **5(200)** in (*R*)-limonene (1.21×10^{-1} g/L, path length = 2.0 mm).

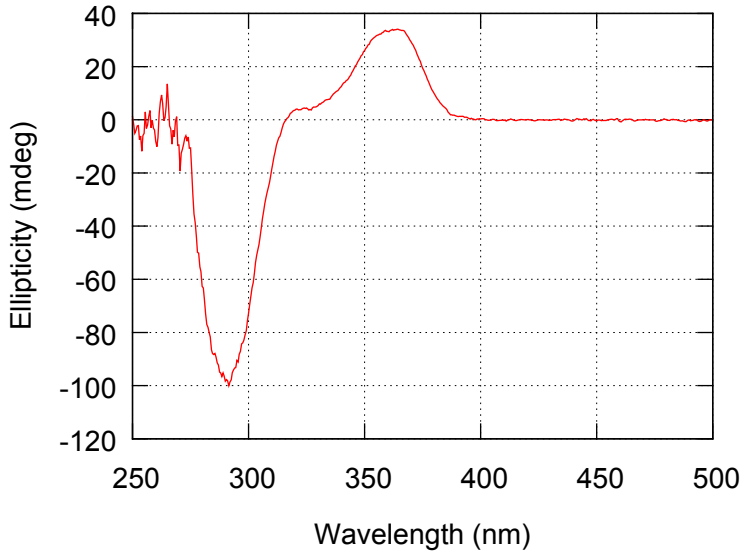

Figure S95. CD spectrum of **5(200)** in (*R*)-limonene (1.21×10^{-1} g/L, path length = 2.0 mm).

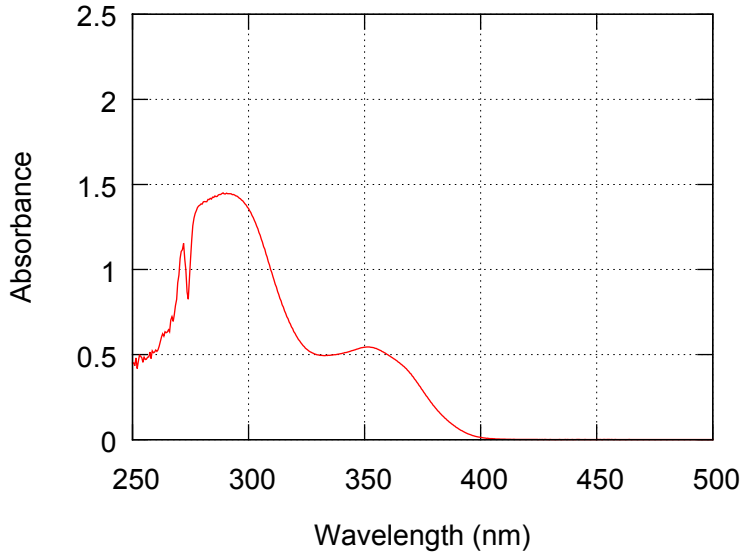

Figure S96. UV-vis absorption spectrum of **5(200)** in (*R*)-limonene (1.21×10^{-1} g/L, path length = 2.0 mm).

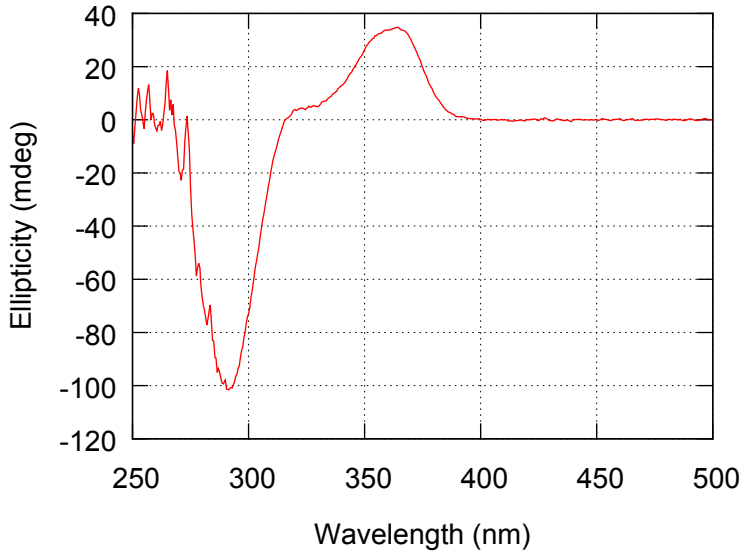

Figure S97. CD spectrum of **5(200)** in (*R*)-limonene (1.21×10^{-1} g/L, path length = 2.0 mm).

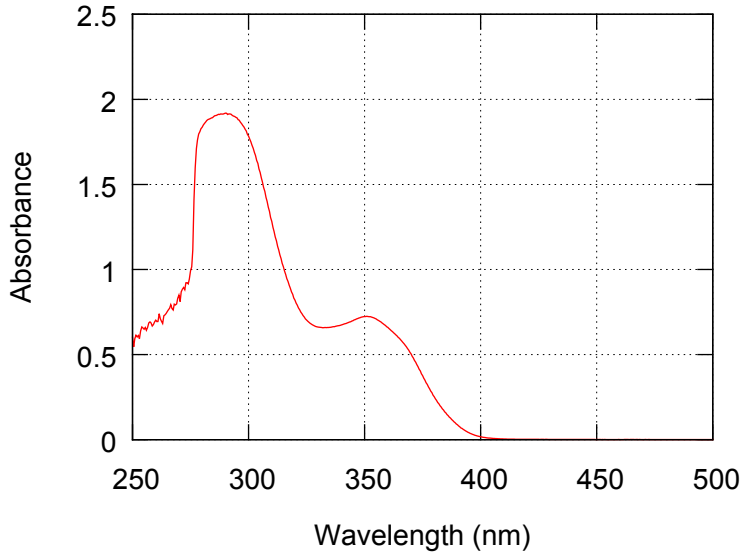

Figure S98. UV-vis absorption spectrum of **5(1000)** in (*R*)-limonene (1.30×10^{-1} g/L, path length = 2.0 mm).

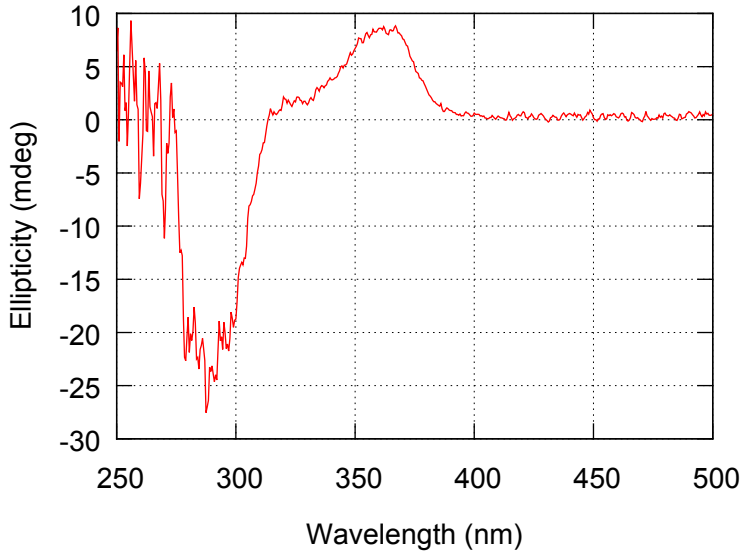

Figure S99. CD spectrum of **5(1000)** in (*R*)-limonene (1.30×10^{-1} g/L, path length = 2.0 mm).

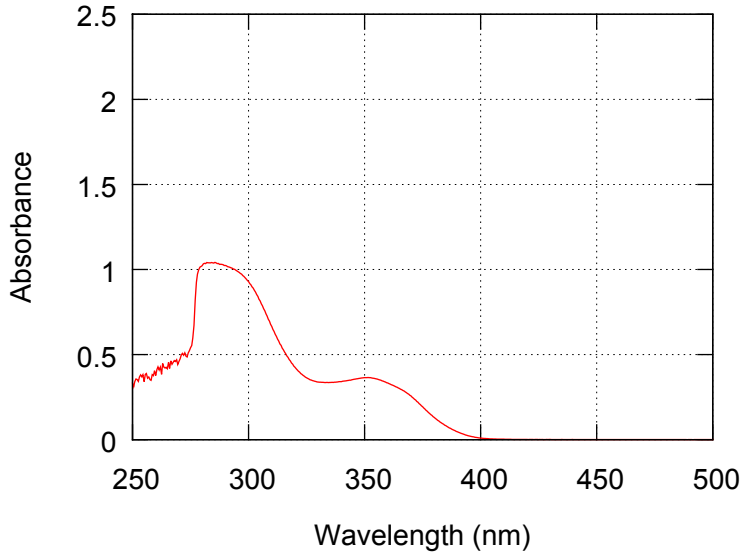

Figure S100. UV-vis absorption spectrum of **5(1000)** in (*R*)-limonene (1.00×10^{-1} g/L, path length = 2.0 mm).

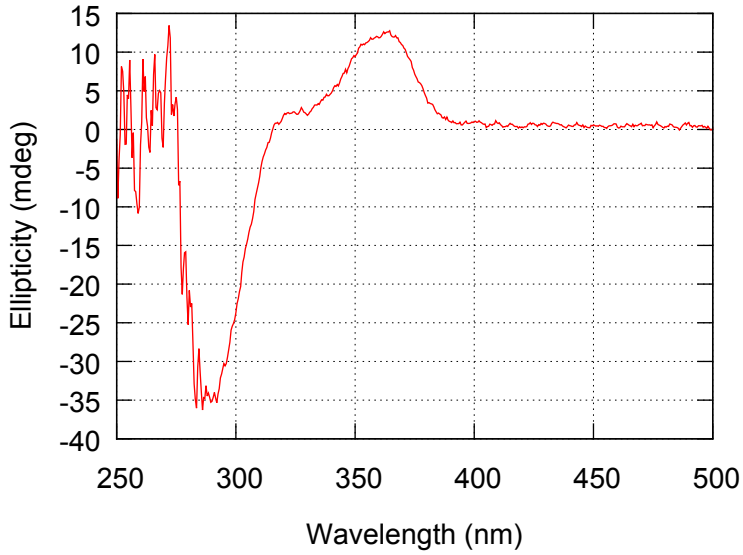

Figure S101. CD spectrum of **5(1000)** in (*R*)-limonene (1.00×10^{-1} g/L, path length = 2.0 mm).

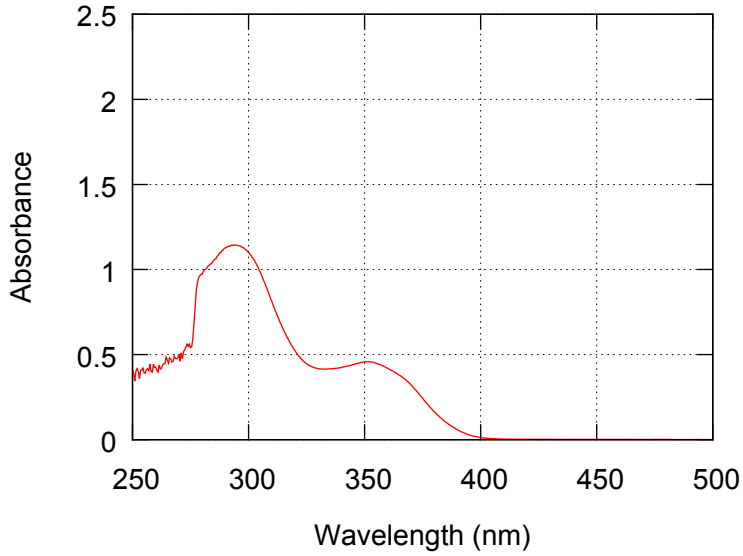

Figure S102. UV-vis absorption spectrum of **5(1000)** in (*R*)-limonene (1.00×10^{-1} g/L, path length = 2.0 mm).

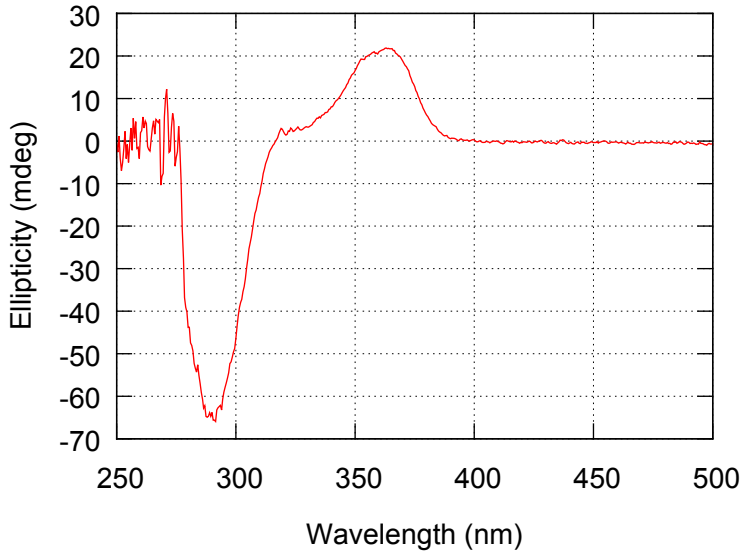

Figure S103. CD spectrum of **5(1000)** in (*R*)-limonene (1.00×10^{-1} g/L, path length = 2.0 mm).

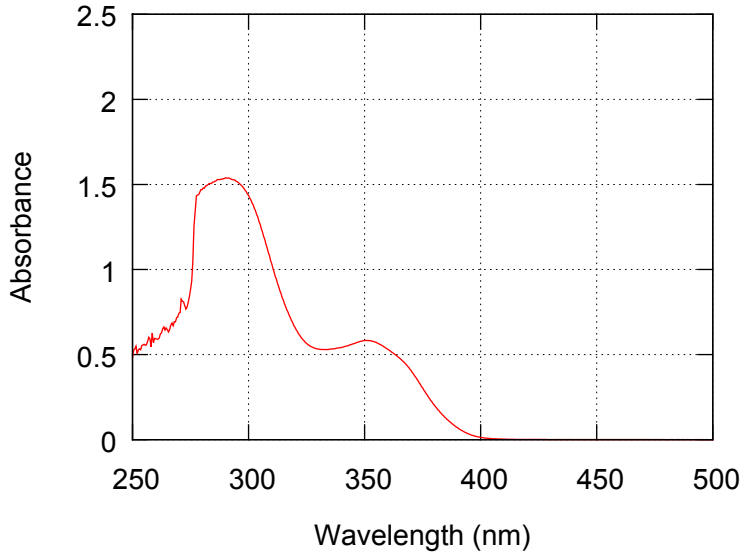

Figure S104. UV-vis absorption spectrum of **5(1000)** in (*R*)-limonene (1.23×10^{-1} g/L, path length = 2.0 mm).

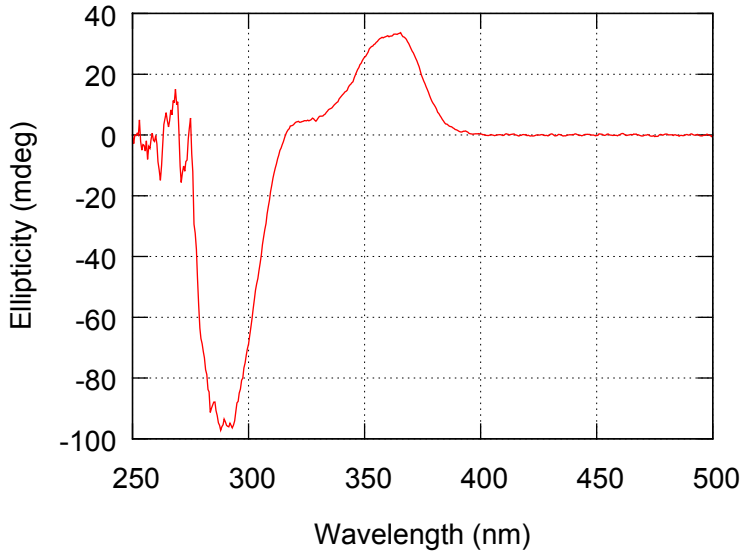

Figure S105. CD spectrum of **5(1000)** in (*R*)-limonene (1.23×10^{-1} g/L, path length = 2.0 mm).

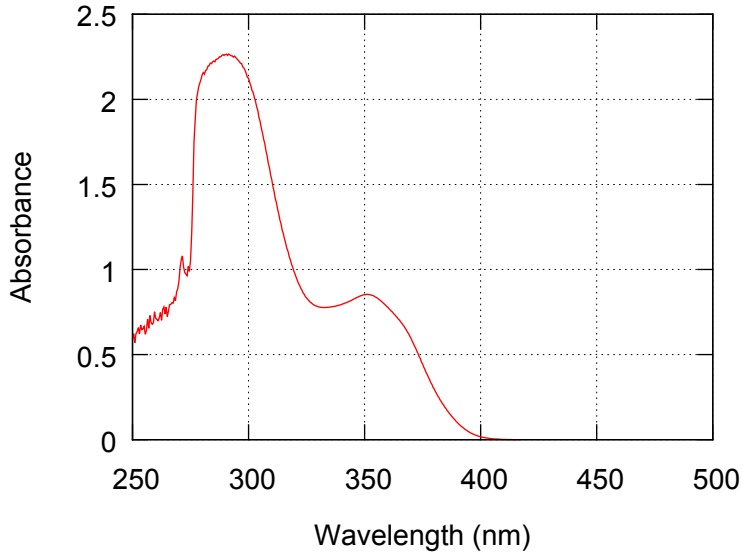

Figure S106. UV-vis absorption spectrum of **5(1000)** in (*R*)-limonene (1.28×10^{-1} g/L, path length = 2.0 mm).

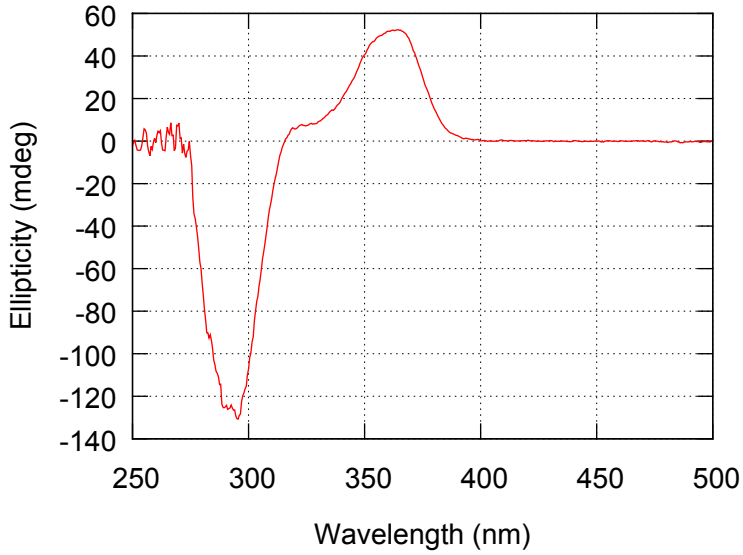

Figure S107. CD spectrum of **5(1000)** in (*R*)-limonene (1.28×10^{-1} g/L, path length = 2.0 mm).

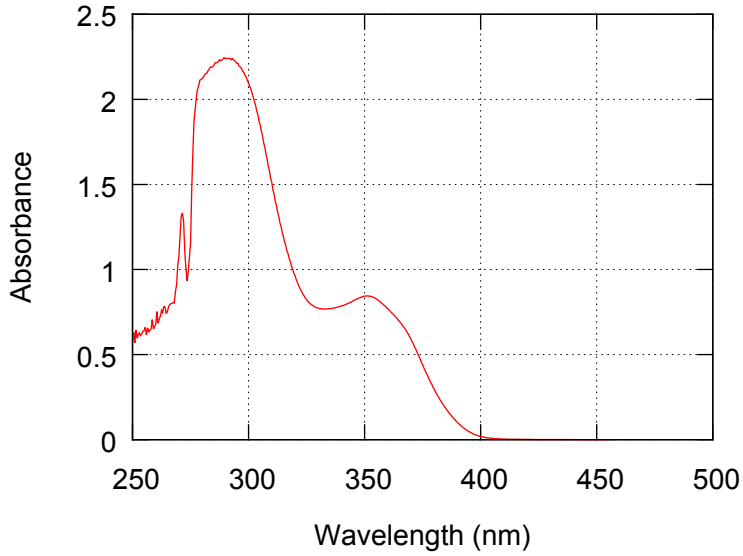

Figure S108. UV-vis absorption spectrum of **5(1000)** in (*R*)-limonene (1.27×10^{-1} g/L, path length = 2.0 mm).

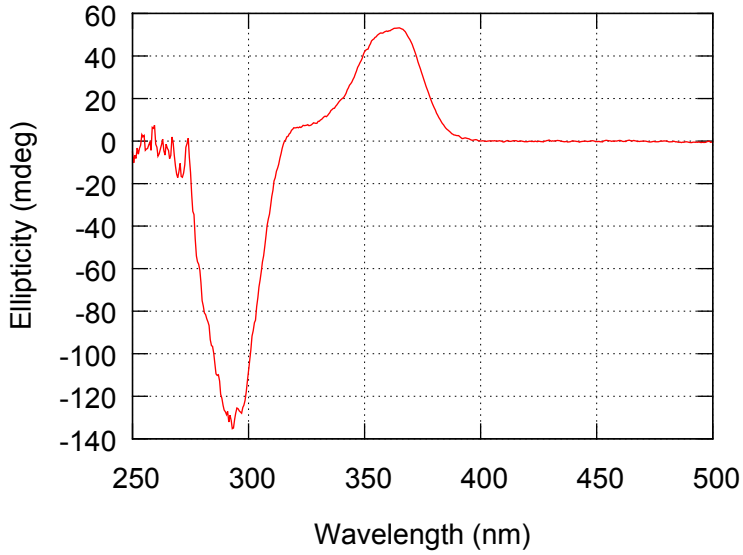

Figure S109. CD spectrum of **5(1000)** in (*R*)-limonene (1.27×10^{-1} g/L, path length = 2.0 mm).

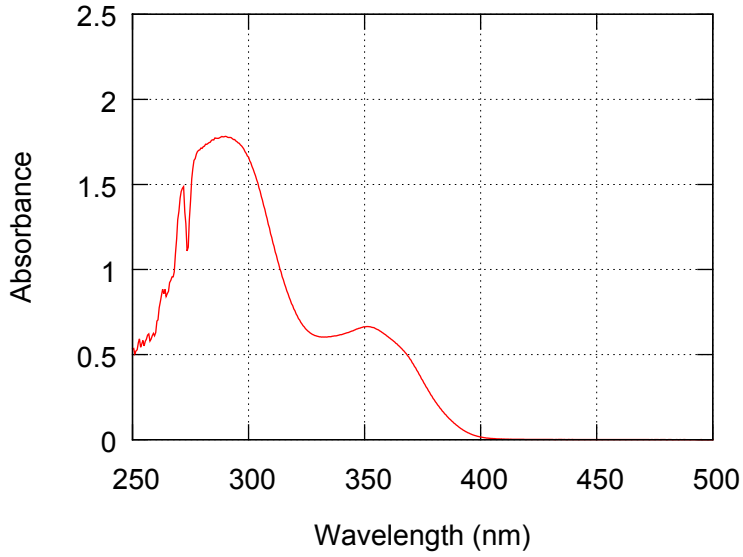

Figure S110. UV-vis absorption spectrum of **5(1000)** in (*R*)-limonene (1.30×10^{-1} g/L, path length = 2.0 mm).

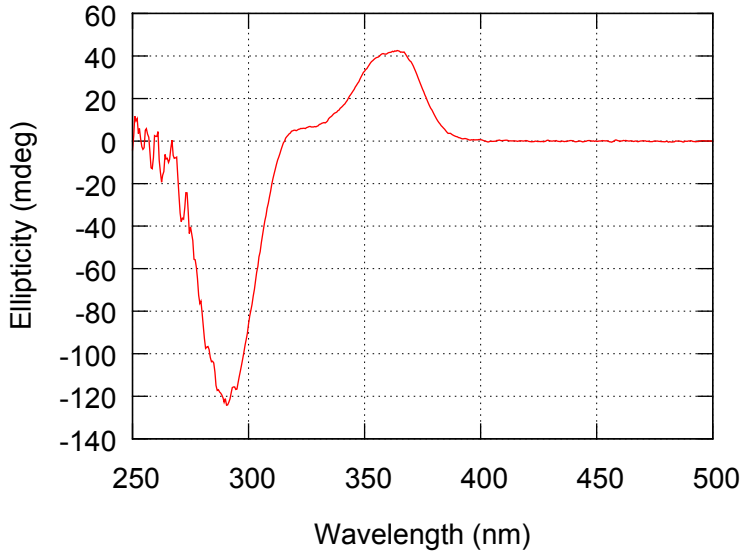

Figure S111. CD spectrum of **5(1000)** in (*R*)-limonene (1.30×10^{-1} g/L, path length = 2.0 mm).

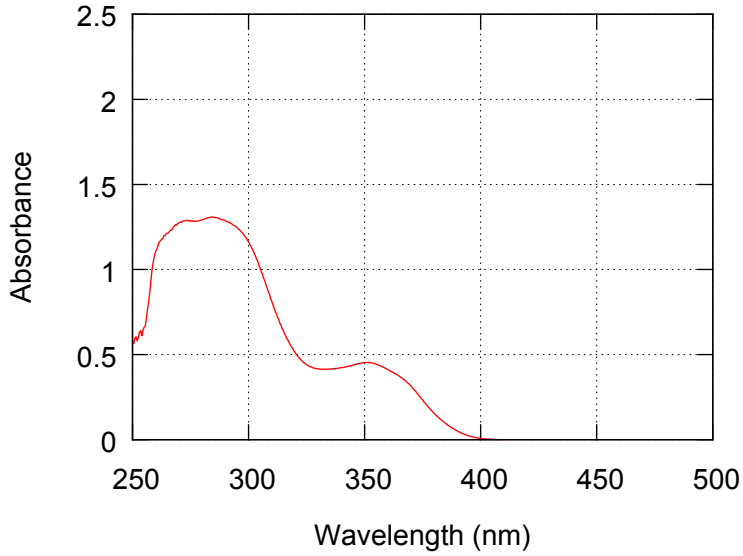

Figure S112. UV-vis absorption spectrum of **5(1000)** in (*R*)-limonene (2.02×10^{-2} g/L, path length = 10 mm).

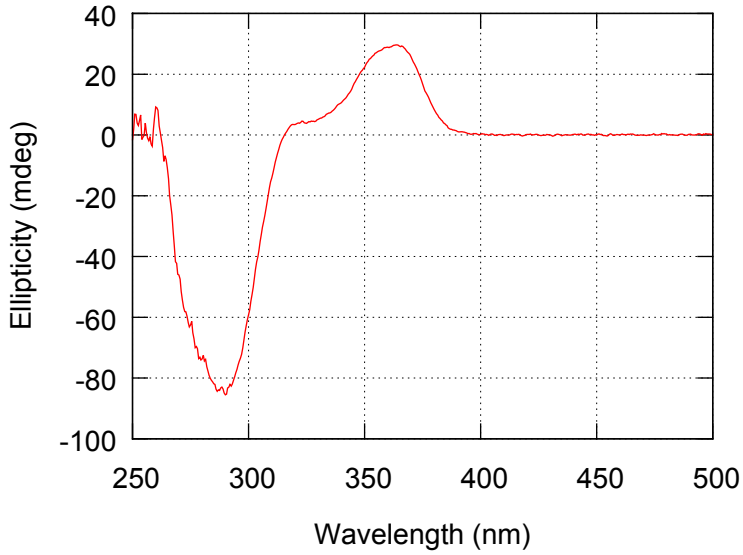

Figure S113. CD spectrum of **5(1000)** in (*R*)-limonene (2.02×10^{-2} g/L, path length = 10 mm).

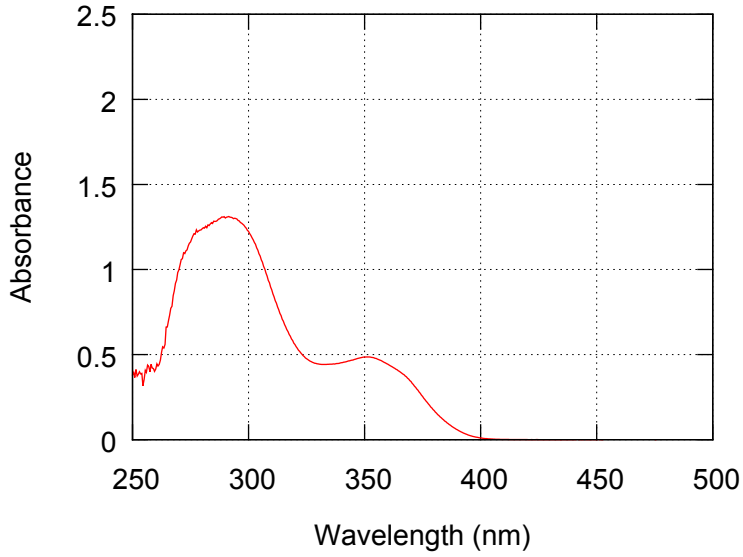

Figure S114. UV-vis absorption spectrum of **L1** in (*R*)-limonene (11.60×10^{-1} g/L, path length = 2.0 mm).

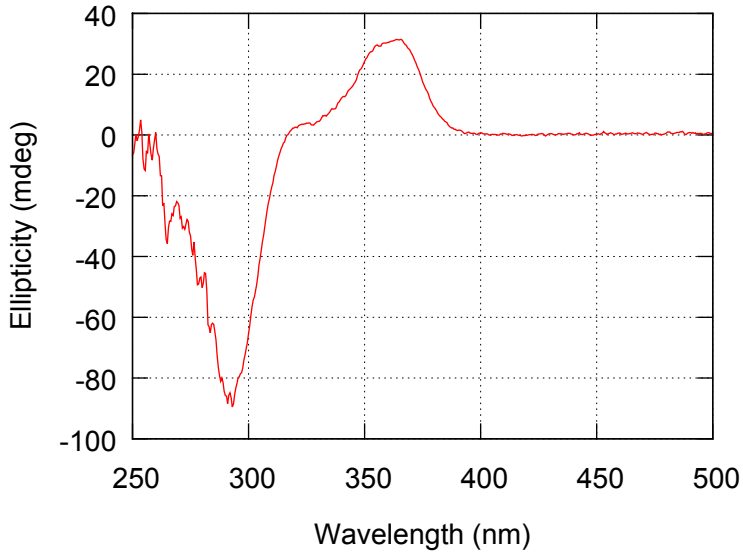

Figure S115. CD spectrum of **L1** in (*R*)-limonene (11.60×10^{-1} g/L, path length = 2.0 mm).

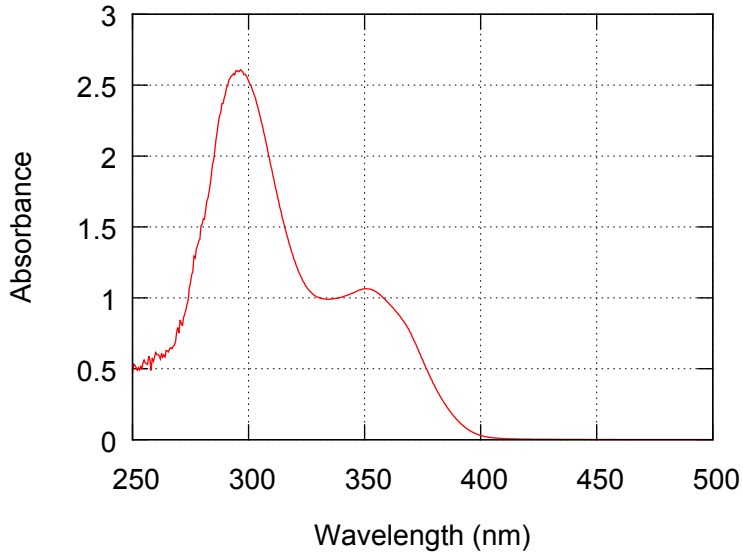

Figure S116. UV-vis absorption spectrum of **L2** in (*R*)-limonene (25.00×10^{-1} g/L, path length = 2.0 mm).

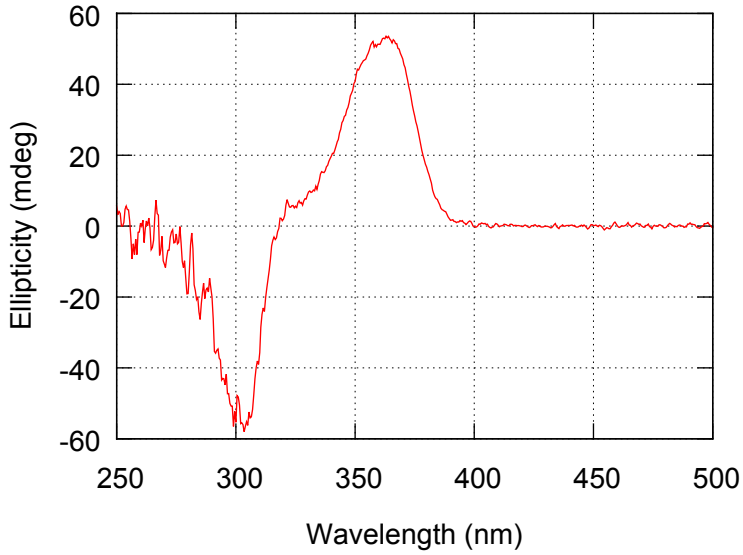

Figure S117. CD spectrum of **L2** in (*R*)-limonene (25.00×10^{-1} g/L, path length = 2.0 mm).

6 NMR Spectra of New Compounds

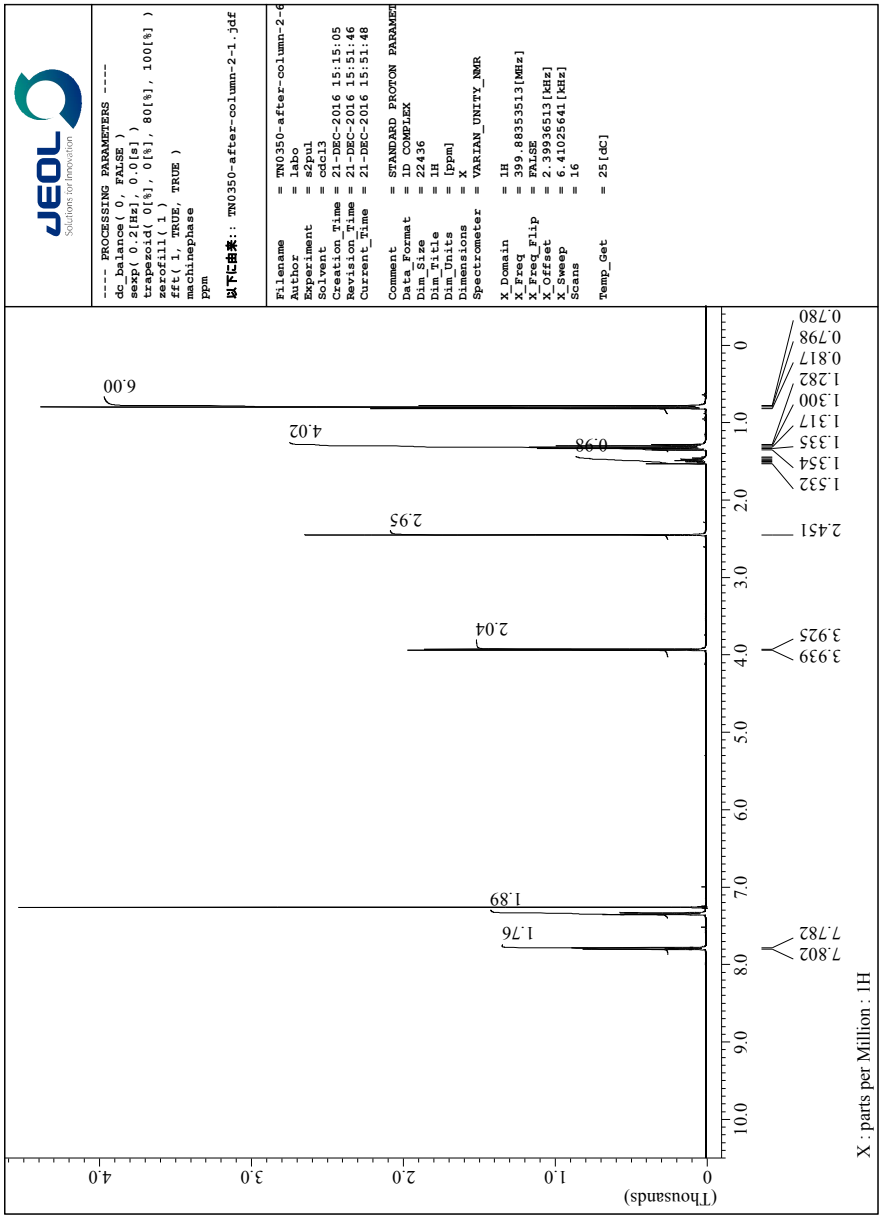

Figure S118. ^{1}H NMR spectrum of **2-Tos** in $CDCl_3$.

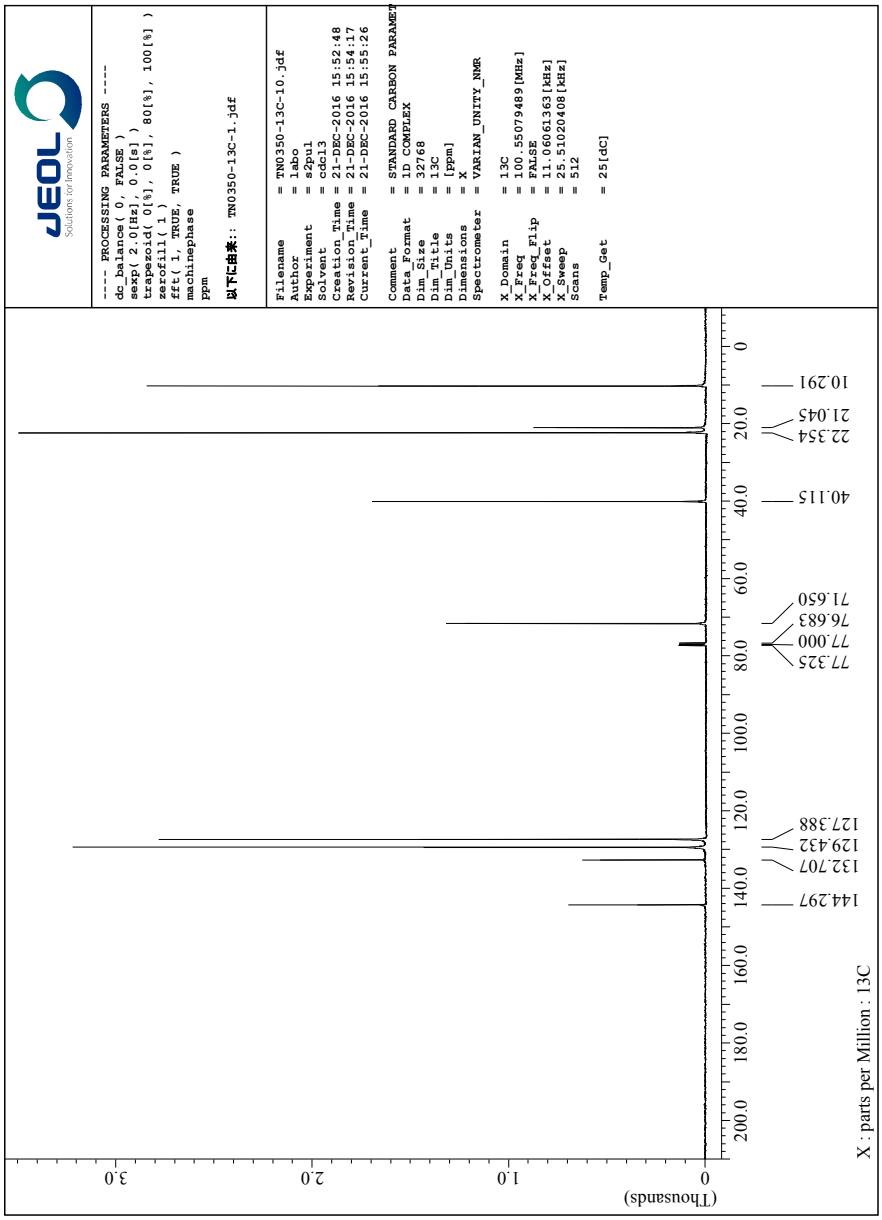

Figure S119. ^{13}C NMR spectrum of **2-Tos** in $CDCl_3$.

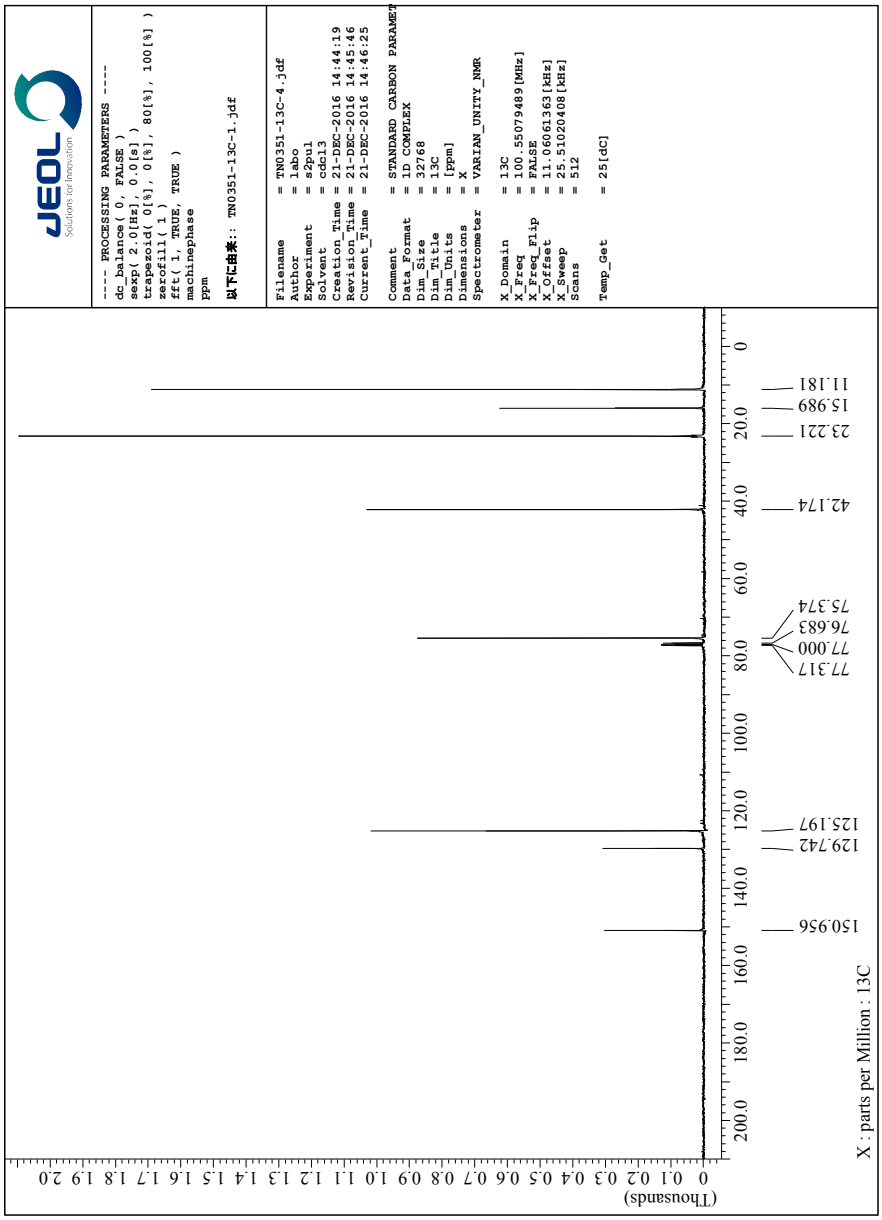

Figure S120. ^{1}H NMR spectrum of **2-H** in $CDCl_3$.

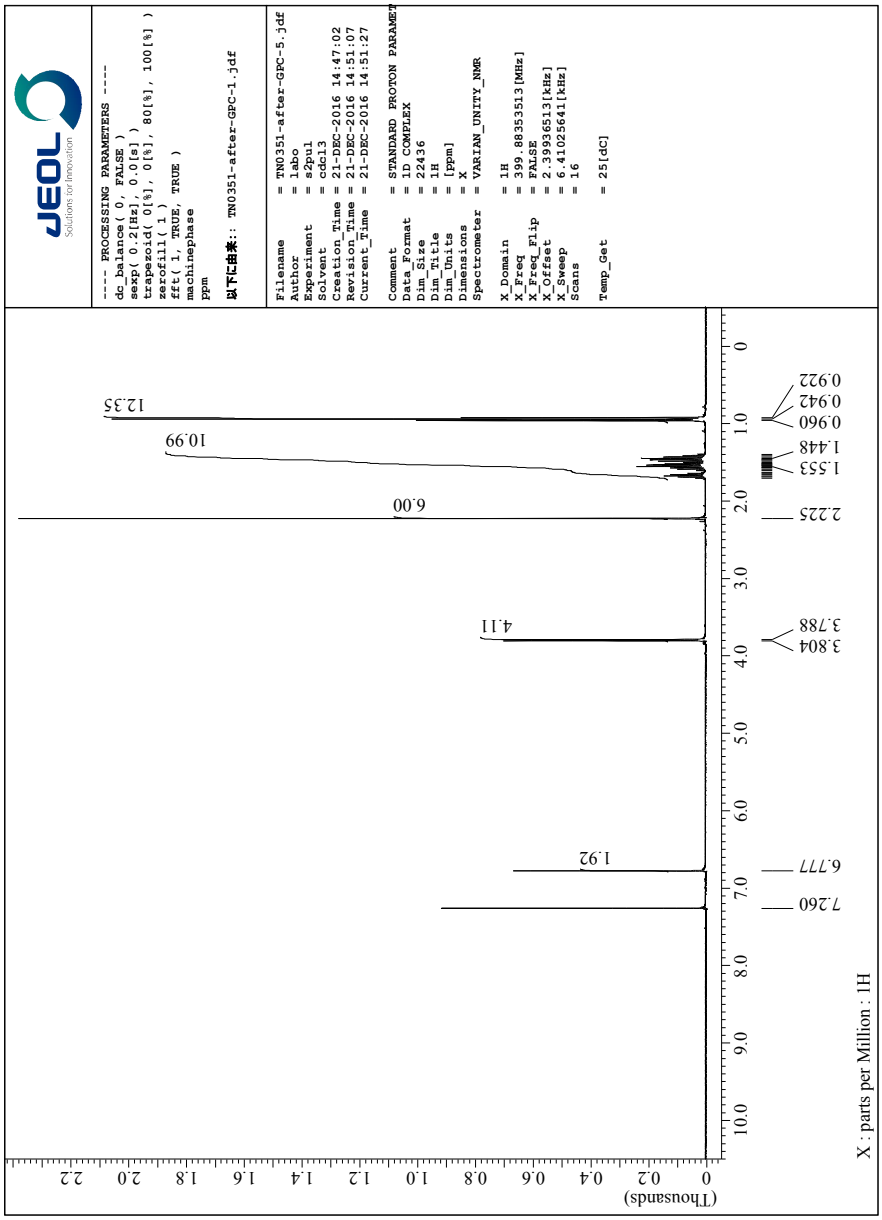

Figure S121. ^{13}C NMR spectrum of **2-H** in $CDCl_3$.

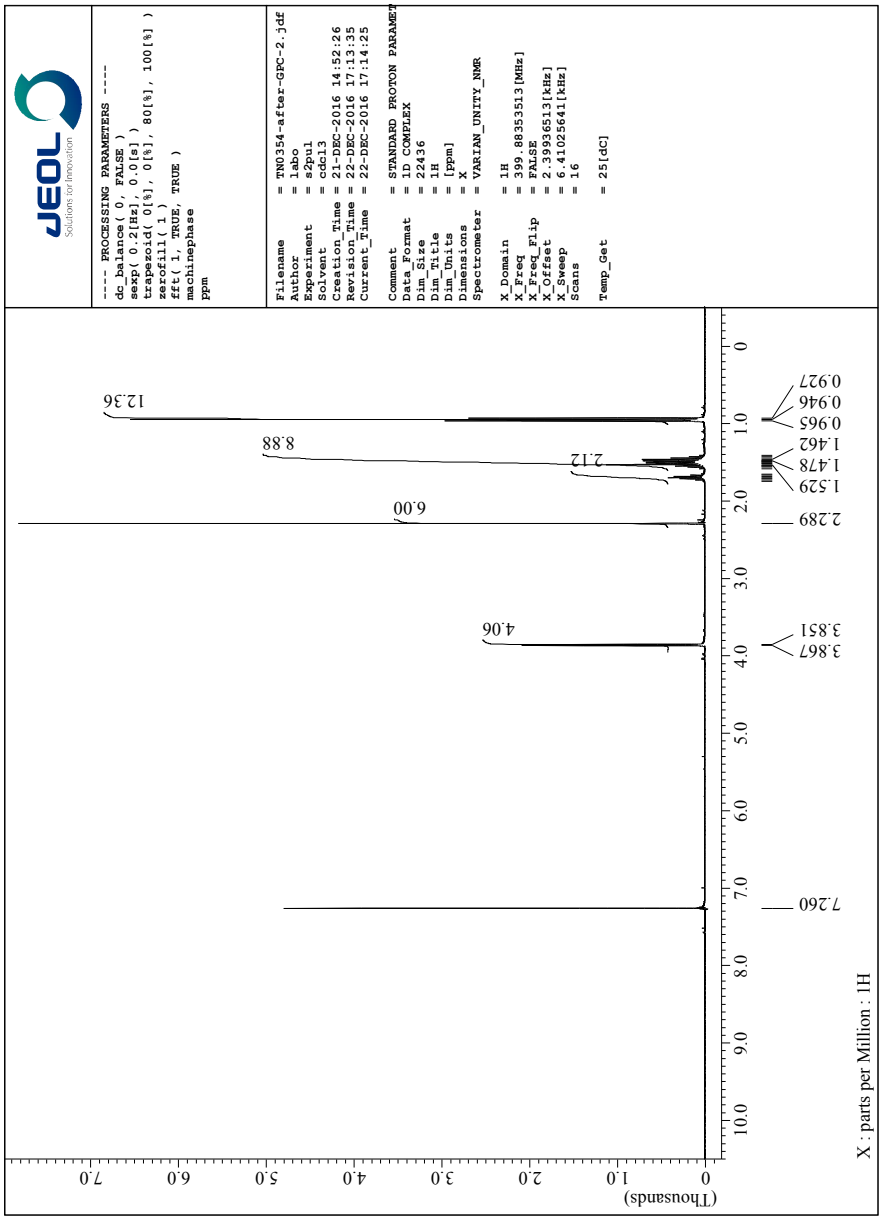

Figure S122. ^{1}H NMR spectrum of **2-NO2** in $CDCl_3$.

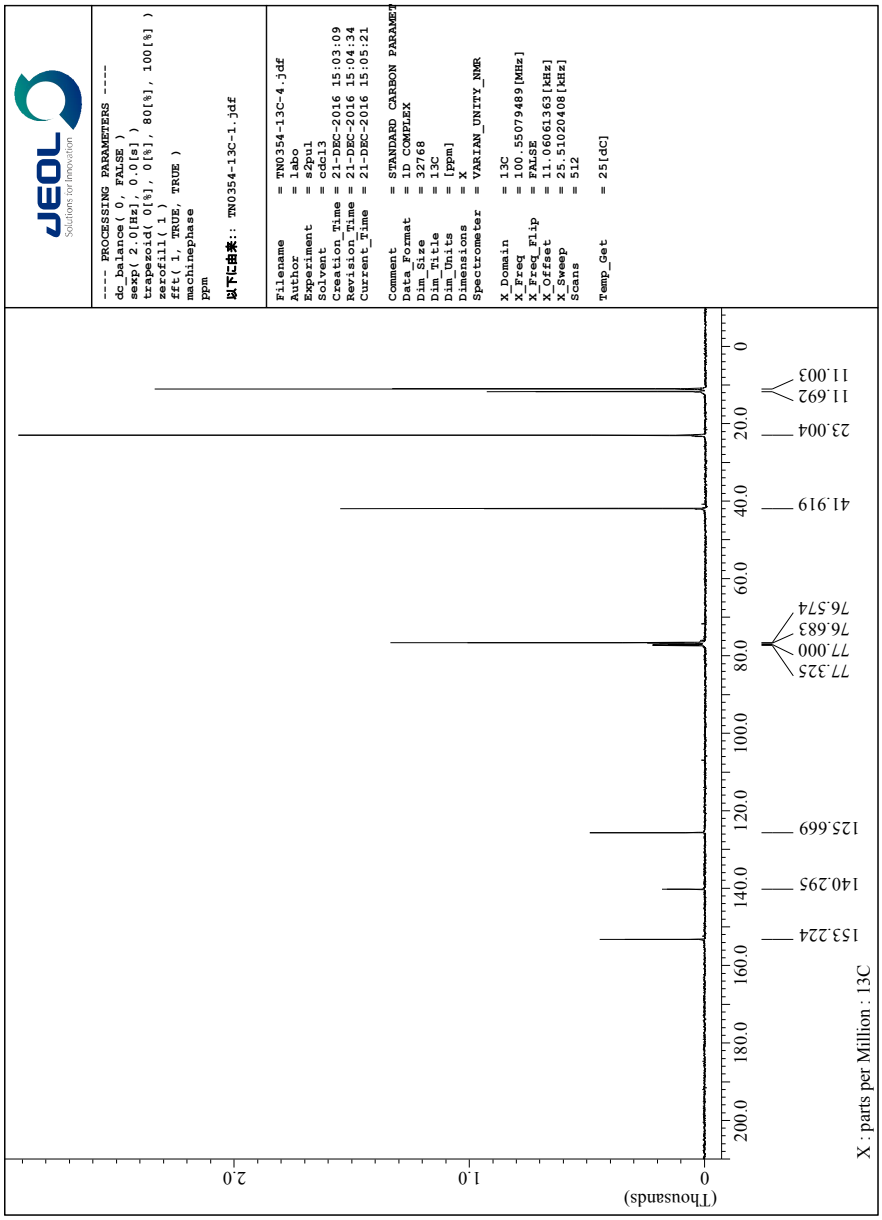

Figure S123. ^{13}C NMR spectrum of **2-NO2** in $CDCl_3$.

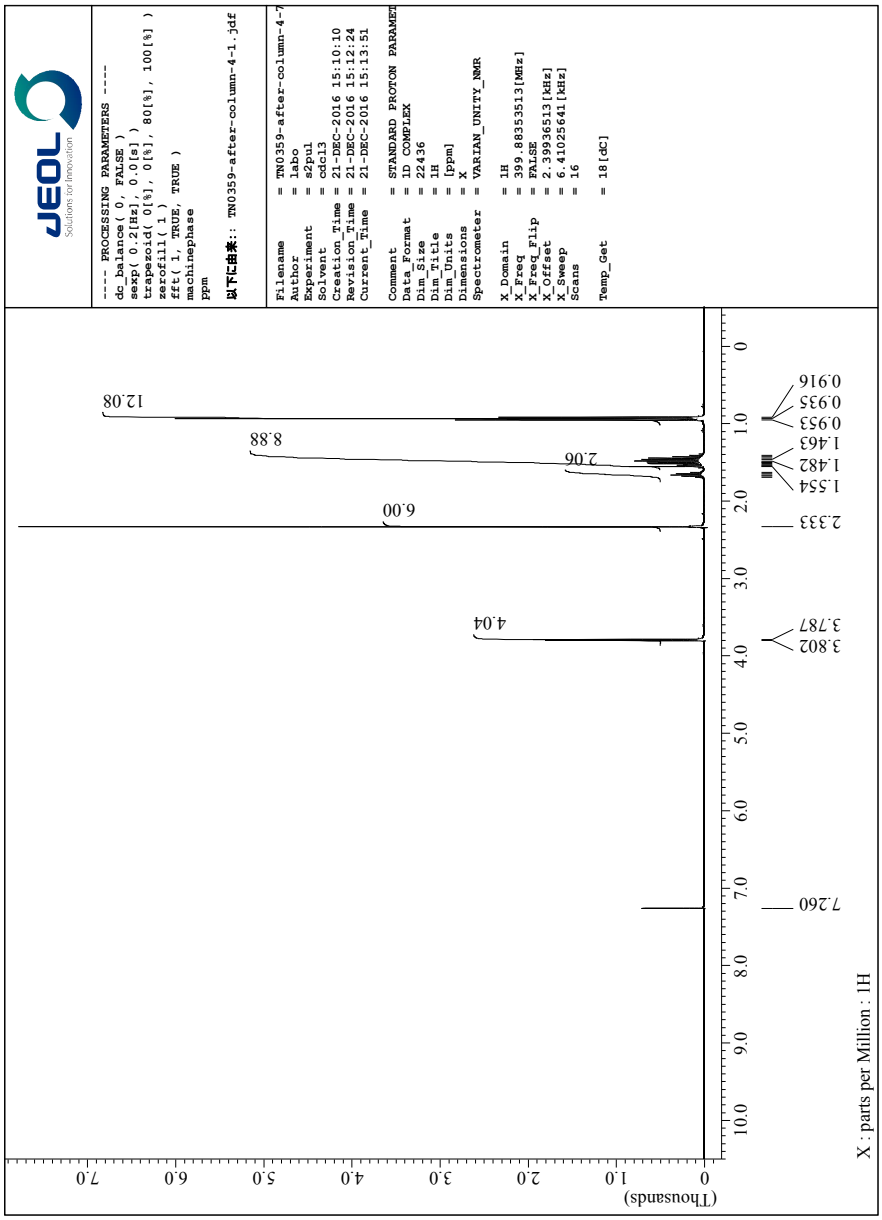

Figure S124. ^{1}H NMR spectrum of **2-NC** in $CDCl_3$.

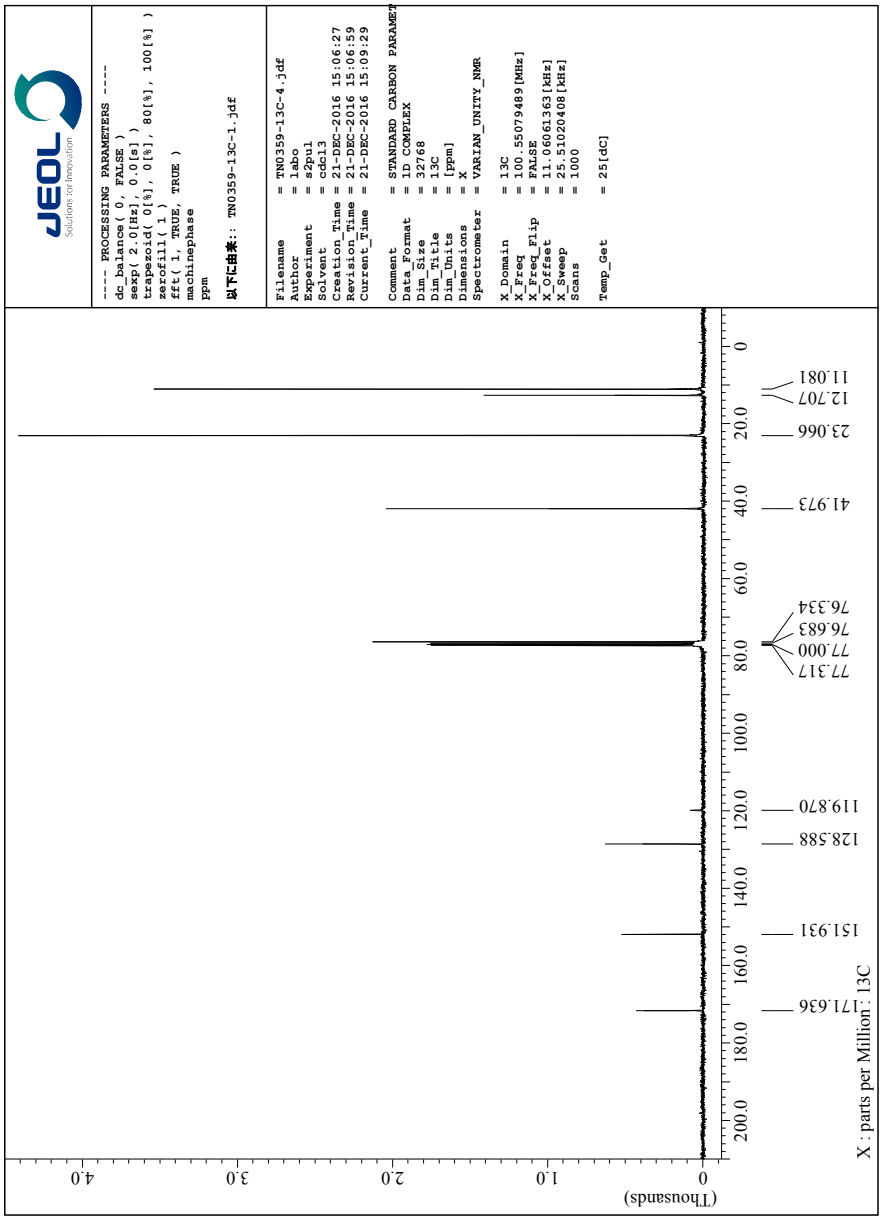

Figure S125. ^{13}C NMR spectrum of **2-NC** in $CDCl_3$.

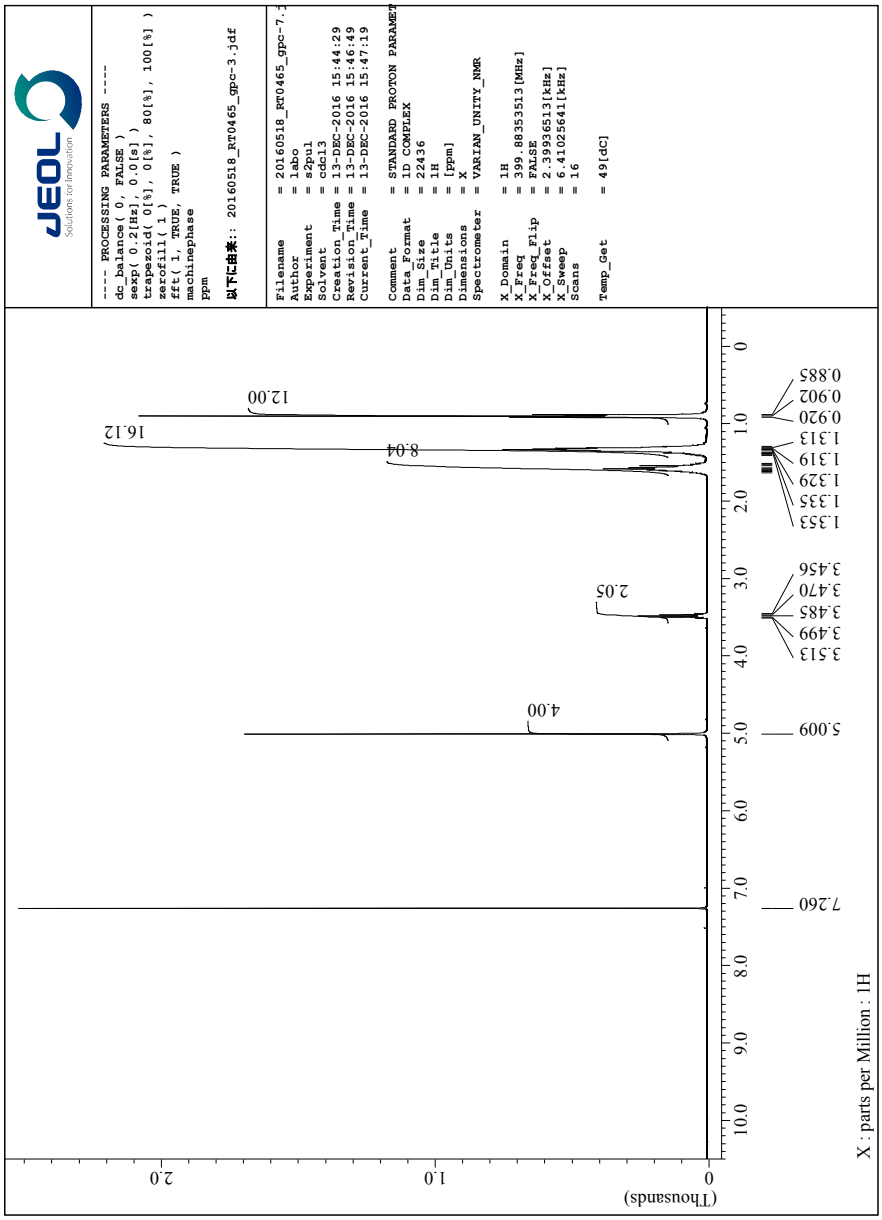

Figure S126. ^{1}H NMR spectrum of **3-Br** in $CDCl_3$.

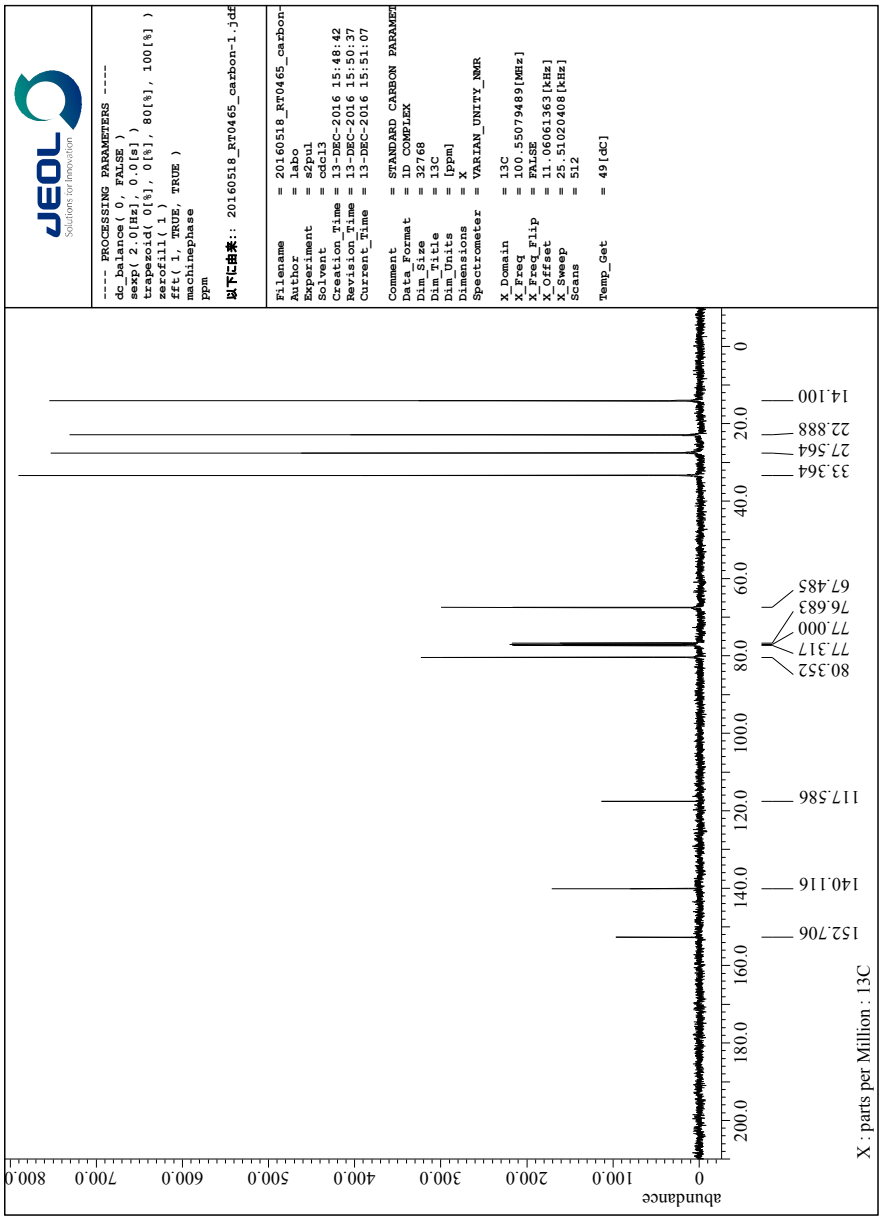

Figure S127. ^{13}C NMR spectrum of **3-Br** in $CDCl_3$.

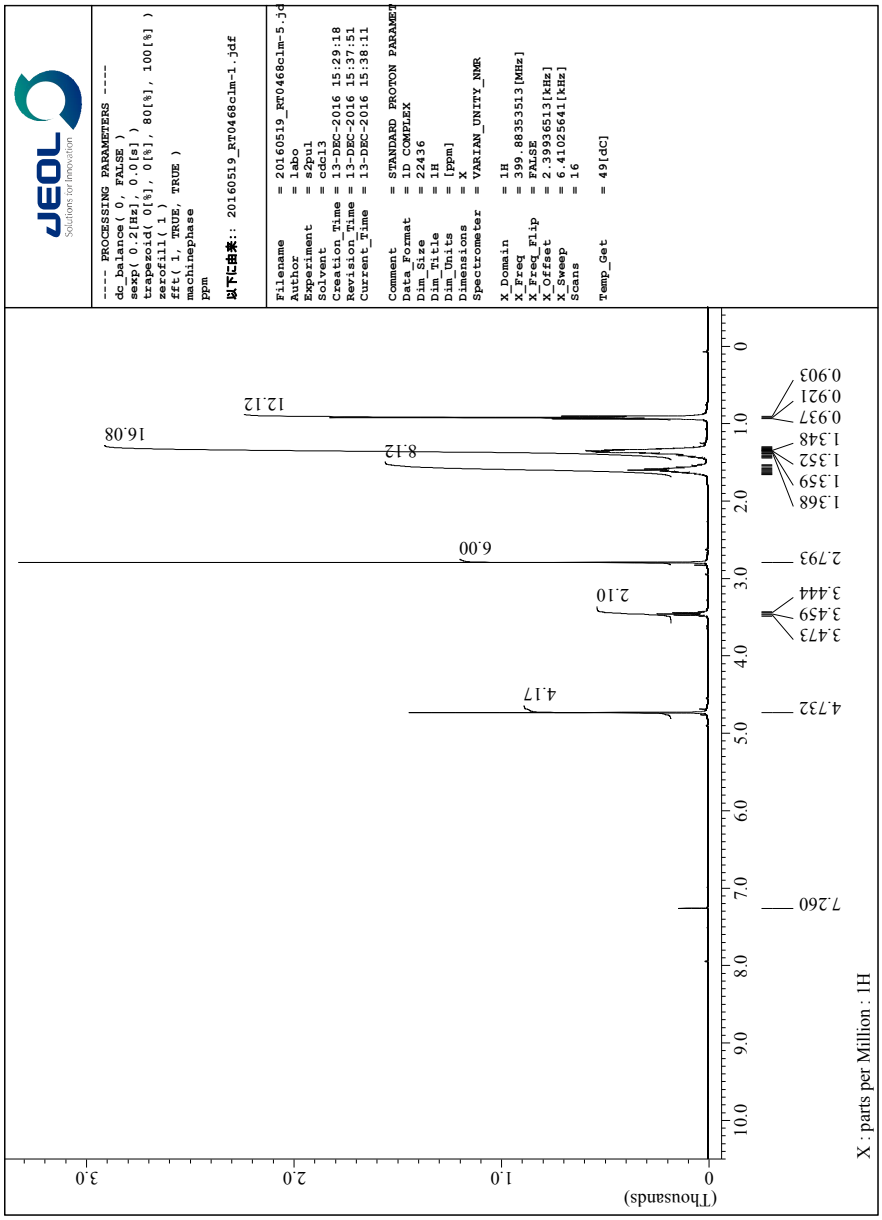

Figure S128. ^{1}H NMR spectrum of **3-Me** in $CDCl_3$.

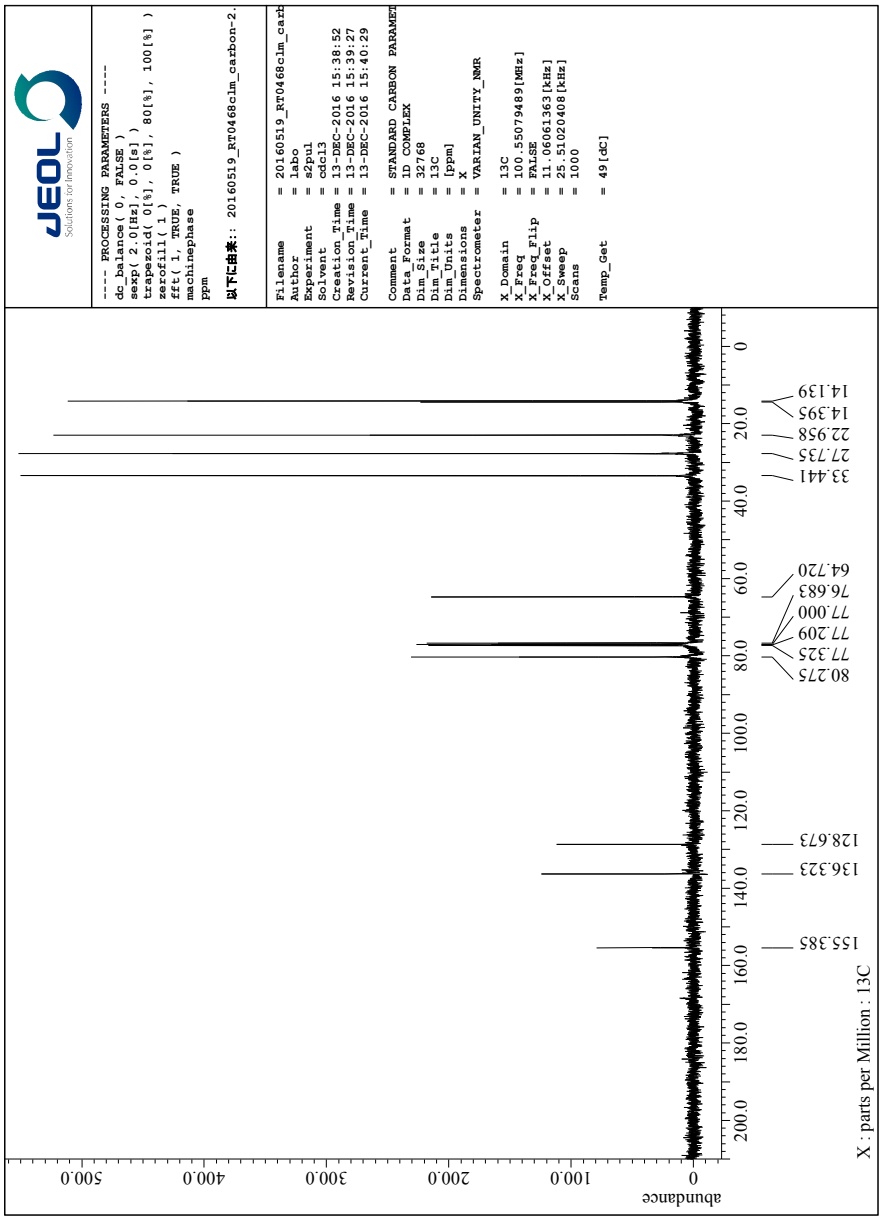

Figure S129. ^{13}C NMR spectrum of **3-Me** in $CDCl_3$.

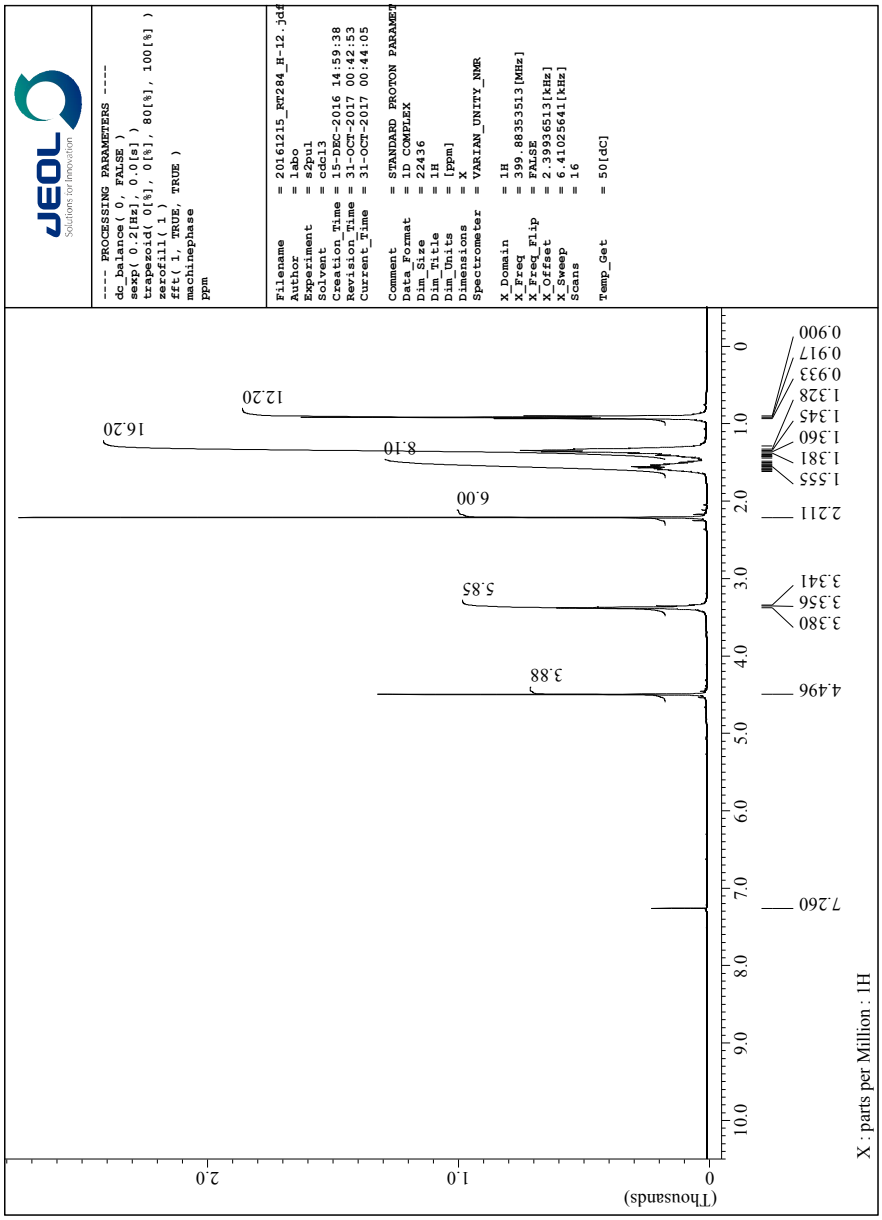

Figure S130. ^{1}H NMR spectrum of **3-NH2** in $CDCl_3$.

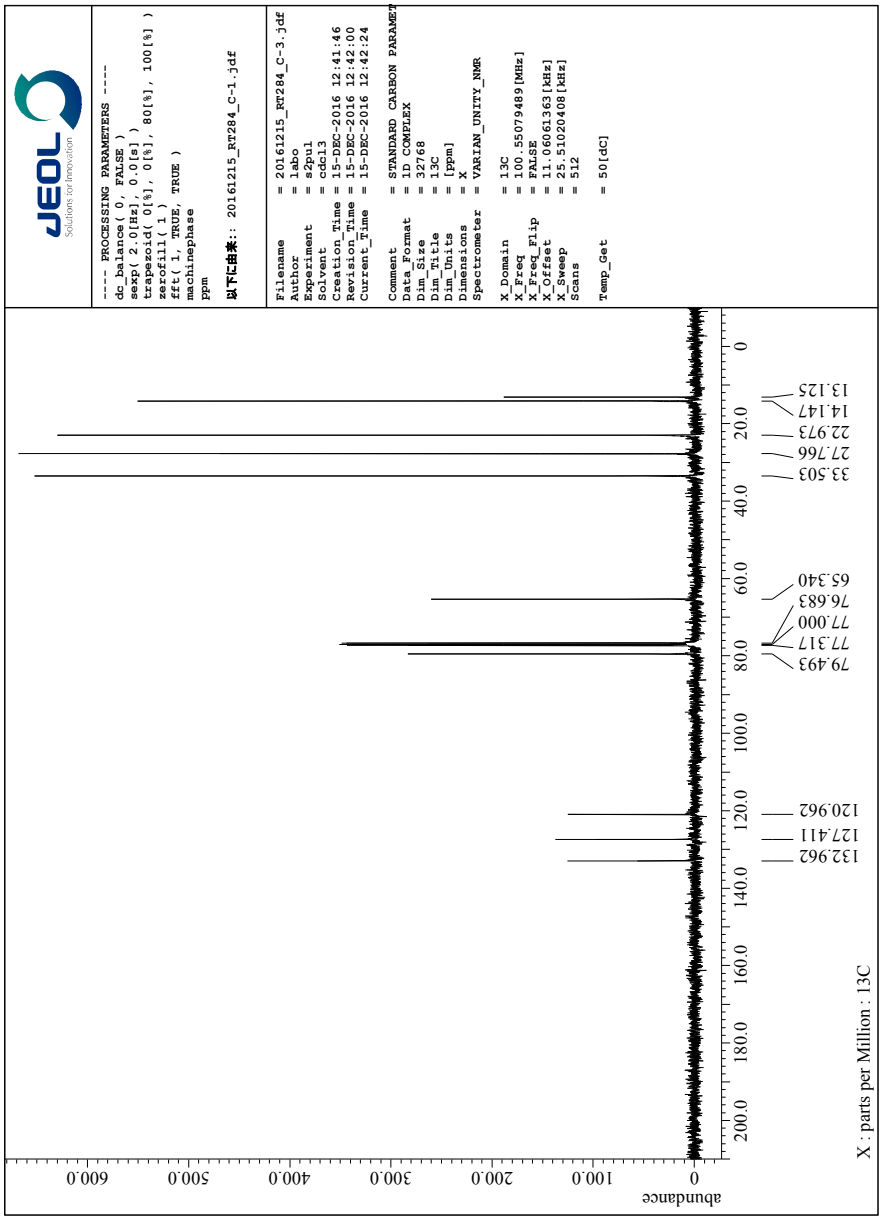

Figure S131. ^{13}C NMR spectrum of **3-NH2** in $CDCl_3$.

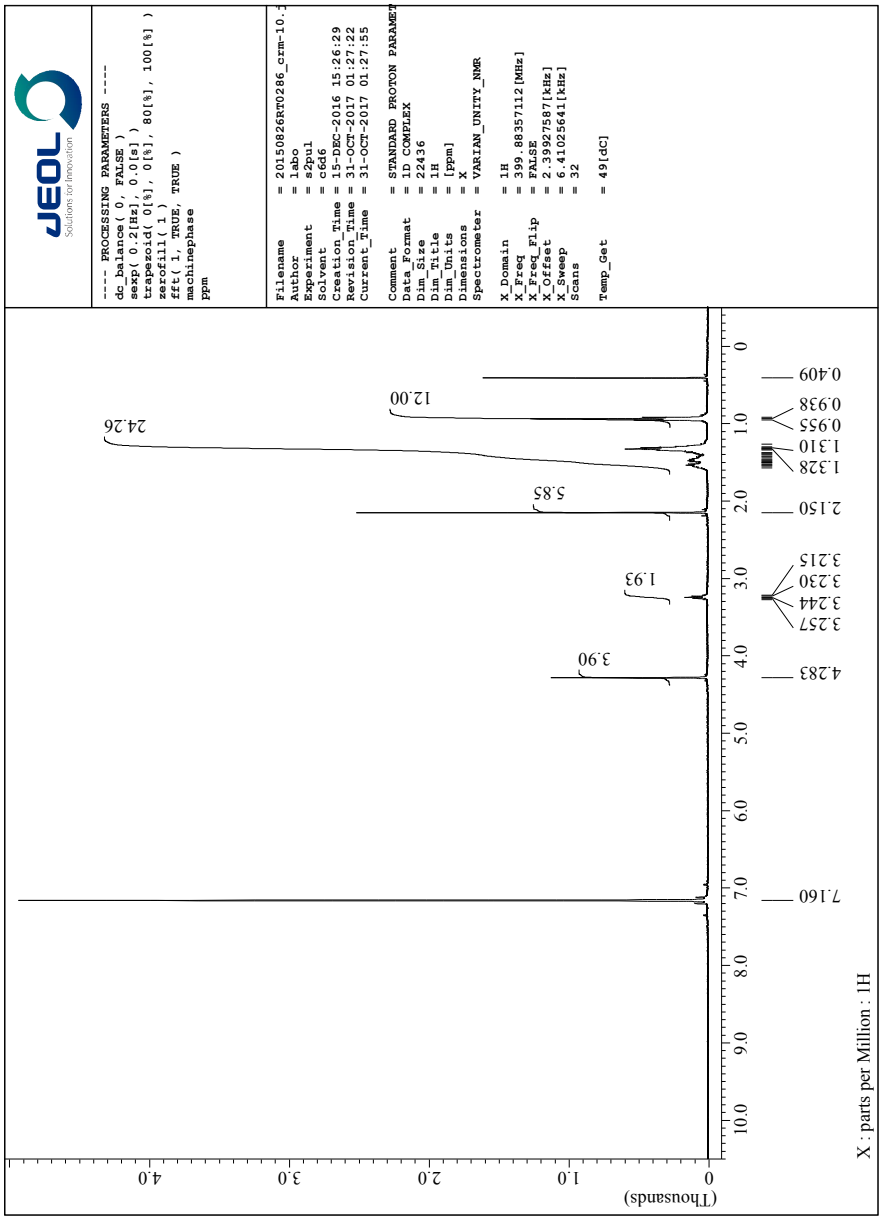

Figure S132. ^{1}H NMR spectrum of **3-NC** in $CDCl_3$.

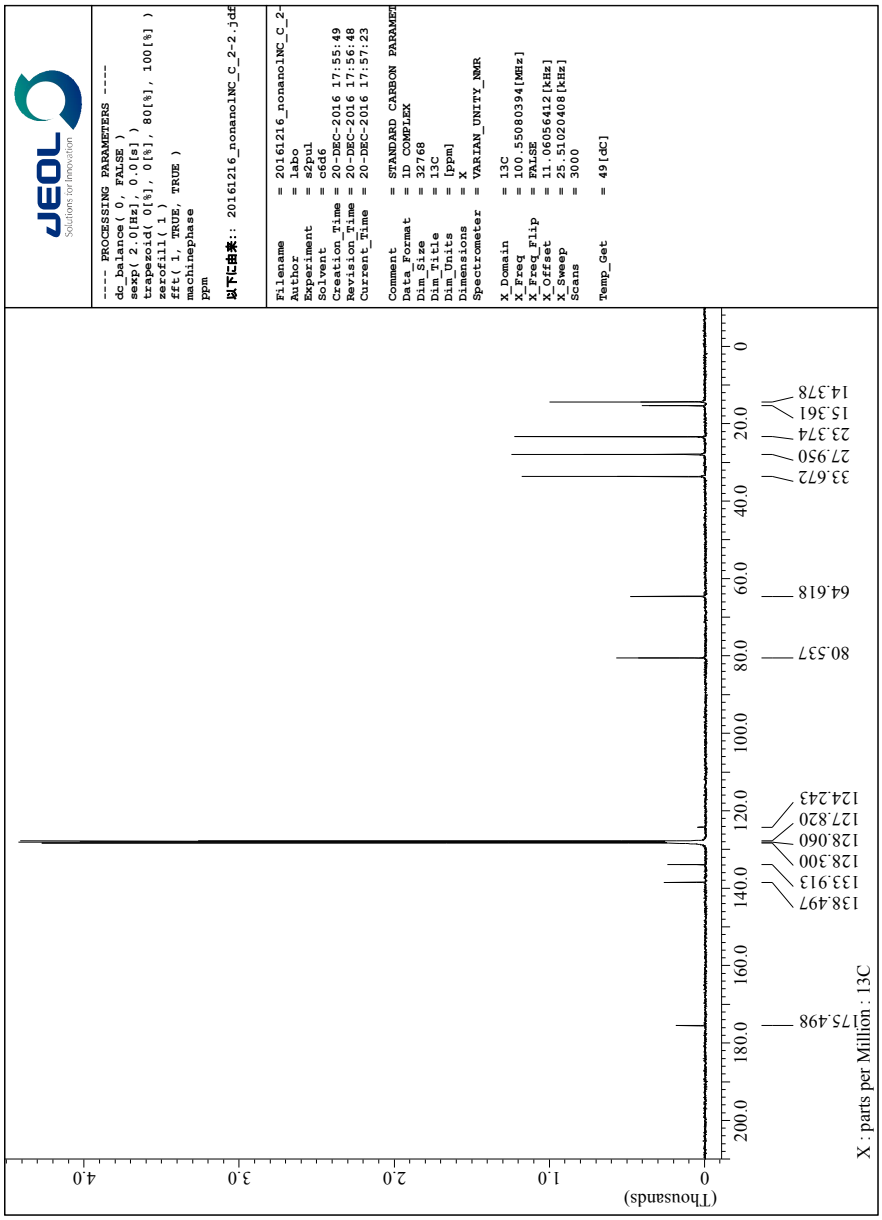

Figure S133. ^{13}C NMR spectrum of **3-NC** in $CDCl_3$.

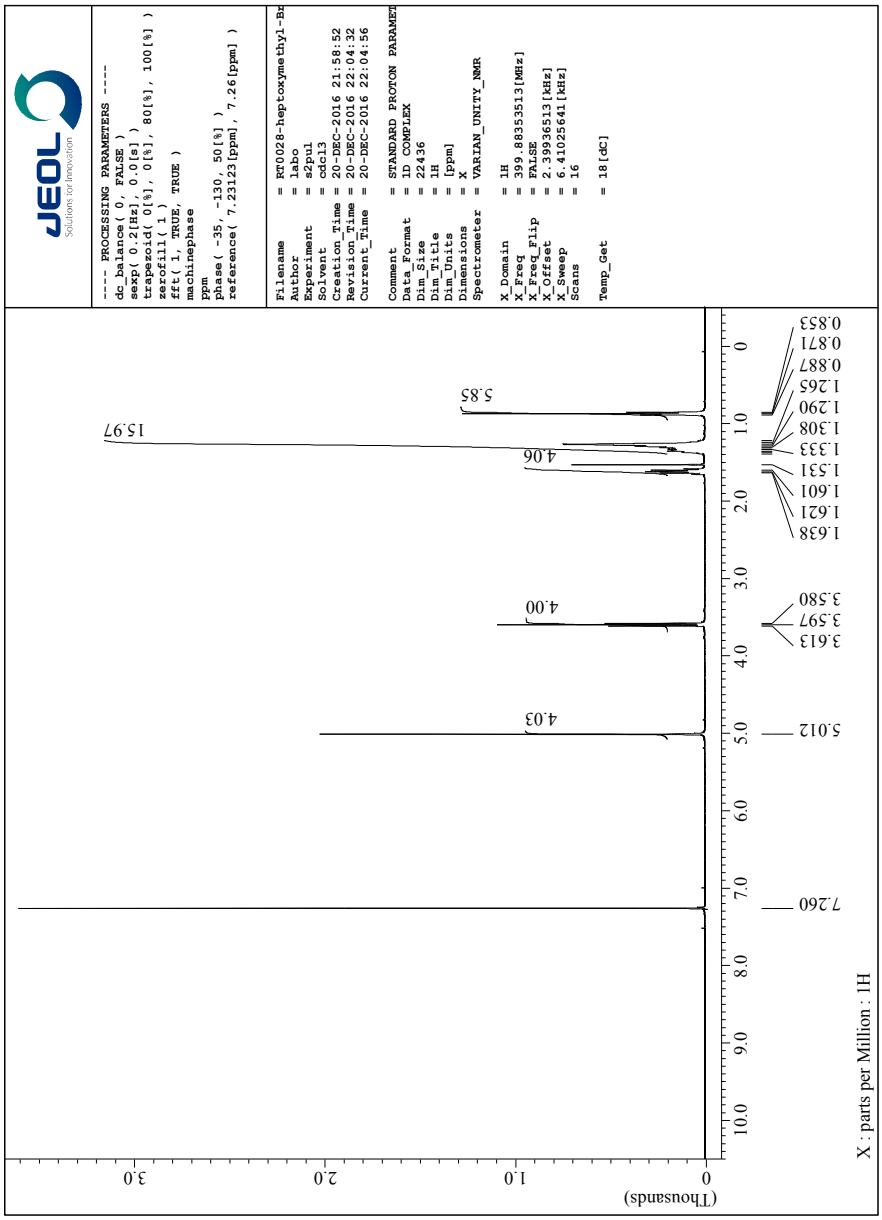

Figure S134. ^{1}H NMR spectrum of **4-Br** in $CDCl_3$.

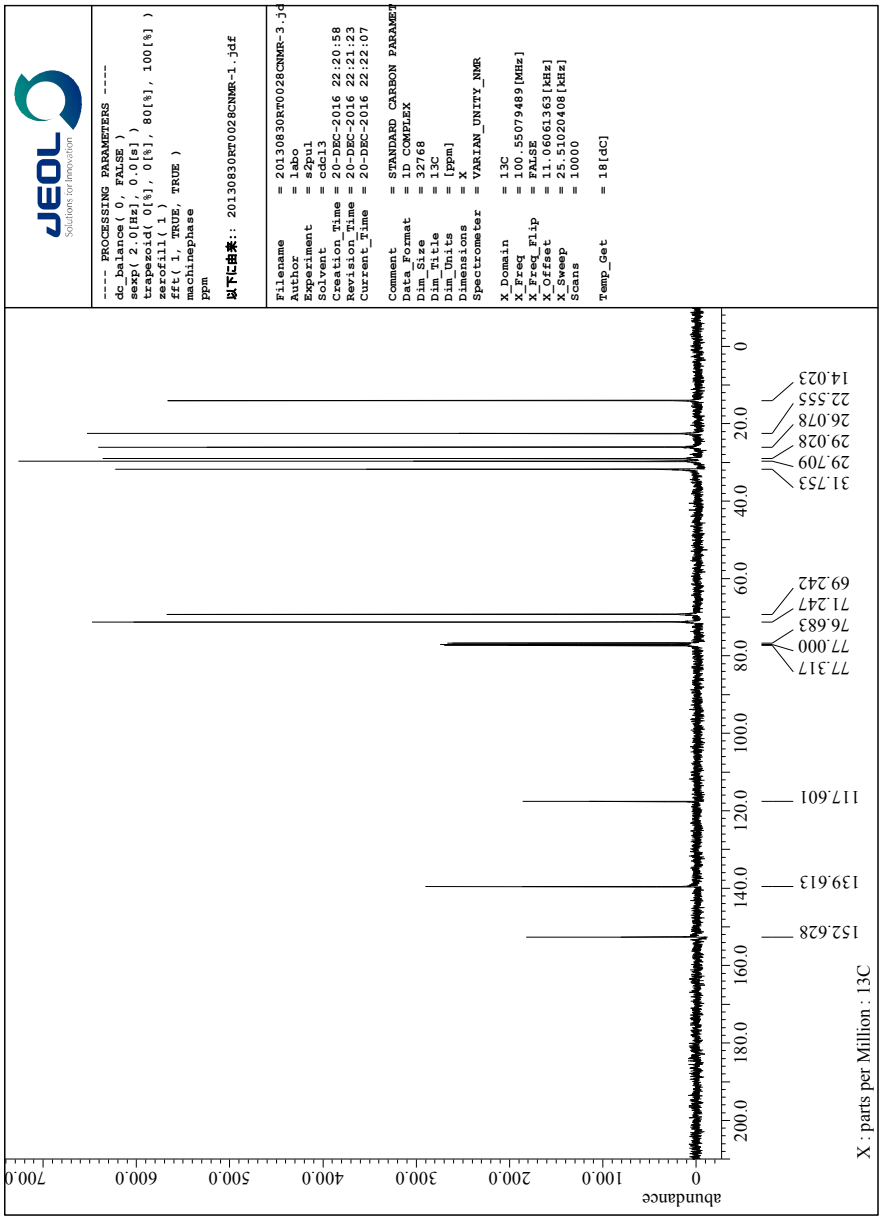

Figure S135. ^{13}C NMR spectrum of **4-Br** in $CDCl_3$.

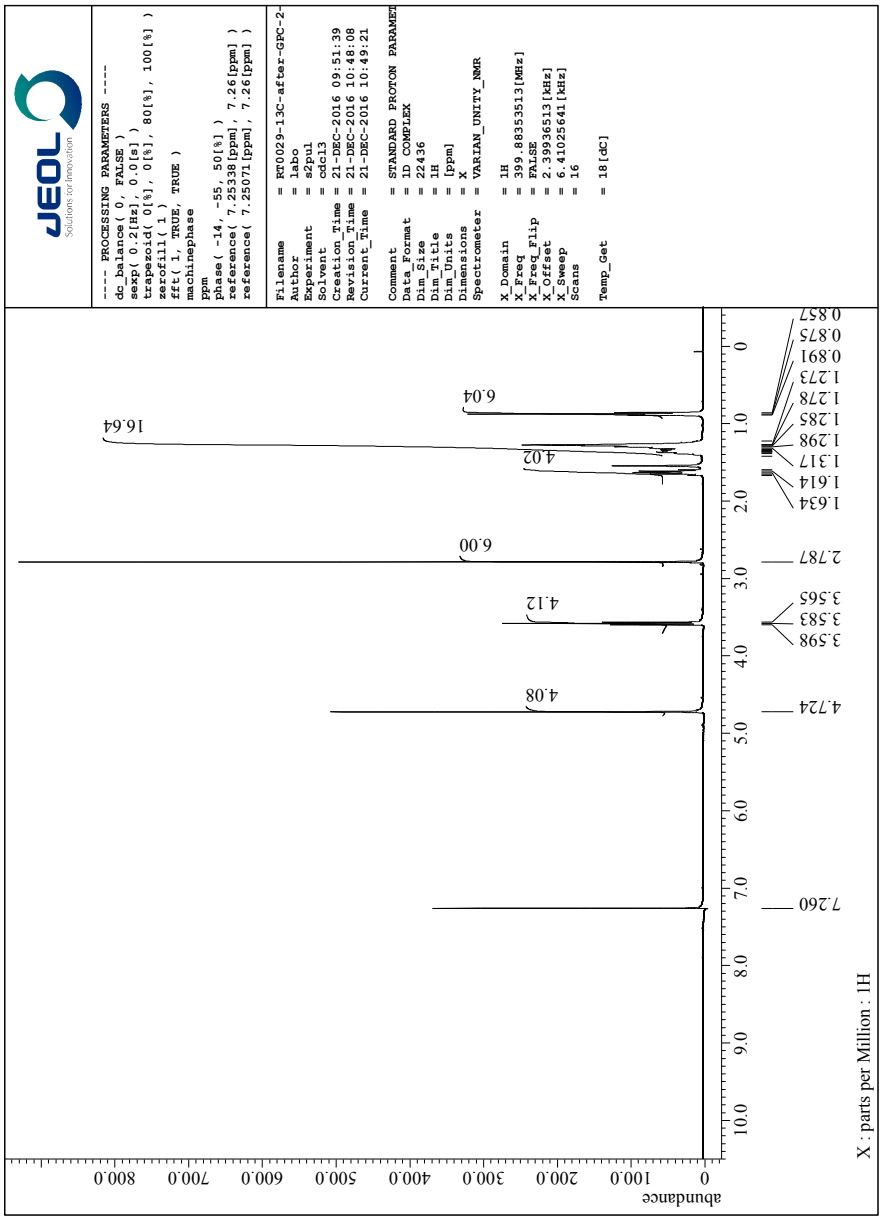

Figure S136. ^{1}H NMR spectrum of **4-Me** in $CDCl_3$.

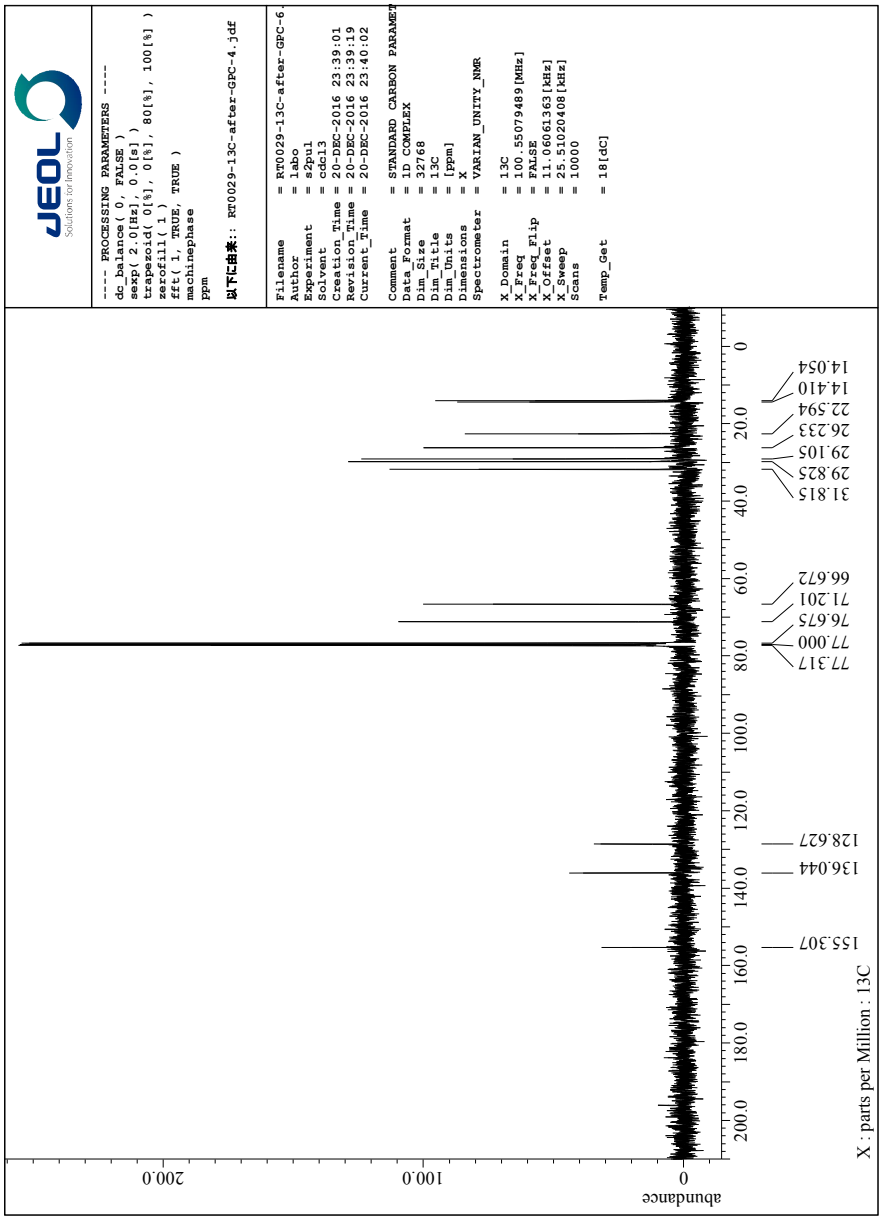

Figure S137. ^{13}C NMR spectrum of **4-Me** in $CDCl_3$.

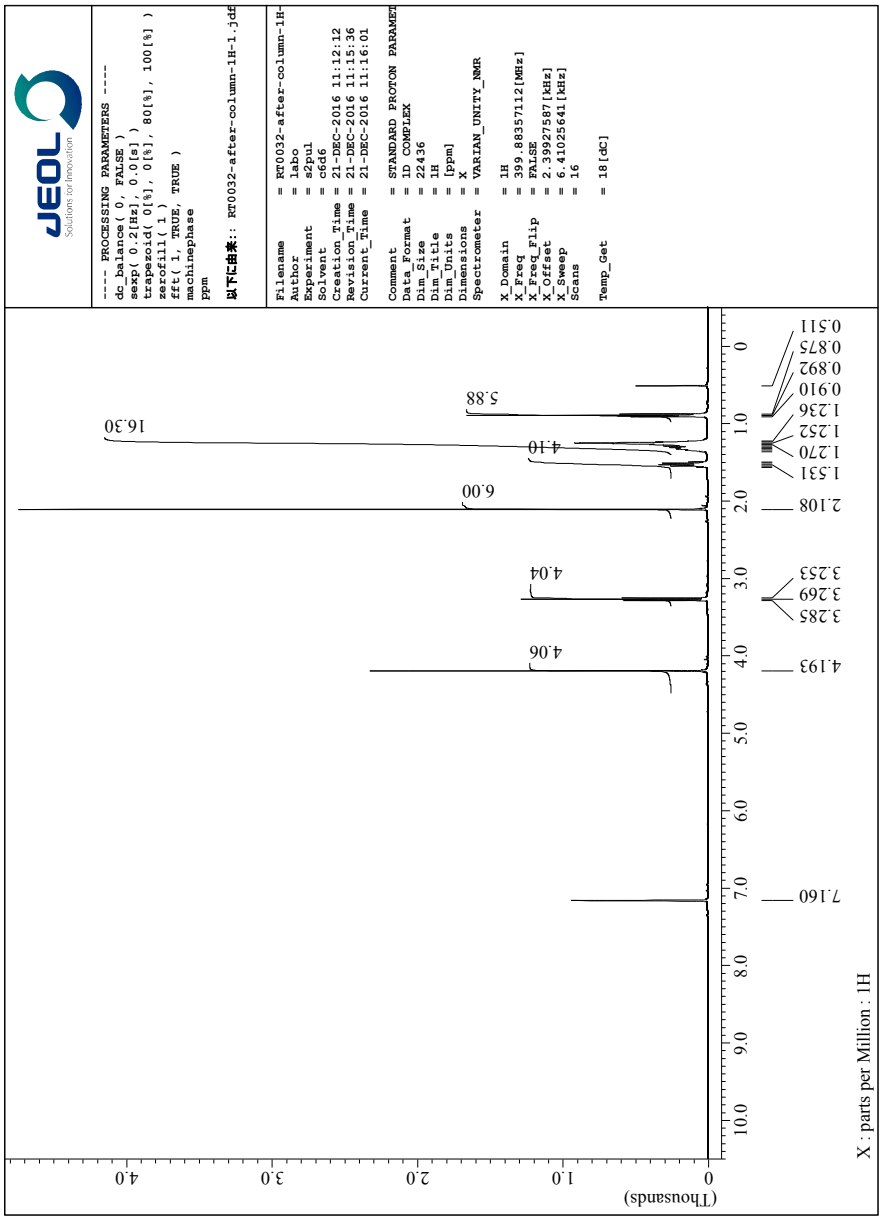

Figure S138. ^{1}H NMR spectrum of **4-NC** in $CDCl_3$.

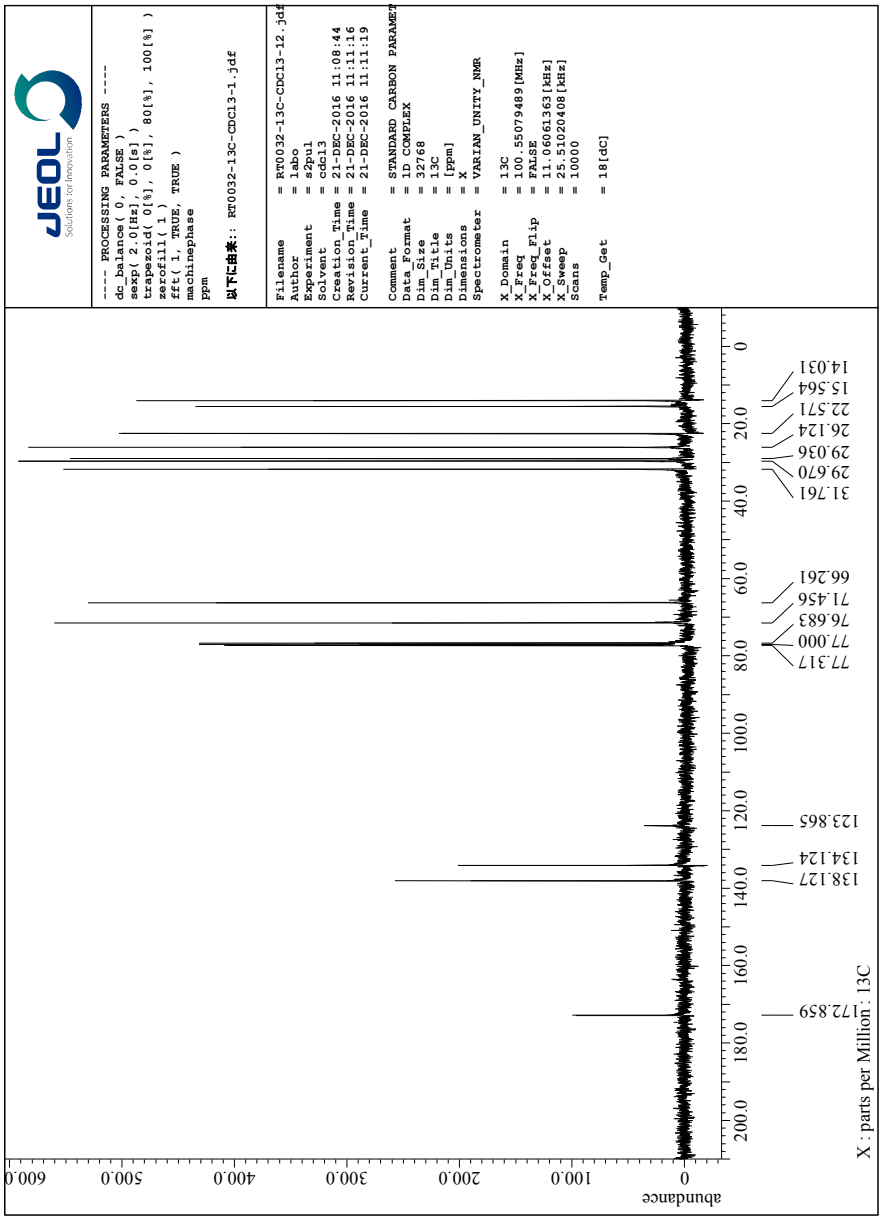

Figure S139. ^{13}C NMR spectrum of **4-NC** in $CDCl_3$.

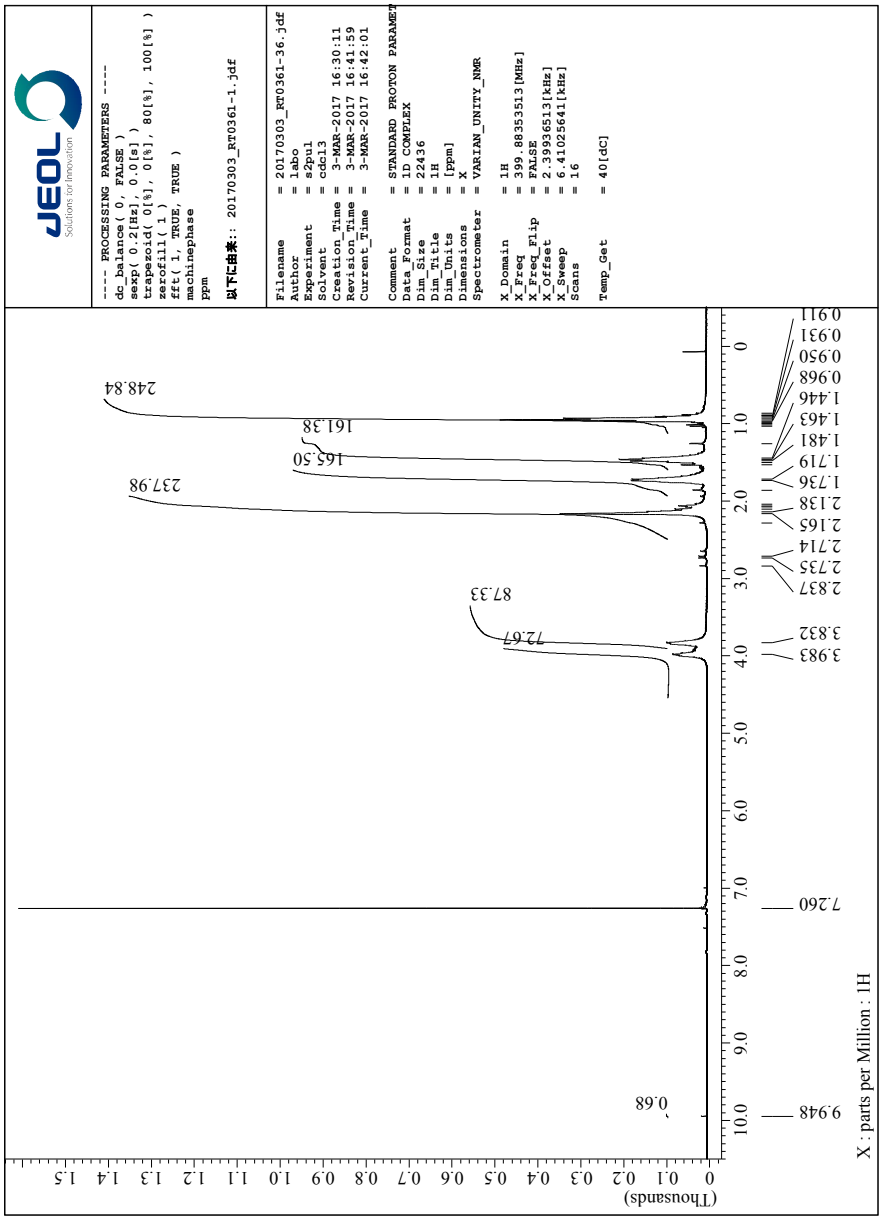

Figure S140. ^{1}H NMR spectrum of **1(40)** in $CDCl_3$.

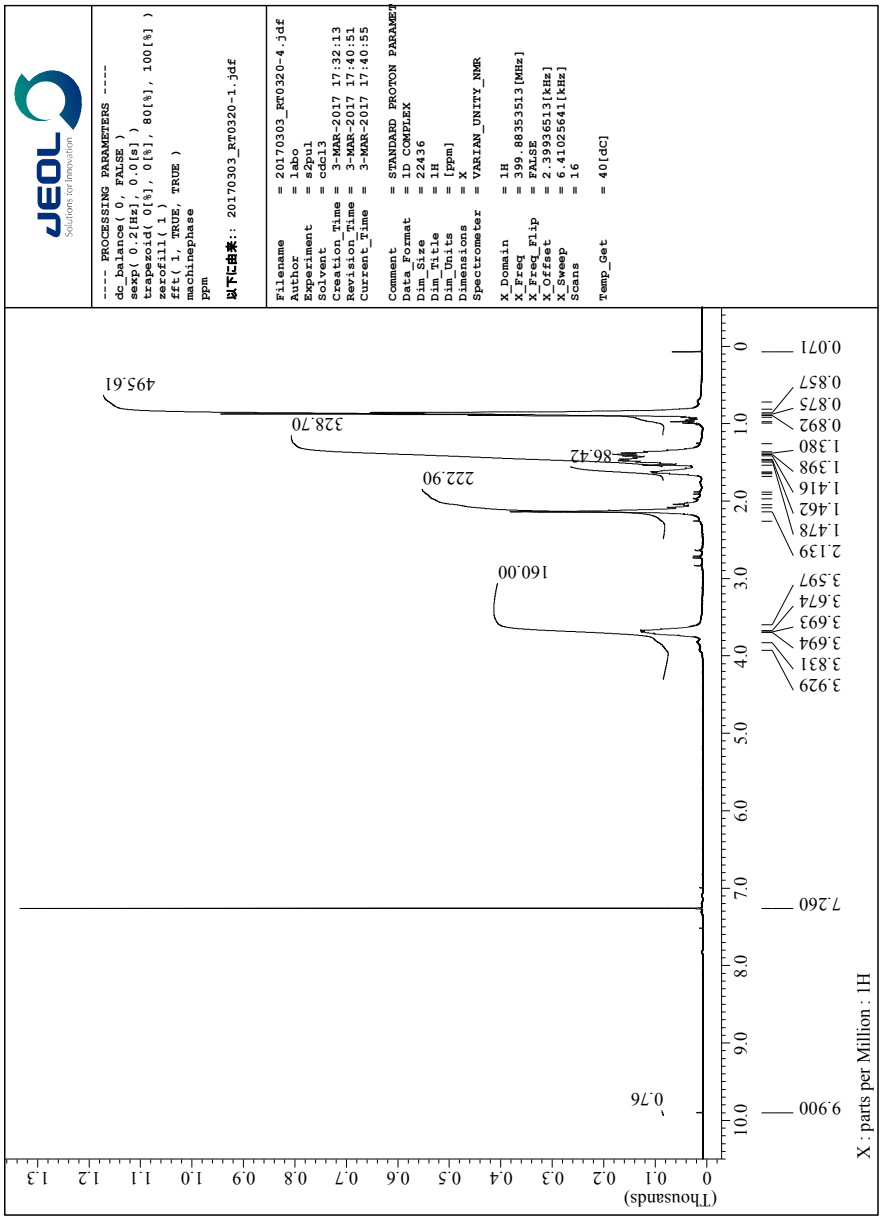

Figure S141. ^{1}H NMR spectrum of **2(40)** in $CDCl_3$.

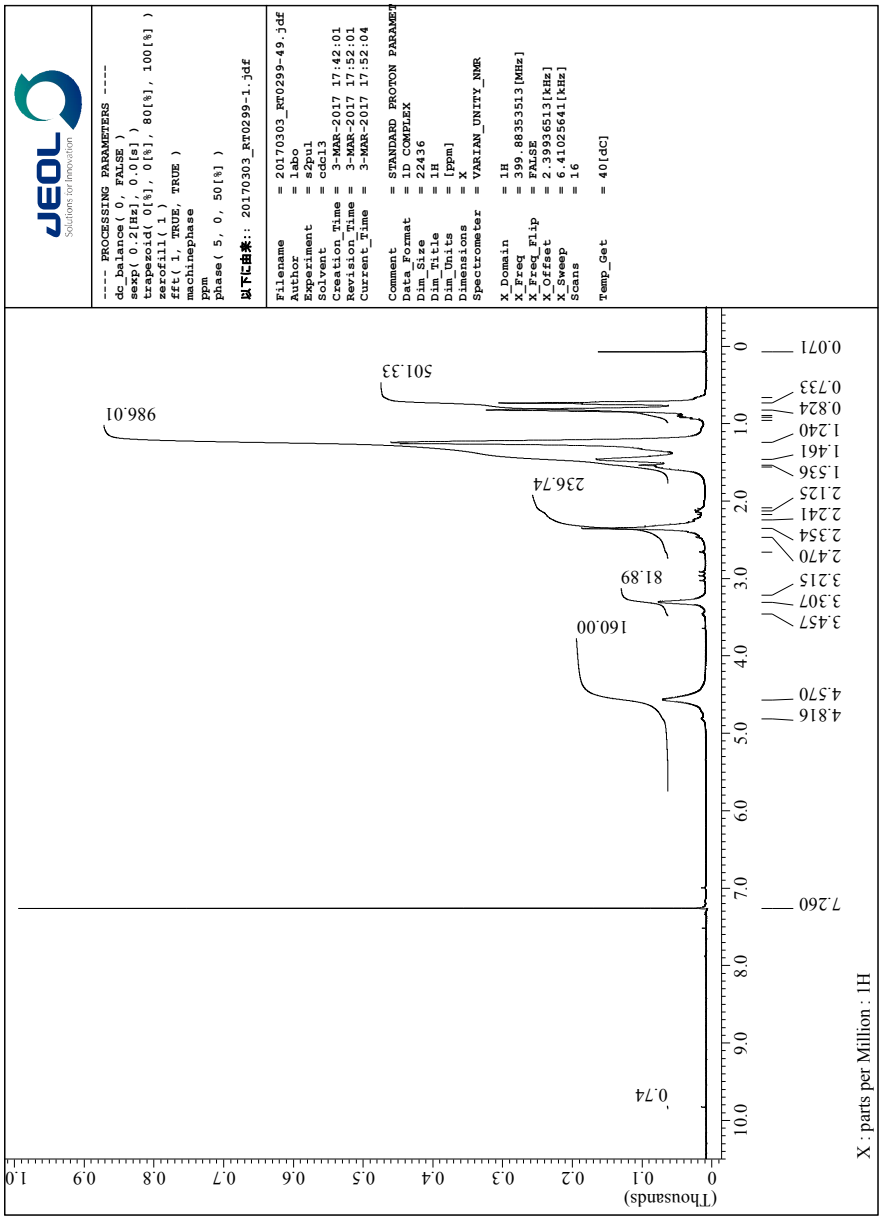

Figure S142. ^{1}H NMR spectrum of **3(40)** in $CDCl_3$.

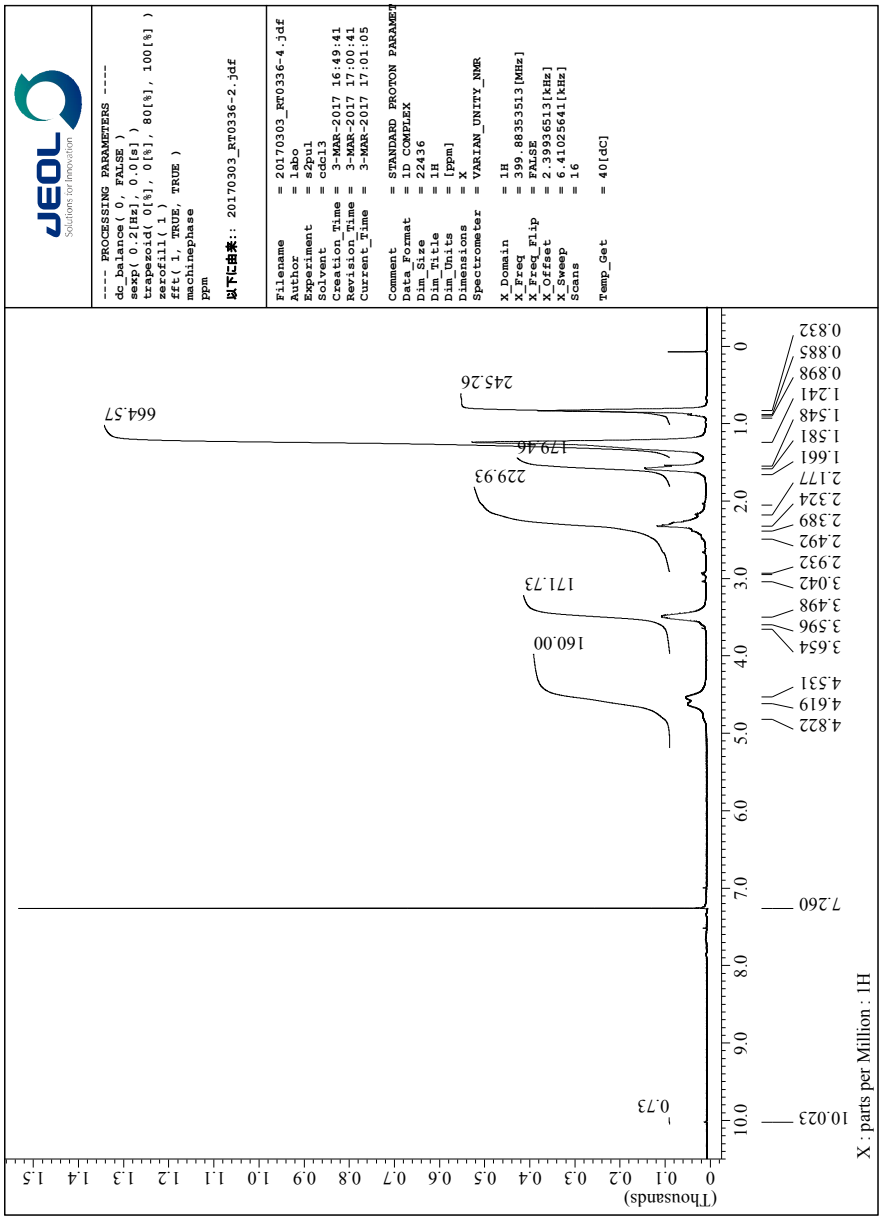

Figure S143. ^{1}H NMR spectrum of **4(40)** in $CDCl_3$.

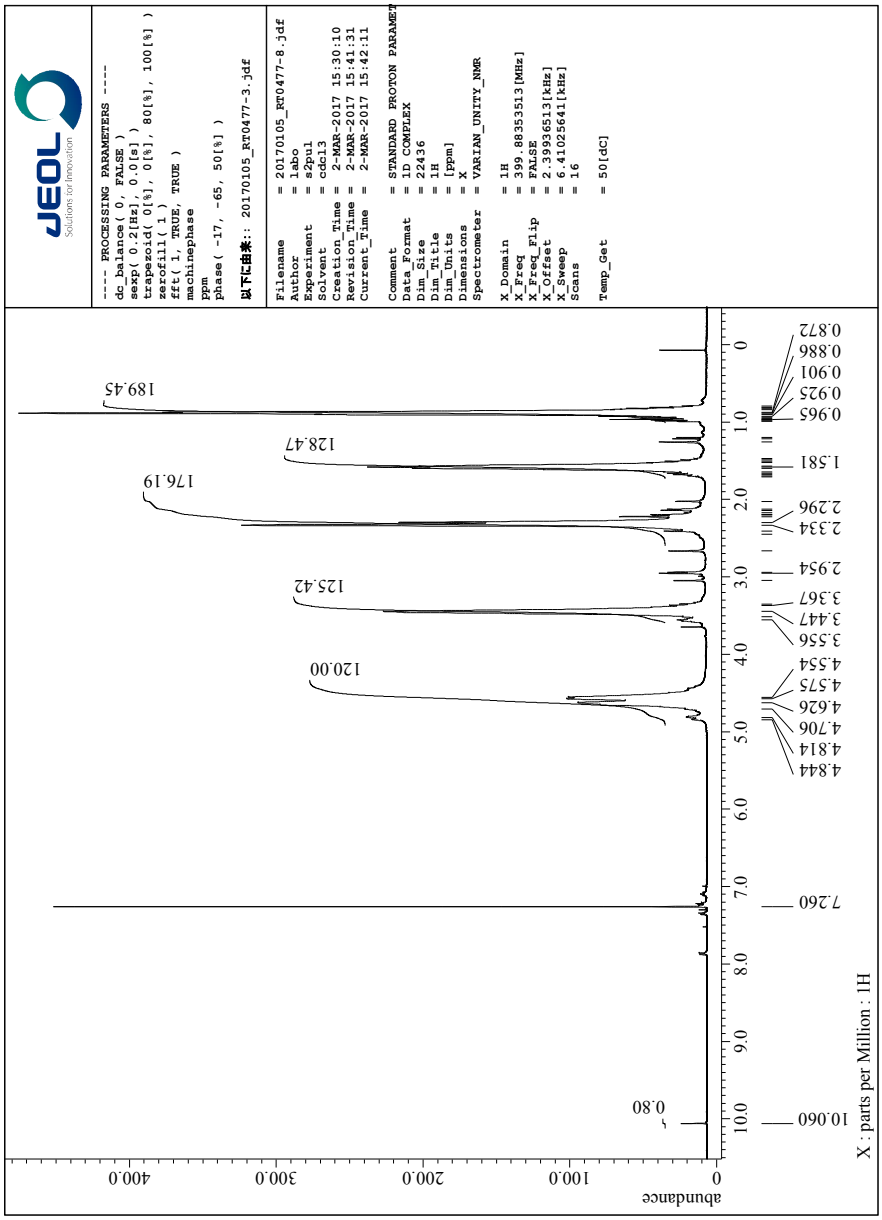

Figure S144. ^{1}H NMR spectrum of **5(30)** in $CDCl_3$.

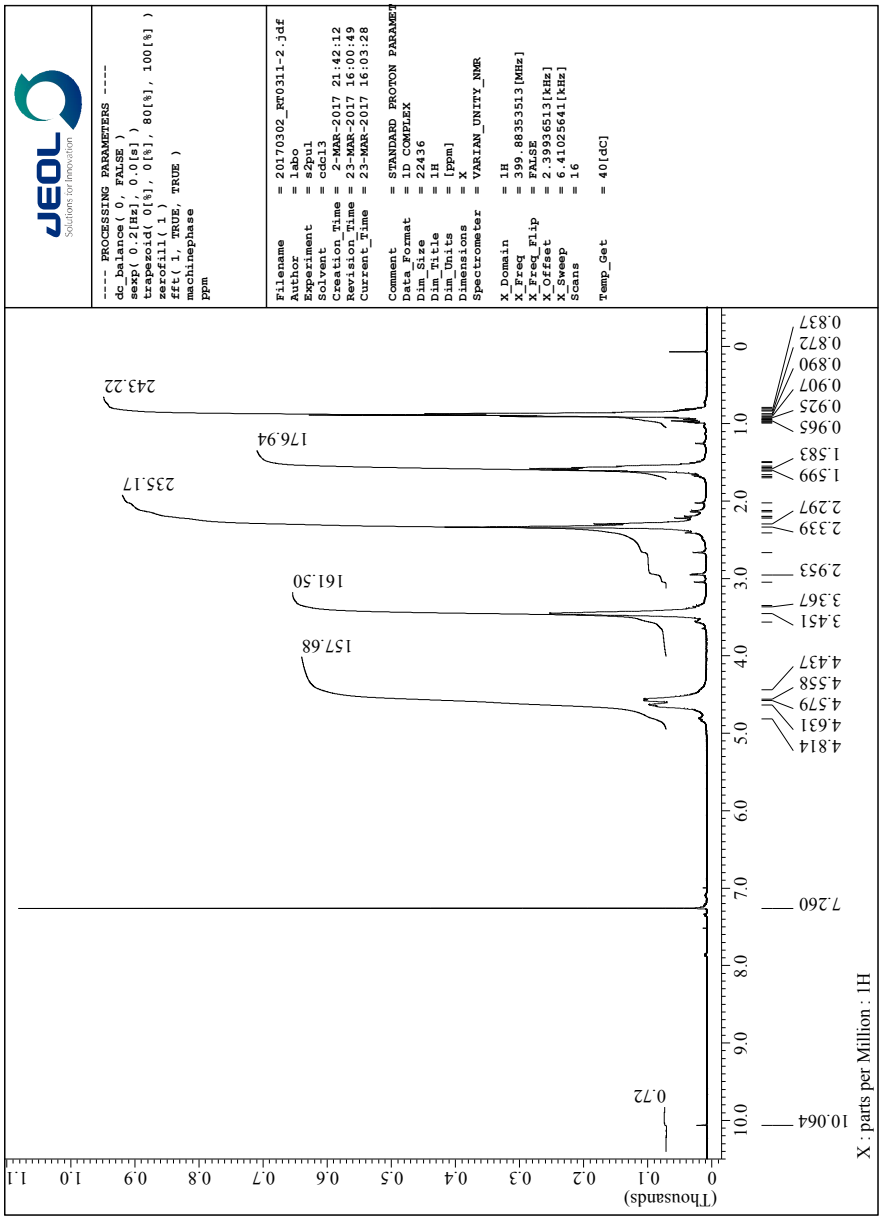

Figure S145. ^{1}H NMR spectrum of **5(40)** in $CDCl_3$.

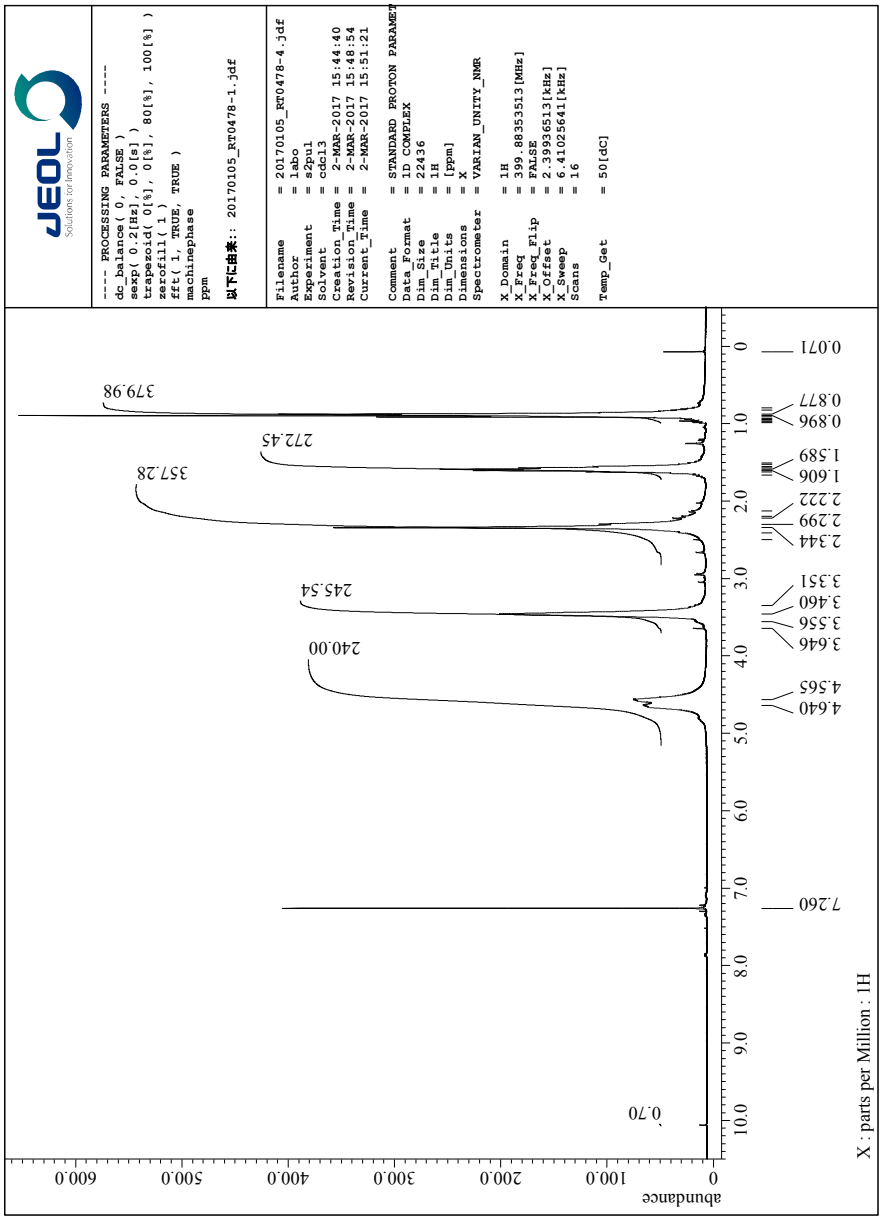

Figure S146. ^{1}H NMR spectrum of **5(60)** in $CDCl_3$.

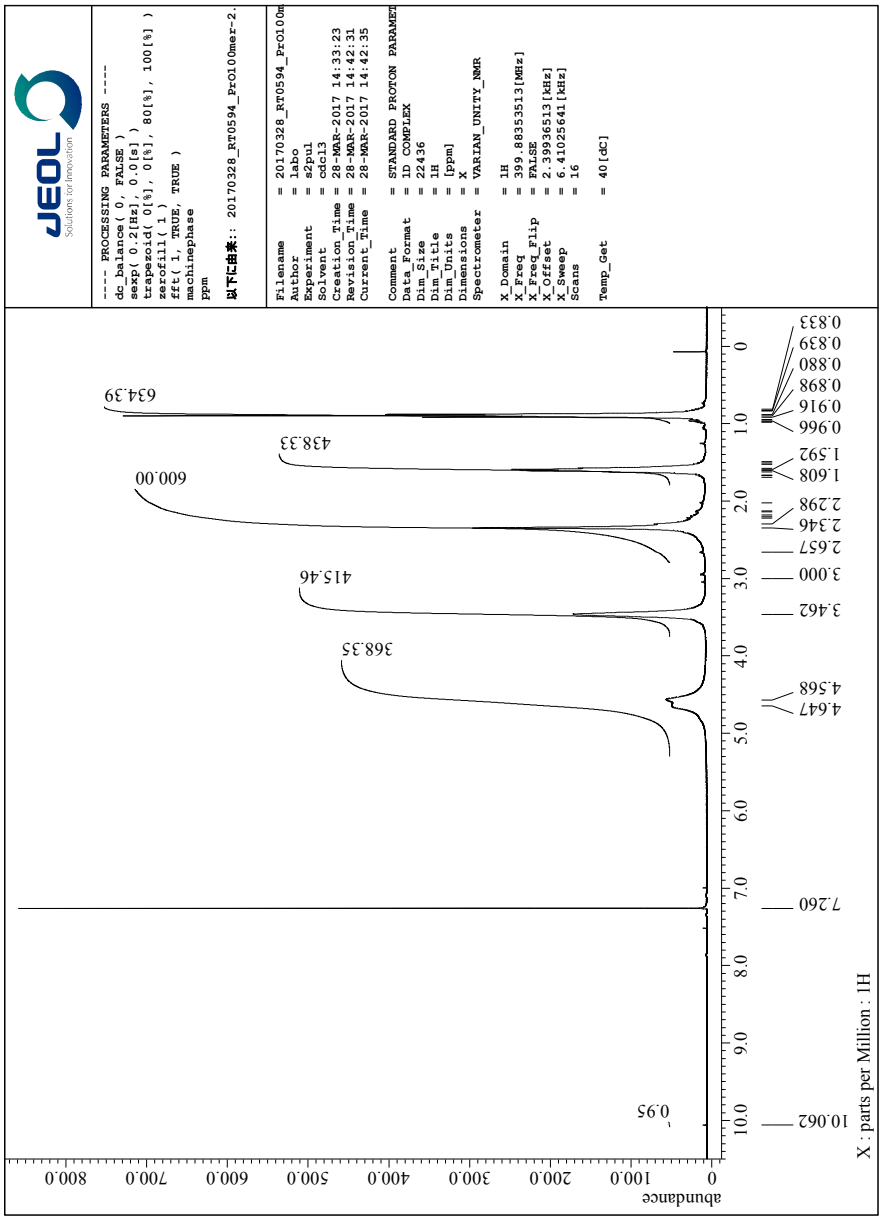

Figure S147. ^{1}H NMR spectrum of **5(100)** in $CDCl_3$.

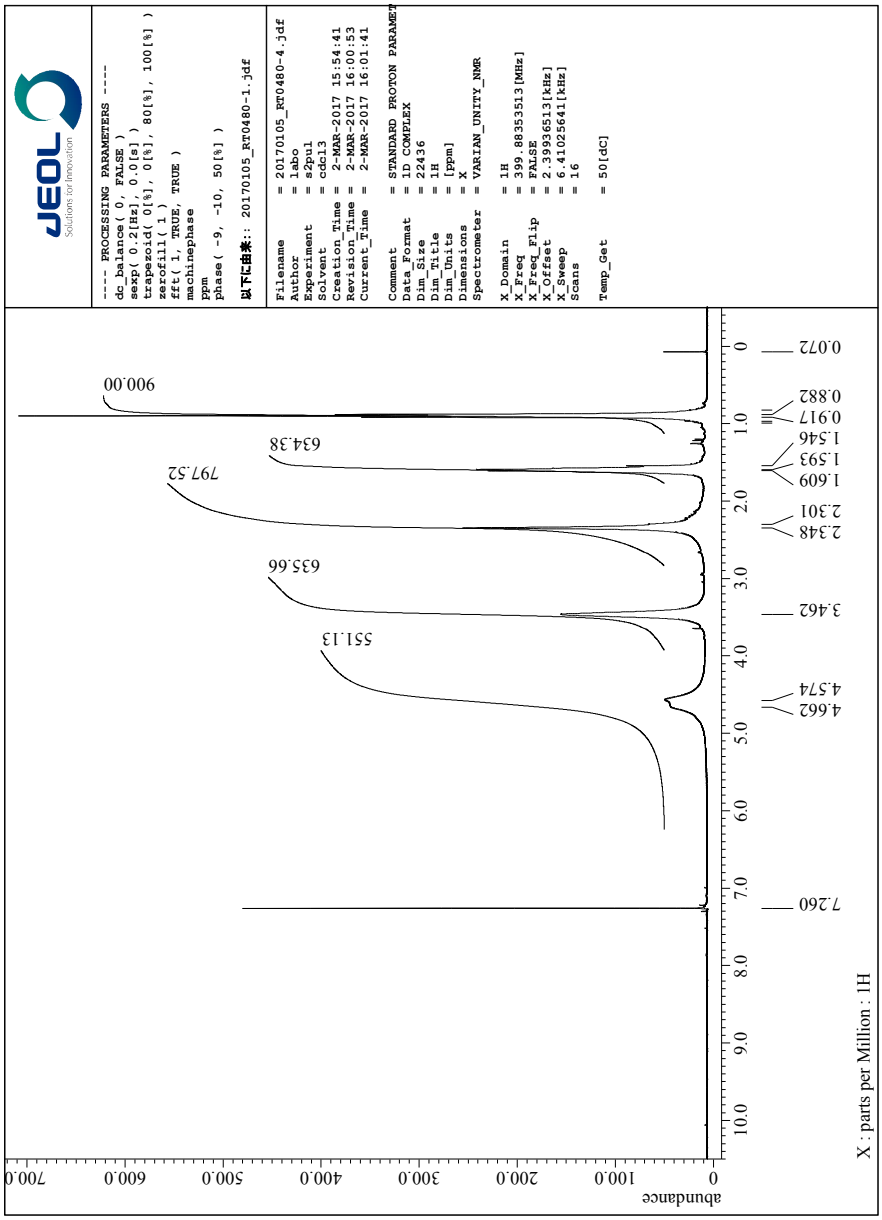

Figure S148. ^{1}H NMR spectrum of **5(150)** in $CDCl_3$.

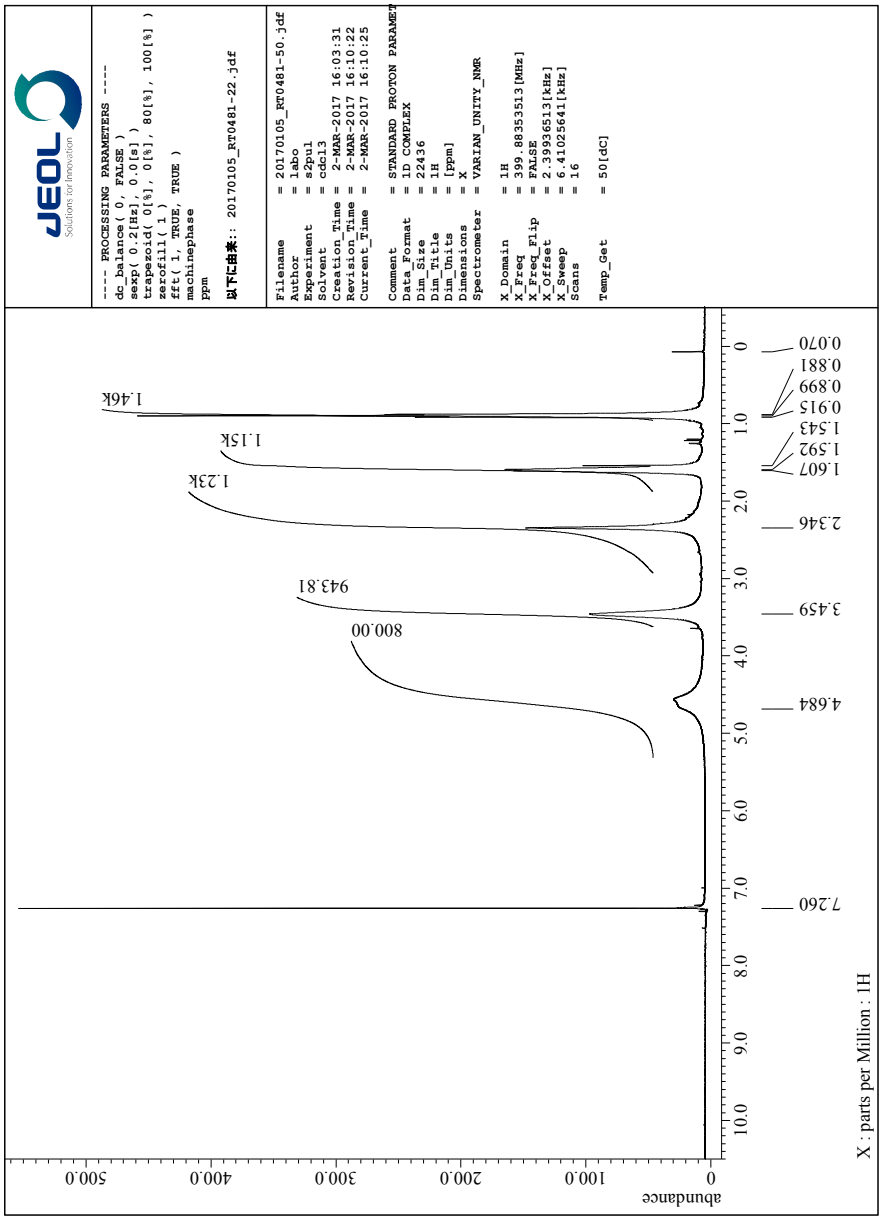

Figure S149. ^{1}H NMR spectrum of **5(200)** in $CDCl_3$.

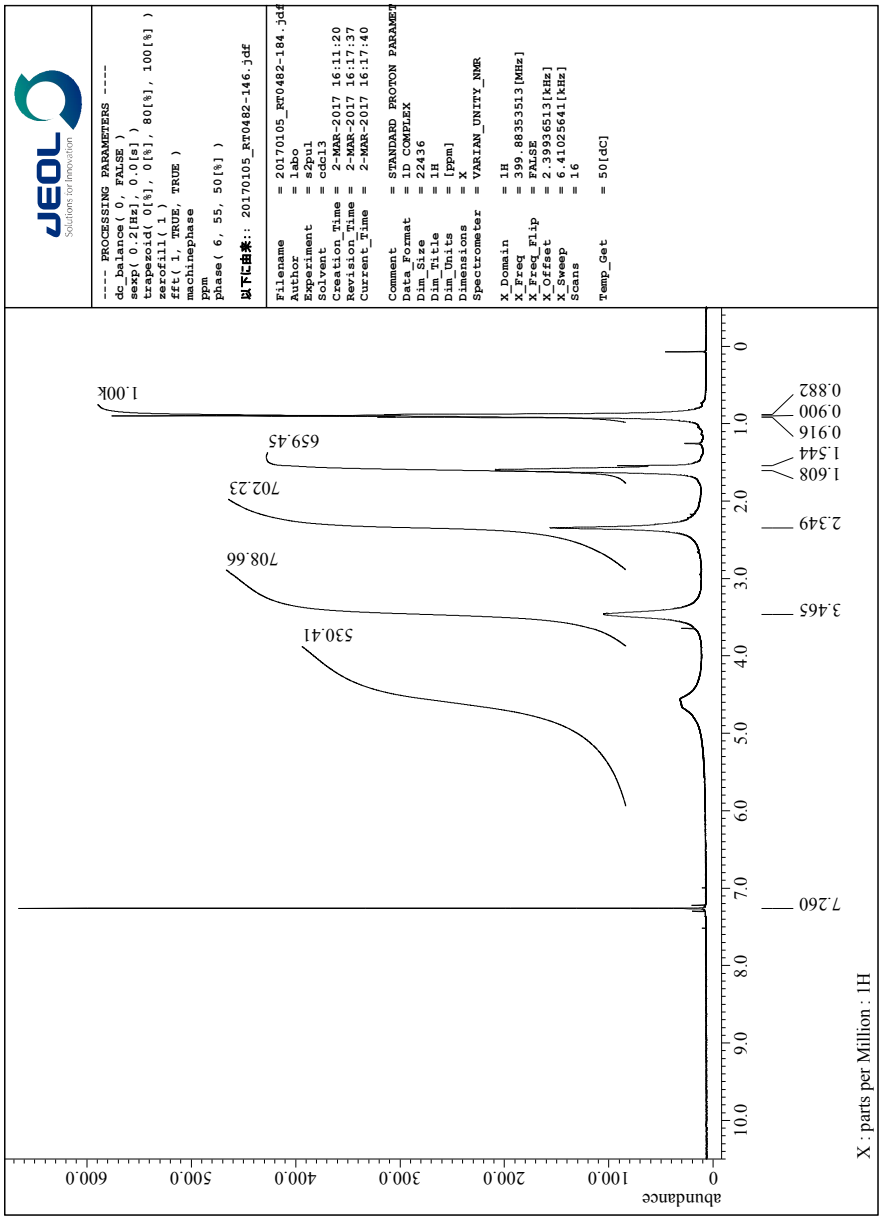

Figure S150. ^{1}H NMR spectrum of **5(250)** in $CDCl_3$.

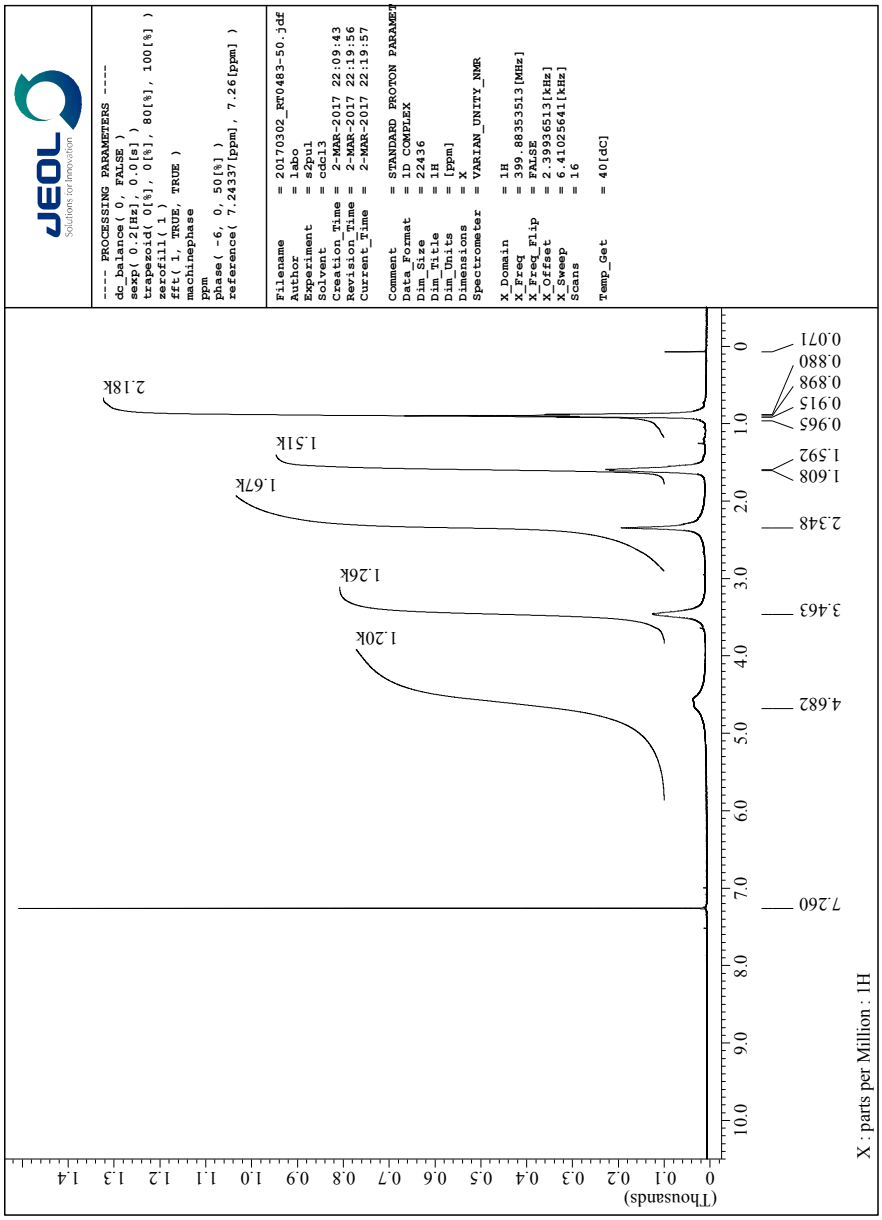

Figure S151. ^{1}H NMR spectrum of **5(300)** in $CDCl_3$.

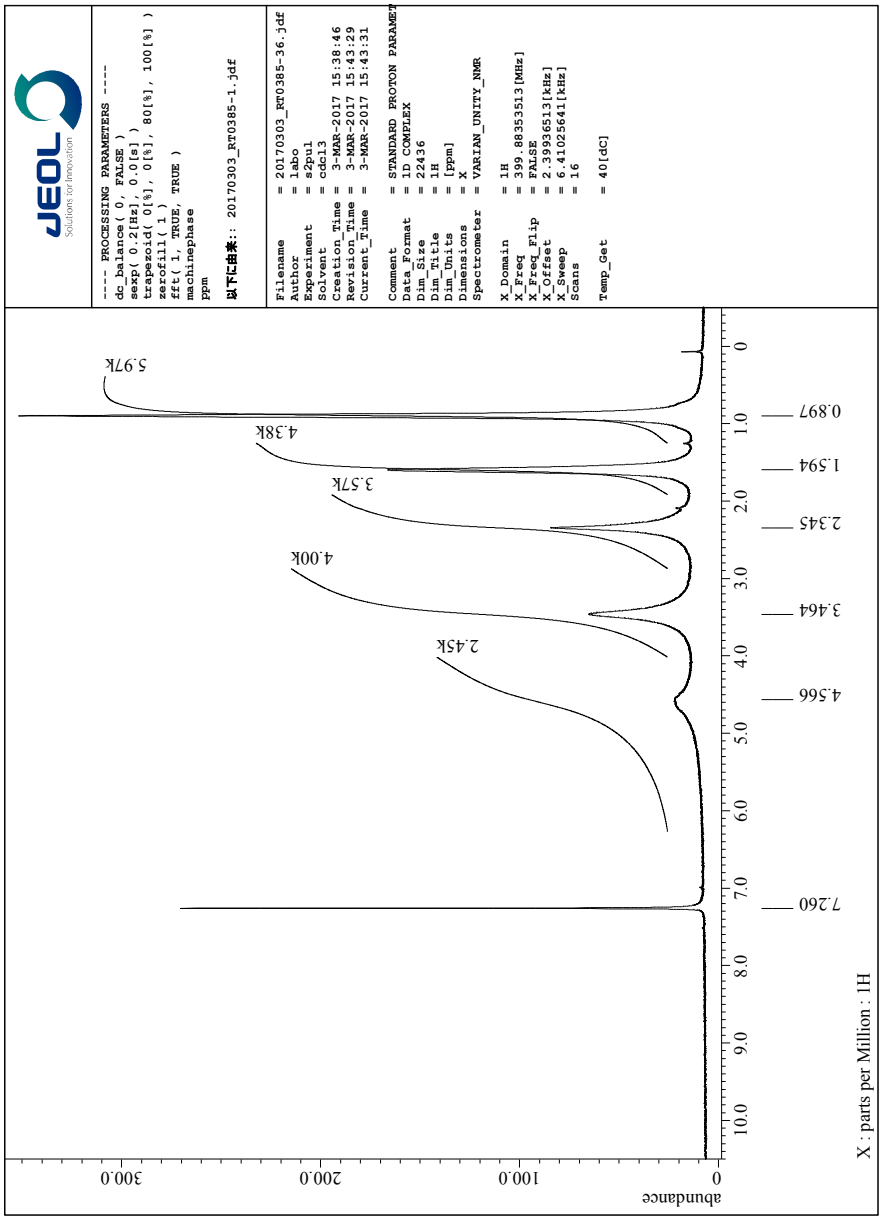

Figure S152. ^{1}H NMR spectrum of **5(1000)** in $CDCl_3$.

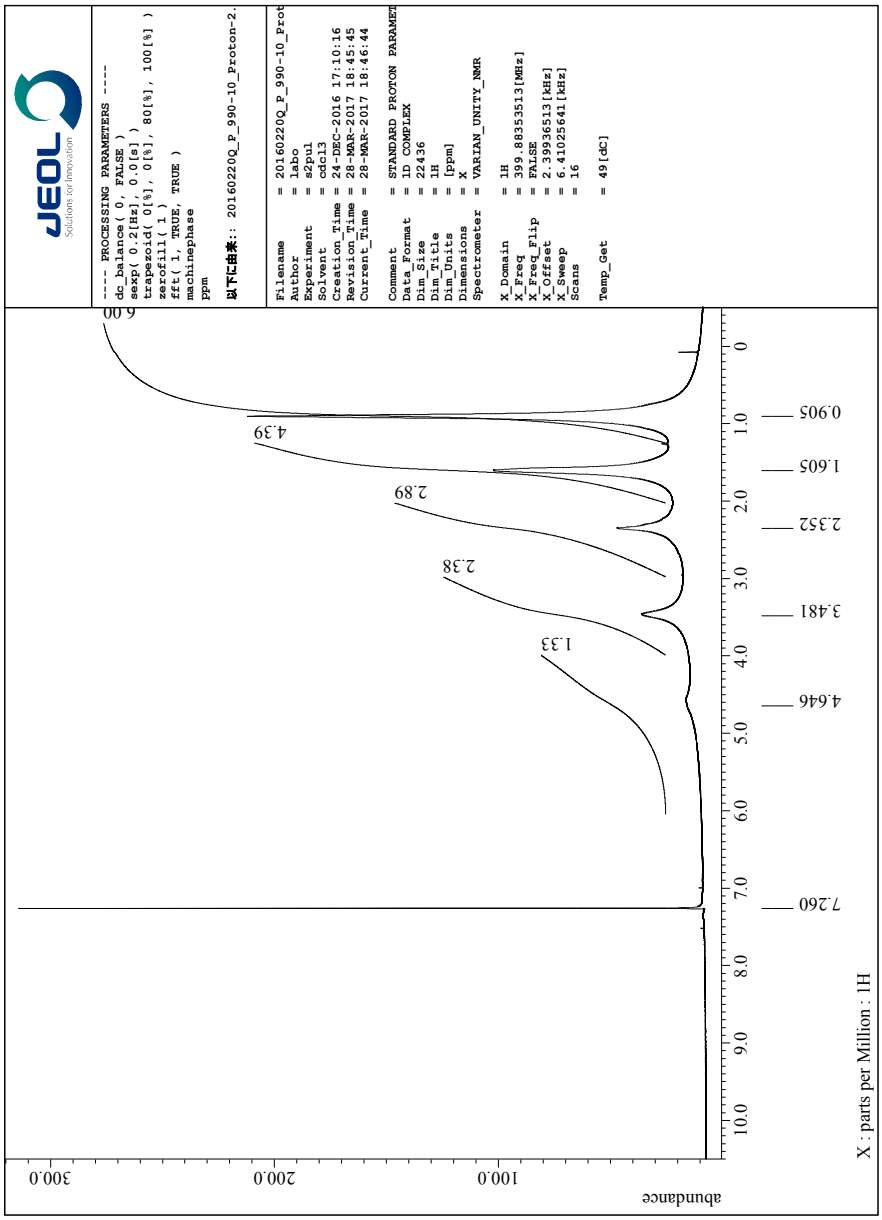

Figure S153. ^{1}H NMR spectrum of **L1** in $CDCl_3$.

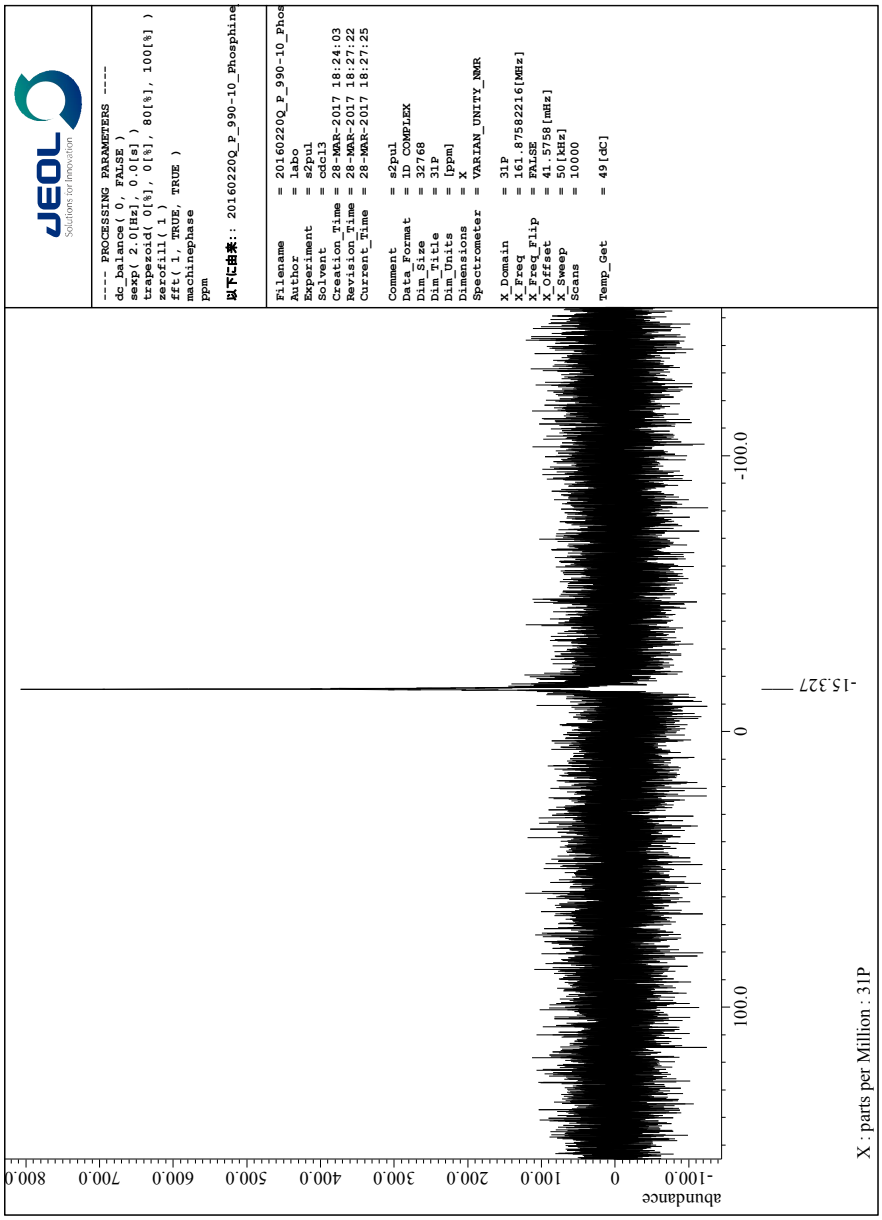

Figure S154. ^{31}P NMR spectrum of **L1** in $CDCl_3$.

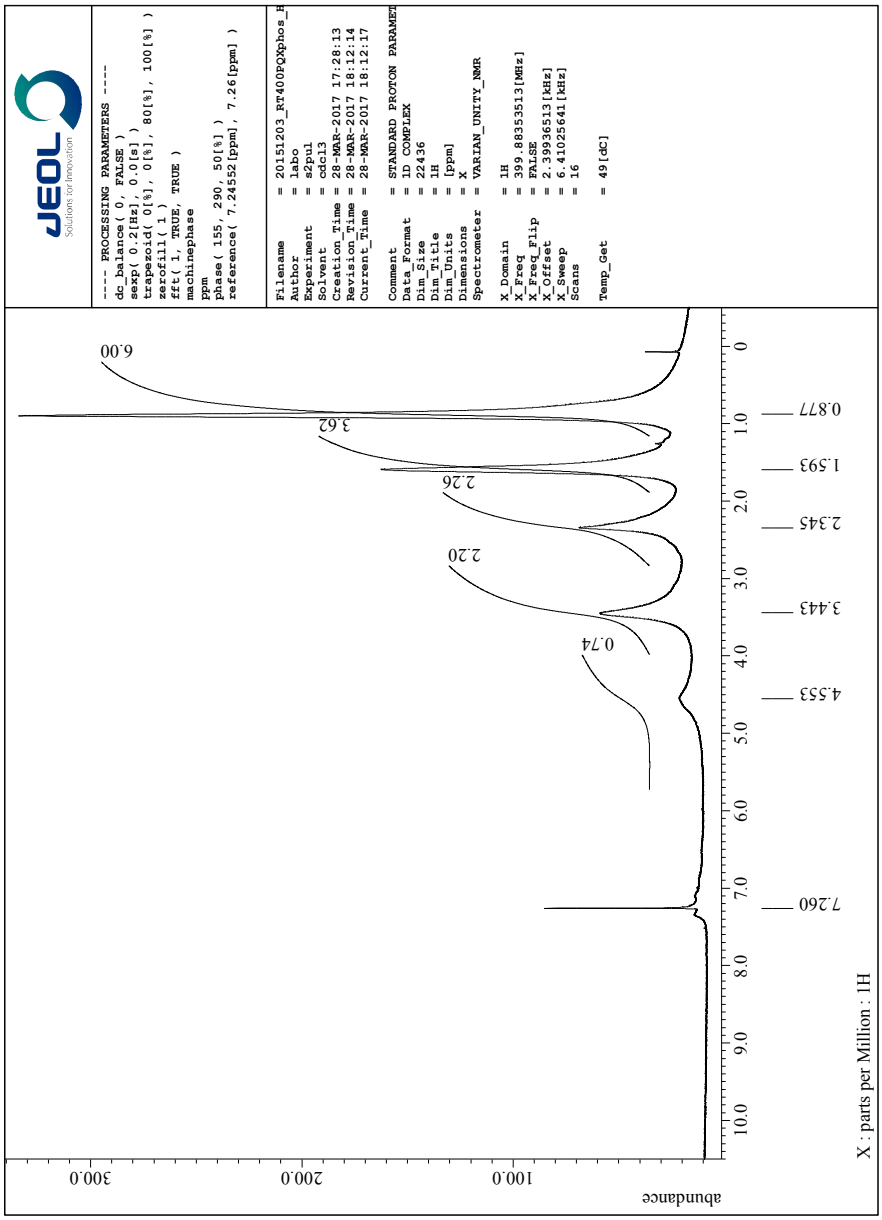

Figure S155. ^{1}H NMR spectrum of **L2** in $CDCl_3$.

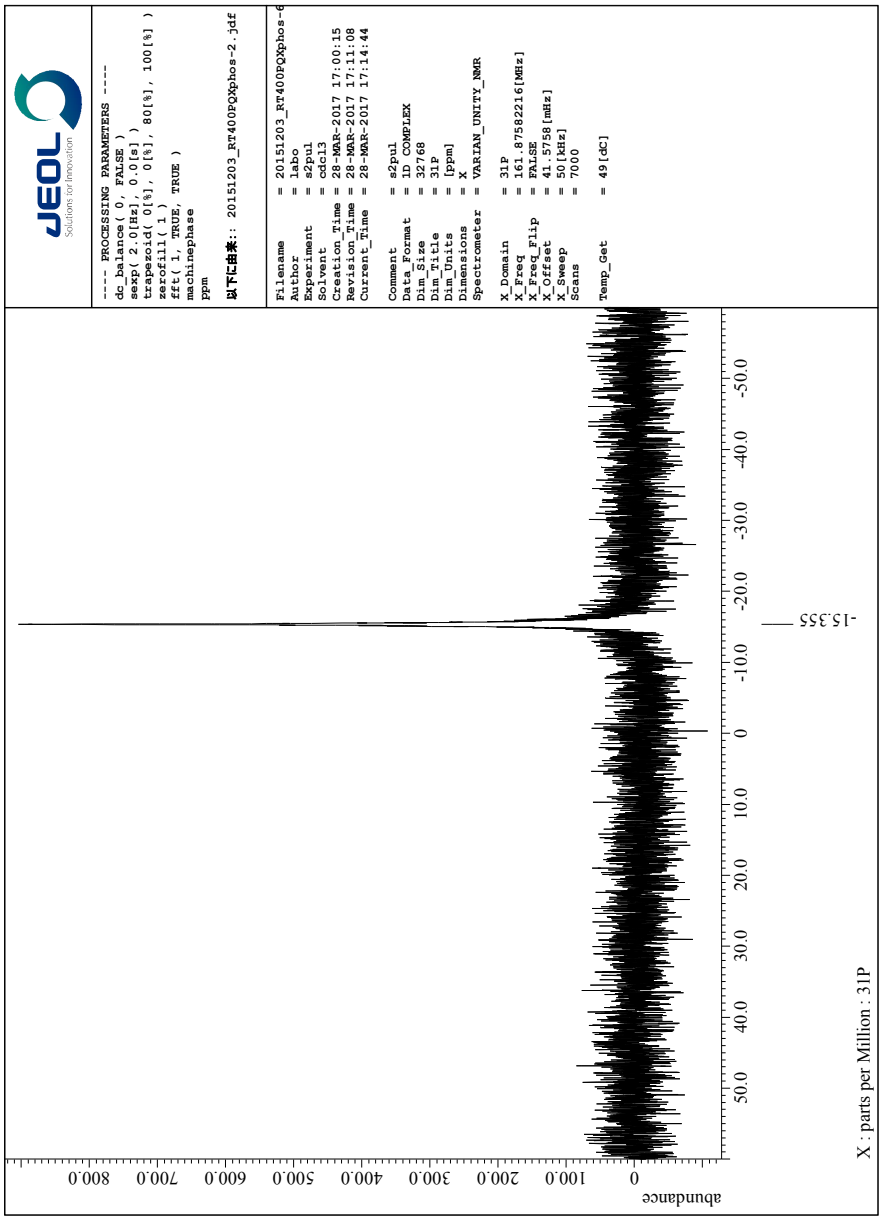

Figure S156. ^{31}P NMR spectrum of **L2** in $CDCl_3$.

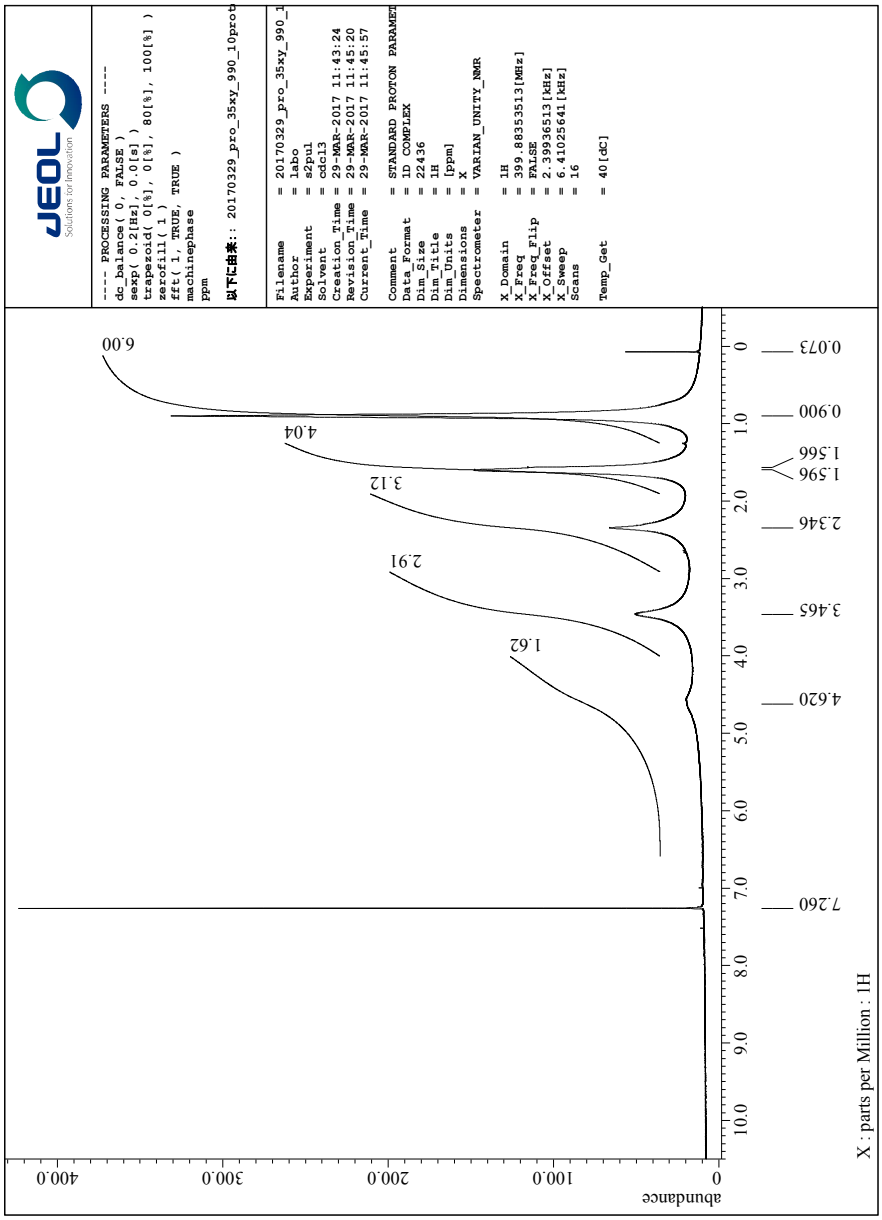

Figure S157. ^{1}H NMR spectrum of **L6** in $CDCl_3$.

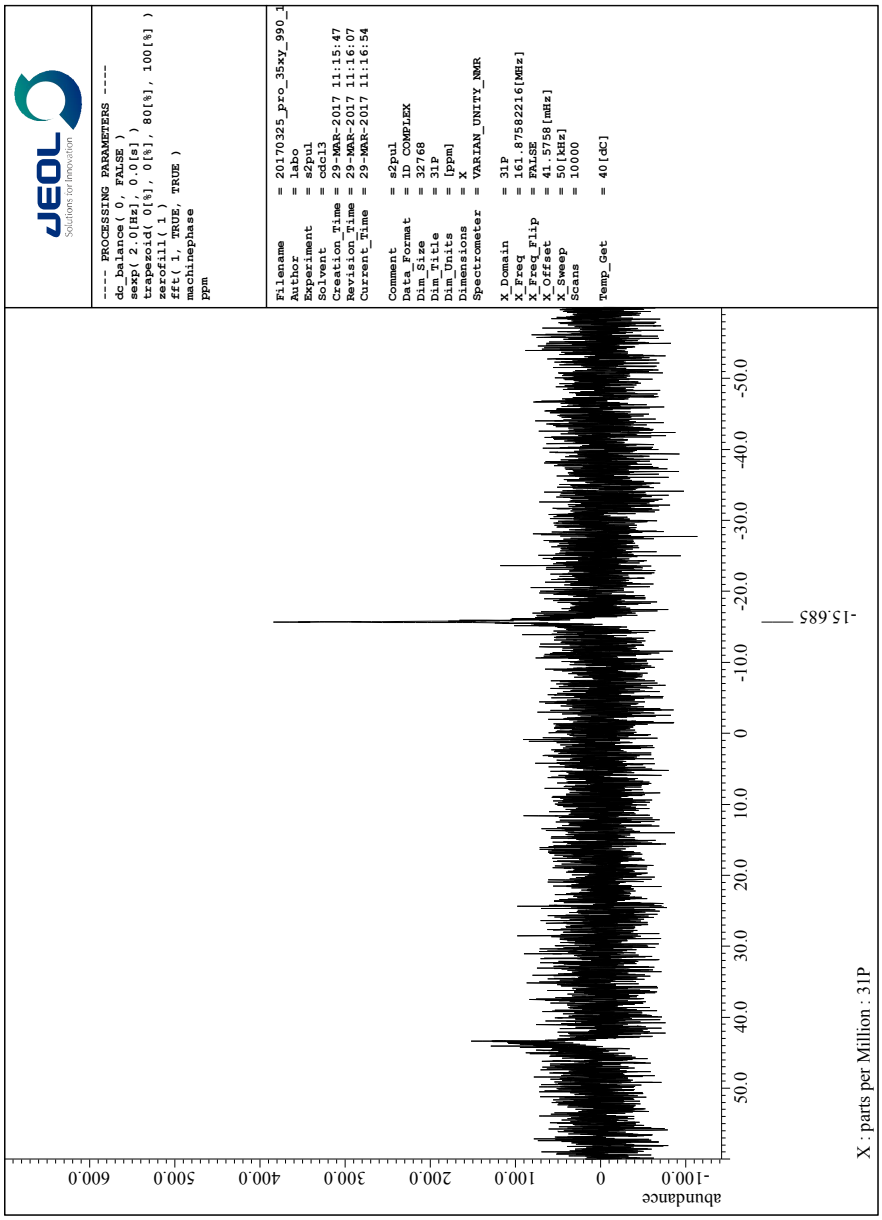

Figure S158. ^{31}P NMR spectrum of **L6** in $CDCl_3$.

7 Chiral HPLC traces of the Reactions

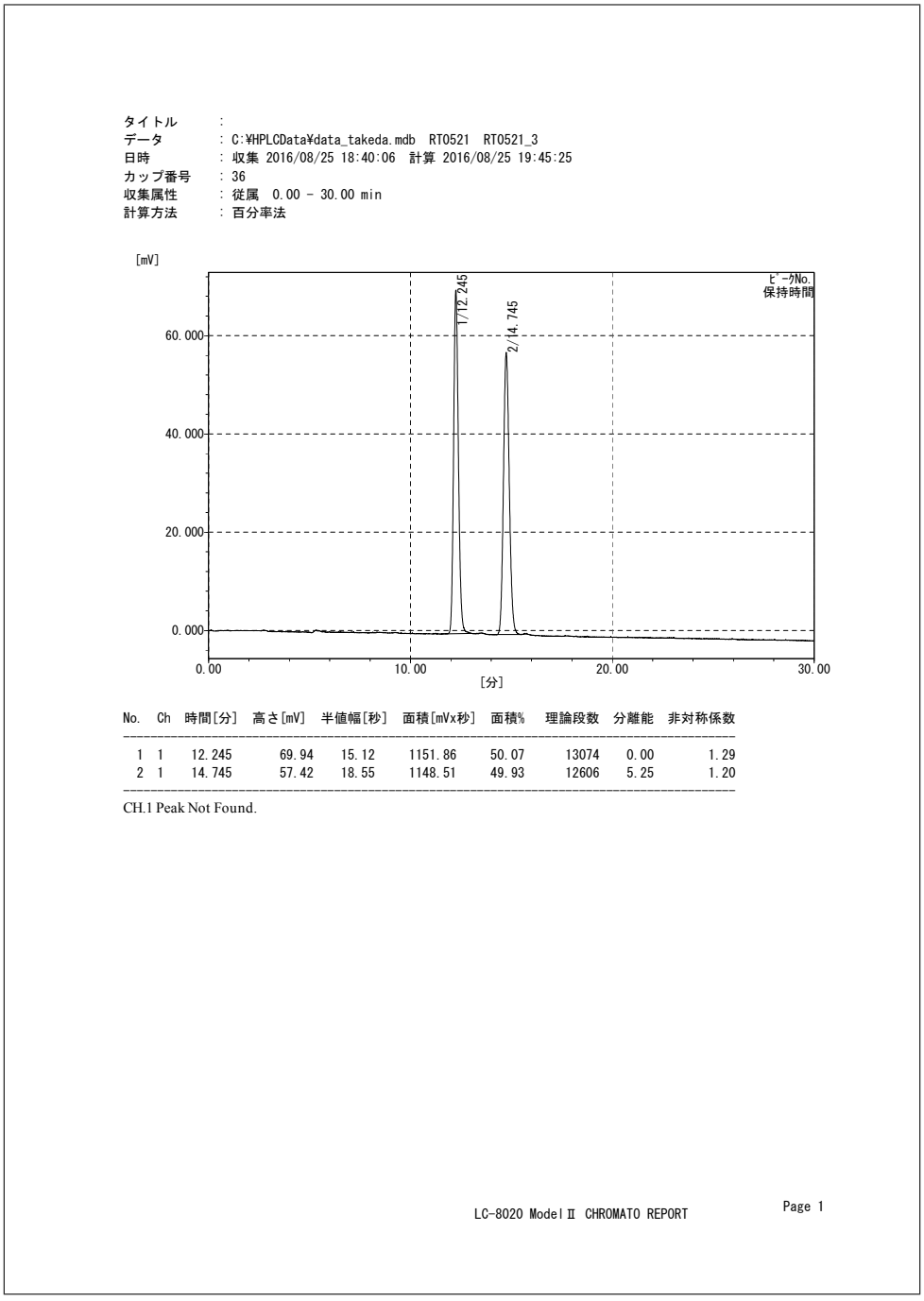

Figure S159. HPLC trace of the product of the asymmetric Suzuki-Miyaura cross coupling reaction in THF. Enantiomeric excess was found to be less than 1% (DAICEL CHIRALCEL® OZ-H, Eluent; *n*-hexane/2-PrOH (80/20), Flow rate; 0.6 mL/min).

タイトル　　:
データ　　: C:¥HPLCData¥data_takeda.mdb　20161207_3rtO608　RTO608
日時　　: 収集 2016/12/07 22:16:28　計算 2016/12/07 22:53:38
カップ番号　: 34
収集属性　　: 従属　0.00 - 20.00 min
計算方法　　: 百分率法

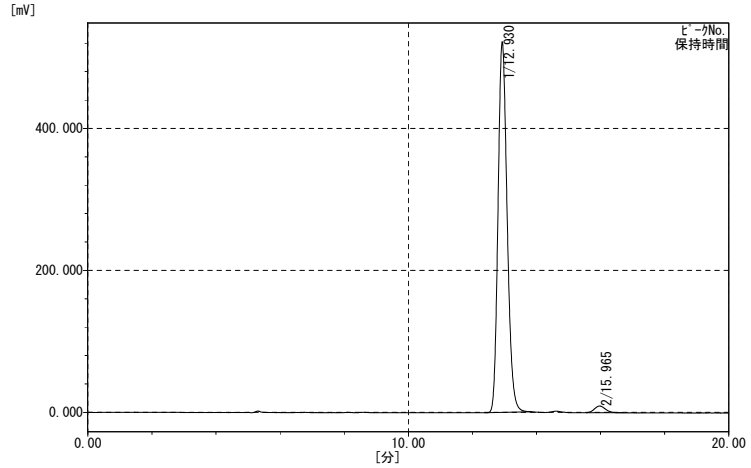

No.	Ch	時間[分]	高さ[mV]	半値幅[秒]	面積[mVx秒]	面積%	理論段数	分離能	非対称係数
1	1	12.930	522.28	18.20	10318.36	97.86	10067	0.00	1.32
2	1	15.965	9.53	22.24	225.86	2.14	10278	5.30	1.26

CH.1 Peak Not Found.

LC-8020 ModelⅡ CHROMATO REPORT　Page 1

Figure S160. HPLC trace of the product of the asymmetric Suzuki-Miyaura cross coupling reaction in (*R*)-limonene/THF (70/30). Enantiomeric excess was found to be 96% (*S*) (DAICEL CHIRALCEL® OZ-H, Eluent; *n*-hexane/2-PrOH (80/20), Flow rate; 0.6 mL/min).

タイトル　　：
データ　　：C:¥HPLCData¥data_takeda.mdb　1609230001　RT0561
日時　　：収集 2016/09/23 01:47:54　計算 2016/09/23 02:18:47
カップ番号　：34
収集属性　　：従属　0.00 - 30.00 min
計算方法　　：百分率法

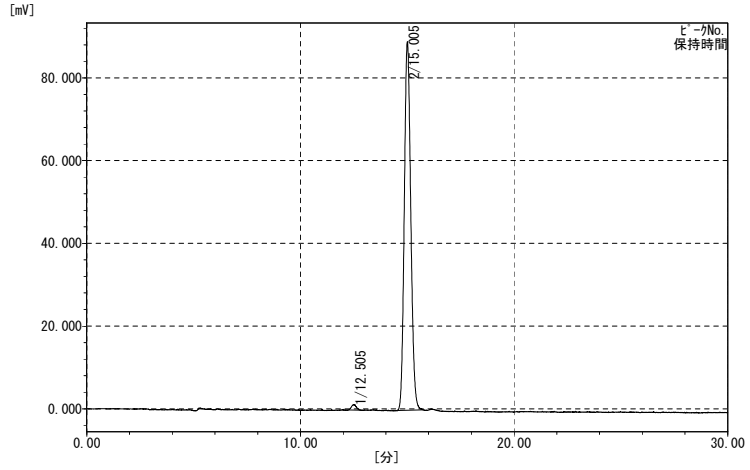

No.	Ch	時間[分]	高さ[mV]	半値幅[秒]	面積[mVx秒]	面積%	理論段数	分離能	非対称係数
1	1	12.505	1.36	14.94	22.55	1.19	13971	0.00	1.22
2	1	15.005	89.13	19.44	1867.47	98.81	11882	5.14	1.20

CH.1 Peak Not Found.

LC-8020 ModelⅡ CHROMATO REPORT　　Page 1

Figure S161. HPLC trace of the product of the asymmetric Suzuki-Miyaura cross coupling reaction in (*S*)-limonene/THF (95/5). Enantiomeric excess was found to be 98% (*R*) (DAICEL CHIRALCEL® OZ-H, Eluent; *n*-hexane/2-PrOH (80/20), Flow rate; 0.6 mL/min).

タイトル　　:
データ　　: C:¥HPLCData¥data_takeda.mdb　20161207_3rtO609　RTO609
日時　　: 収集 2016/12/07 22:41:29　計算 2016/12/07 23:06:34
カップ番号　: 35
収集属性　　: 従属　0.00 - 20.00 min
計算方法　　: 百分率法

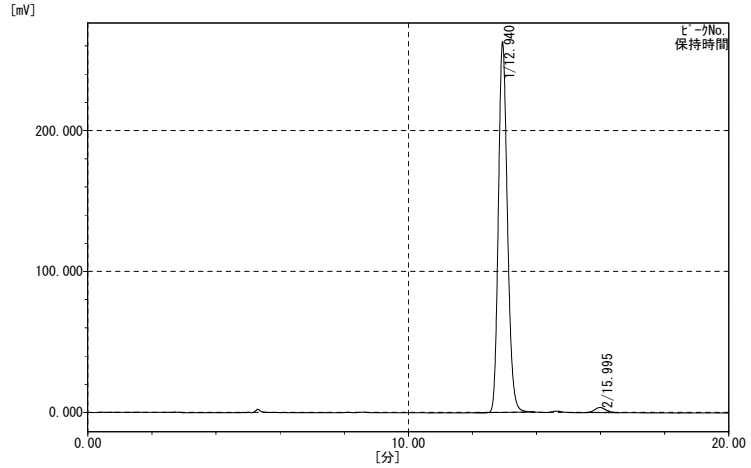

No.	Ch	時間[分]	高さ[mV]	半値幅[秒]	面積[mVx秒]	面積%	理論段数	分離能	非対称係数
1	1	12.940	263.10	18.02	5158.94	98.29	10285	0.00	1.31
2	1	15.995	3.72	22.22	89.62	1.71	10330	5.37	1.16

CH.1 Peak Not Found.

LC-8020 ModelⅡ CHROMATO REPORT　Page 1

Figure S162. HPLC trace of the product of the asymmetric Suzuki-Miyaura cross coupling reaction in (*R*)-limonene/THF (98/2). Enantiomeric excess was found to be 97% (*S*) (DAICEL CHIRALCEL® OZ-H, Eluent; *n*-hexane/2-PrOH (80/20), Flow rate; 0.6 mL/min).

タイトル　　:
データ　　: C:¥HPLCData¥data_takeda.mdb　201701190003　RT0621
日時　　: 収集 2017/01/19 19:32:20　計算 2017/01/19 20:37:05
カップ番号　: 35
収集属性　　: 従属　0.00 - 20.00 min
計算方法　　: 百分率法

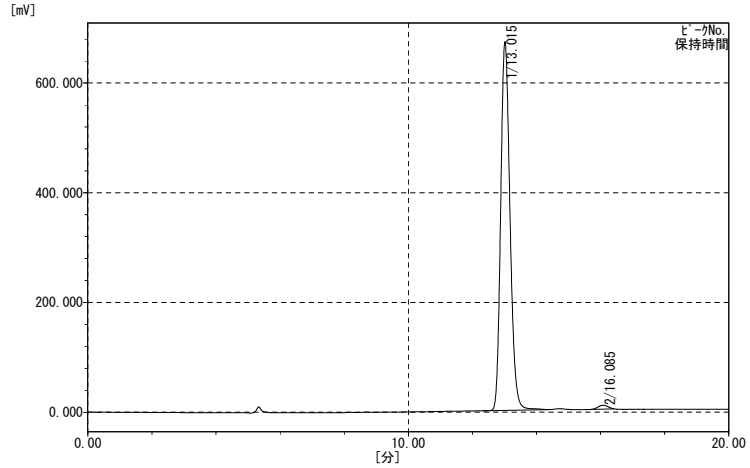

No.	Ch	時間[分]	高さ[mV]	半値幅[秒]	面積[mVx秒]	面積%	理論段数	分離能	非対称係数
1	1	13.015	672.18	18.57	13561.79	98.90	9800	0.00	1.33
2	1	16.085	7.12	20.77	151.42	1.10	11957	5.52	0.95

CH.1 Peak Not Found.

LC-8020 ModelⅡ CHROMATO REPORT　　Page 1

Figure S163. HPLC trace of the product of the asymmetric Suzuki-Miyaura cross coupling reaction in (*S*)-limonene/THF (95/5). Enantiomeric excess was found to be 98% (*R*) (DAICEL CHIRALCEL® OZ-H, Eluent; *n*-hexane/2-PrOH (80/20), Flow rate; 0.6 mL/min).

タイトル　　:
データ　　: C:¥HPLCData¥data_takeda.mdb　201702030003　RT0635
日時　　: 収集 2017/02/03 21:58:54　計算 2017/08/31 21:26:16
カップ番号　: 34
収集属性　　: 従属　0.00 - 20.00 min
計算方法　　: 百分率法

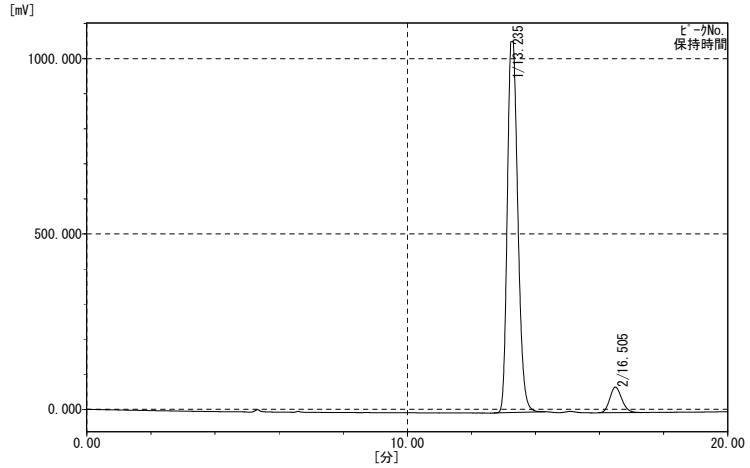

No.	Ch	時間[分]	高さ[mV]	半値幅[秒]	面積[mVx秒]	面積%	理論段数	分離能	非対称係数
1	1	13.235	1058.01	21.18	24153.94	92.74	7784	0.00	1.73
2	1	16.505	73.08	23.97	1892.14	7.26	9456	5.12	1.18

CH.1 Peak Not Found.

LC-8020 ModelⅡ CHROMATO REPORT　　Page 1

Figure S164. HPLC trace of the product of the asymmetric Suzuki-Miyaura cross coupling reaction in (*R*)-limonene/THF (95/5). Enantiomeric excess was found to be 85% (*S*) (DAICEL CHIRALCEL® OZ-H, Eluent; *n*-hexane/2-PrOH (80/20), Flow rate; 0.6 mL/min).

タイトル　　:
データ　　: C:¥HPLCData¥data_takeda.mdb　201702030004　RT0638
日時　　: 収集 2017/02/03 22:23:54　計算 2017/02/03 22:44:37
カップ番号　: 35
収集属性　　: 従属　0.00 - 20.00 min
計算方法　　: 百分率法

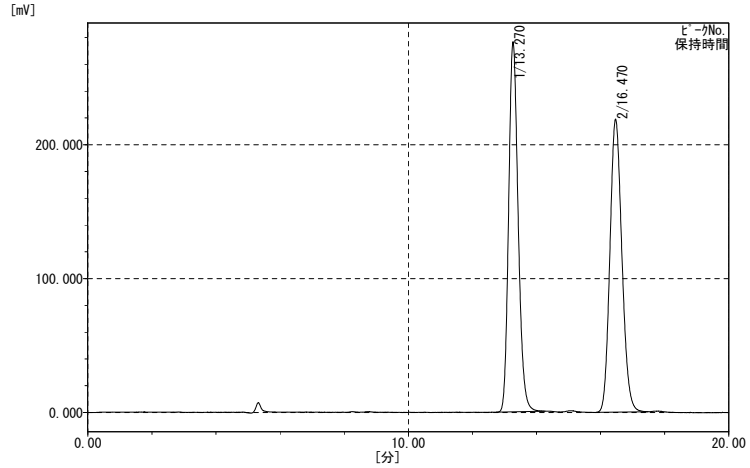

No.	Ch	時間[分]	高さ[mV]	半値幅[秒]	面積[mVx秒]	面積%	理論段数	分離能	非対称係数
1	1	13.270	276.51	18.88	5691.92	50.10	9847	0.00	1.29
2	1	16.470	218.84	23.99	5669.27	49.90	9400	5.28	1.22

CH.1 Peak Not Found.

LC-8020 ModelⅡ CHROMATO REPORT　Page 1

Figure S165. HPLC trace of the product of the asymmetric Suzuki-Miyaura cross coupling reaction in (*R*)-limonene/THF (95/5). Enantiomeric excess was found to be less than 1% (DAICEL CHIRALCEL® OZ-H, Eluent; *n*-hexane/2-PrOH (80/20), Flow rate; 0.6 mL/min).

タイトル　　：
データ　　：C:¥HPLCData¥data_takeda.mdb　201701170003　RT0619
日時　　：収集 2017/01/17 16:59:05　計算 2017/01/17 17:21:33
カップ番号　：35
収集属性　　：従属　0.00 - 20.00 min
計算方法　　：百分率法

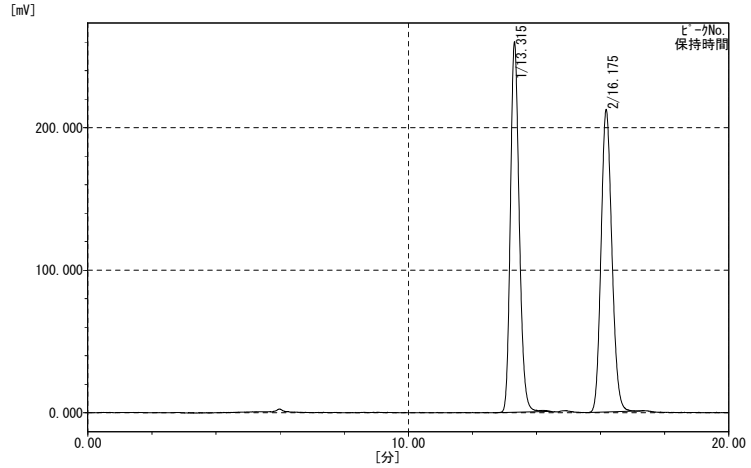

No.	Ch	時間[分]	高さ[mV]	半値幅[秒]	面積[mVx秒]	面積%	理論段数	分離能	非対称係数
1	1	13.315	259.93	17.56	4988.87	50.02	11470	0.00	1.29
2	1	16.175	212.36	21.73	4984.67	49.98	11048	5.15	1.23

CH.1 Peak Not Found.

LC-8020 ModelⅡ CHROMATO REPORT　　Page 1

Figure S166. HPLC trace of the product of the asymmetric Suzuki-Miyaura cross coupling reaction in (*R*)-limonene/THF (95/5). Enantiomeric excess was found to be less than 1% (DAICEL CHIRALCEL® OZ-H, Eluent; *n*-hexane/2-PrOH (80/20), Flow rate; 0.6 mL/min).

タイトル　　:
データ　　: C:¥HPLCData¥data_takeda.mdb　RT0441　RT0441
日時　　: 収集 2016/03/01 20:30:39　計算 2016/03/01 21:05:37
カップ番号　: 35
収集属性　　: 独立　0.00 - 30.00 min
計算方法　　: 百分率法

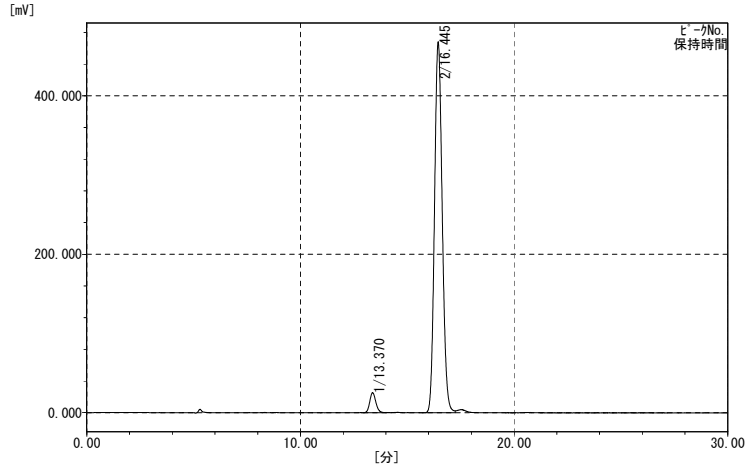

No.	Ch	時間[分]	高さ[mV]	半値幅[秒]	面積[mVx秒]	面積%	理論段数	分離能	非対称係数
1	1	13.370	25.30	18.09	494.11	4.03	10895	0.00	1.30
2	1	16.445	468.52	23.36	11775.96	95.97	9884	5.24	1.20

CH.1 Peak Not Found.

LC-8020 ModelⅡ CHROMATO REPORT　Page 1

Figure S167. HPLC trace of the product of the asymmetric Suzuki-Miyaura cross coupling reaction in (*S*)-HMB. Enantiomeric excess was found to be 92% (*R*) (DAICEL CHIRALCEL® OZ-H, Eluent; *n*-hexane/2-PrOH (80/20), Flow rate; 0.6 mL/min).

タイトル　　：
データ　　：C:¥HPLCData¥data_takeda.mdb　201610130002　RT568
日時　　：収集 2016/10/13 13:48:18　計算 2016/10/13 15:40:32
カップ番号　：34
収集属性　　：従属　0.00 - 30.00 min
計算方法　　：百分率法

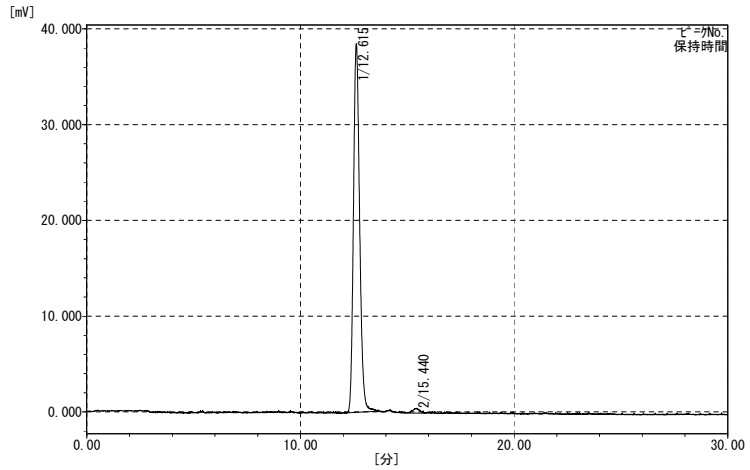

No.	Ch	時間[分]	高さ[mV]	半値幅[秒]	面積[mVx秒]	面積%	理論段数	分離能	非対称係数
1	1	12.615	38.51	18.29	771.60	98.58	9483	0.00	1.29
2	1	15.440	0.50	24.61	11.11	1.42	7847	4.65	0.90

CH.1 Peak Not Found.

LC-8020 ModelⅡ CHROMATO REPORT　　Page 1

Figure S168. HPLC trace of the product of the asymmetric Suzuki-Miyaura cross coupling reaction in orange oil/THF (95/5). Enantiomeric excess was found to be 97% (*S*) (DAICEL CHIRALCEL® OZ-H, Eluent; *n*-hexane/2-PrOH (80/20), Flow rate; 0.6 mL/min).

タイトル　　：
データ　　：C:¥HPLCData¥data_takeda.mdb　RT0597　RT0597_4ee
日時　　：収集 2016/11/16 19:06:58　計算 2017/03/29 15:24:18
カップ番号　：36
収集属性　　：従属　0.00 - 25.00 min
計算方法　　：百分率法

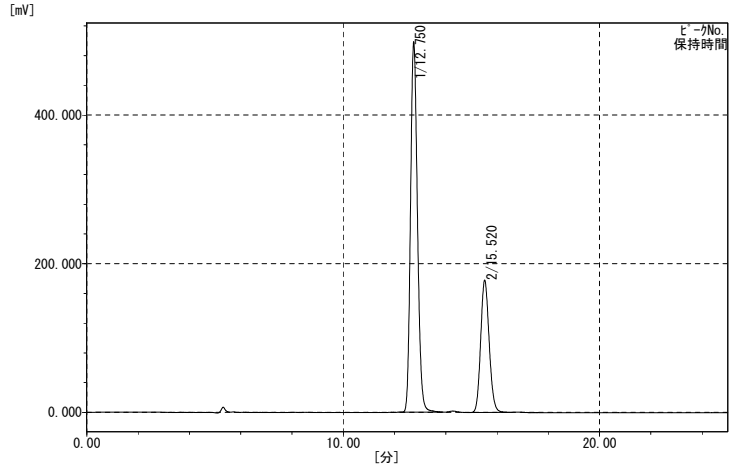

No.	Ch	時間[分]	高さ[mV]	半値幅[秒]	面積[mVx秒]	面積%	理論段数	分離能	非対称係数
1	1	12.750	498.51	17.32	9351.60	69.61	10812	0.00	1.28
2	1	15.520	178.34	21.19	4083.40	30.39	10703	5.09	1.21

CH.1 Peak Not Found.

LC-8020 ModelⅡ CHROMATO REPORT　　Page 1

Figure S169. HPLC trace of the product of the asymmetric Suzuki-Miyaura cross coupling reaction in (*R*)-limonene (6.7% ee) /THF (95/5). Enantiomeric excess was found to be 36% (*S*) (DAICEL CHIRALCEL® OZ-H, Eluent; *n*-hexane/2-PrOH (80/20), Flow rate; 0.6 mL/min).

タイトル　　：
データ　　：C:¥HPLCData¥data_takeda.mdb　RT0598　RT0598_10ee
日時　　：収集 2016/11/16 19:38:39　計算 2016/11/16 21:05:53
カップ番号　：37
収集属性　　：従属　0.00 - 25.00 min
計算方法　　：百分率法

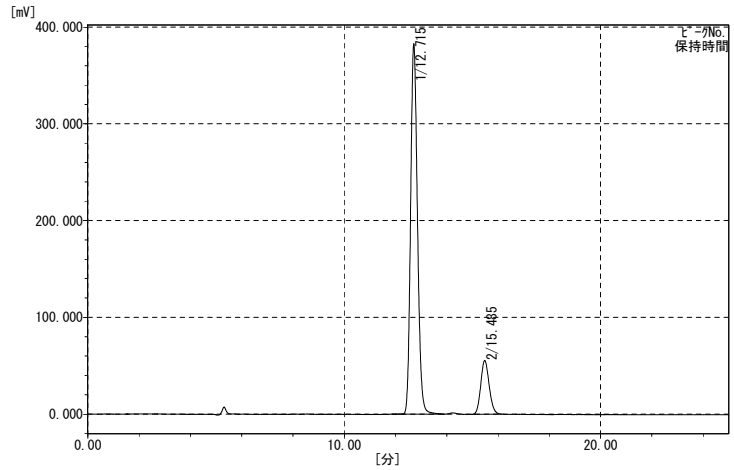

No.	Ch	時間[分]	高さ[mV]	半値幅[秒]	面積[mVx秒]	面積%	理論段数	分離能	非対称係数
1	1	12.715	382.97	17.11	7116.46	84.92	11009	0.00	1.26
2	1	15.485	55.66	21.11	1264.15	15.08	10735	5.12	1.19

CH.1 Peak Not Found.

LC-8020 Model Ⅱ CHROMATO REPORT　　Page 1

Figure S170. HPLC trace of the product of the asymmetric Suzuki-Miyaura cross coupling reaction in (*R*)-limonene (12.6% ee) /THF (95/5). Enantiomeric excess was found to be 70% (*S*) (DAICEL CHIRALCEL® OZ-H, Eluent; *n*-hexane/2-PrOH (80/20), Flow rate; 0.6 mL/min).

タイトル　　：
データ　　：C:¥HPLCData¥data_takeda.mdb　RT0599　RT0599_60ee
日時　　：収集 2016/11/16 21:37:07　計算 2016/11/16 22:03:23
カップ番号　：38
収集属性　　：従属　0.00 - 25.00 min
計算方法　　：百分率法

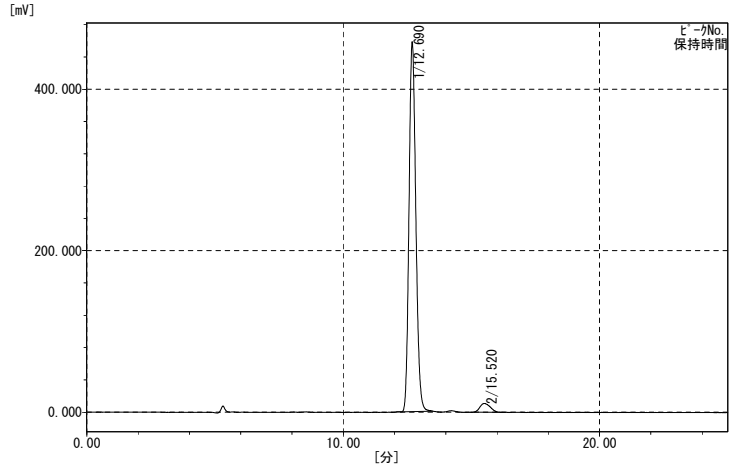

No.	Ch	時間[分]	高さ[mV]	半値幅[秒]	面積[mVx秒]	面積%	理論段数	分離能	非対称係数
1	1	12.690	458.41	17.09	8457.54	96.48	10991	0.00	1.27
2	1	15.520	10.87	27.40	308.32	3.52	6398	4.50	1.32

CH.1 Peak Not Found.

LC-8020 ModelⅡ CHROMATO REPORT　　Page 1

Figure S171. HPLC trace of the product of the asymmetric Suzuki-Miyaura cross coupling reaction in (*R*)-limonene (63.4% ee) /THF (95/5). Enantiomeric excess was found to be 93% (*S*) (DAICEL CHIRALCEL® OZ-H, Eluent; *n*-hexane/2-PrOH (80/20), Flow rate; 0.6 mL/min).

タイトル　　:
データ　　: C:¥HPLCData¥data_takeda.mdb　201701310002　RT0633
日時　　: 収集 2017/01/31 17:57:57　計算 2017/01/31 18:32:38
カップ番号　: 35
収集属性　　: 従属　0.00 - 20.00 min
計算方法　　: 百分率法

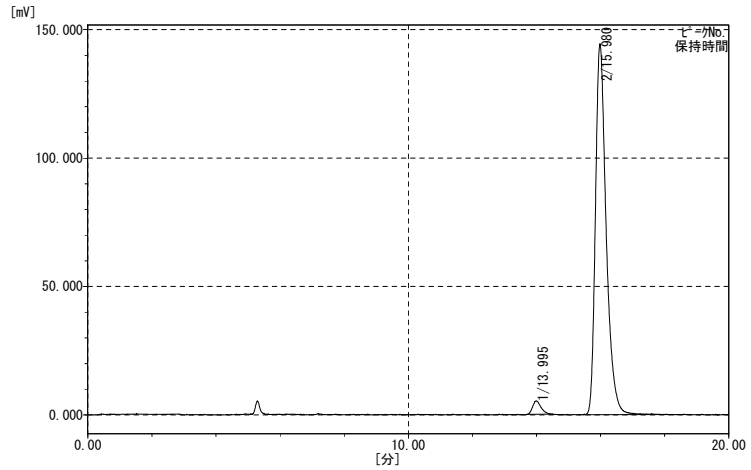

No.	Ch	時間[分]	高さ[mV]	半値幅[秒]	面積[mVx秒]	面積%	理論段数	分離能	非対称係数
1	1	13.995	5.26	16.62	94.89	2.74	14140	0.00	1.55
2	1	15.980	144.48	20.69	3366.17	97.26	11895	3.76	1.67

CH.1 Peak Not Found.

LC-8020 ModelⅡ CHROMATO REPORT　Page 1

Figure S172. HPLC trace of the product of the asymmetric hydrosilylation reaction of styrene in (*R*)-limonene/THF (95/5) after oxidation to 1-phenylethanol. Enantiomeric excess was found to be 95% (*S*) (DAICEL CHIRALCEL® OD-H, Eluent; *n*-hexane/2-PrOH (97/3), Flow rate; 0.6 mL/min).

タイトル　　:
データ　　: C:¥HPLCData¥data_takeda.mdb　RT0583　RT583_7
日時　　: 収集 2016/10/31 22:36:28　計算 2016/11/01 09:35:27
カップ番号　: 34
収集属性　　: 従属　0.00 - 15.00 min
計算方法　　: 百分率法

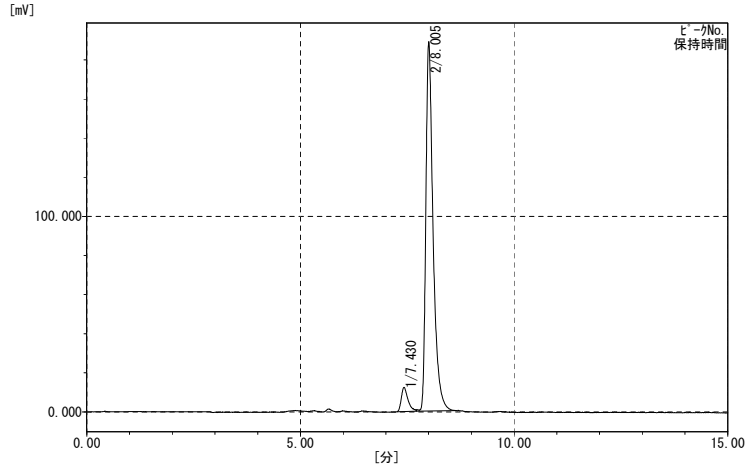

No.	Ch	時間[分]	高さ[mV]	半値幅[秒]	面積[mVx秒]	面積%	理論段数	分離能	非対称係数
1	1	7.430	12.33	9.48	131.63	5.59	12258	0.00	1.74
2	1	8.005	188.88	10.24	2224.53	94.41	12179	2.06	1.80

CH.1 Peak Not Found.

LC-8020 ModelⅡ CHROMATO REPORT　　Page 1

Figure S173. HPLC trace of the product of the silaboration reaction of methylene cyclopropane in (*S*)-limonene/THF (95/5). Enantiomeric excess was found to be 89% (*R*) (DAICEL CHIRALCEL® OD-H, Eluent; *n*-hexane/2-PrOH (99.7/0.3), Flow rate; 0.6 mL/min).